國 立 交 通 大 學

電子工程學系　電子研究所碩士班

碩 士 論 文

閘極介電層氧化釓於
硫鈍化後砷化鎵基板之電物性研究

The Electrical and Material Characteristics of Gd_2O_3 Gate Dielectric on Sulfided GaAs Substrate

研 究 生：曾 治 國

指導教授：簡 昭 欣 博士

中華民國九十六年六月

國 立 交 通 大 學

電子工程學系　電子研究所碩士班

碩 士 論 文

閘極介電層氧化釓於
硫鈍化後砷化鎵基板之電物性研究

The Electrical and Material Characteristics
of Gd_2O_3 Gate Dielectric on Sulfided GaAs Substrate

研 究 生：曾 治 國
指導教授：簡 昭 欣 博士

中華民國九十六年六月

閘極介電層氧化釓於硫鈍化後砷化鎵基板之電物性研究

The Electrical and Material Characteristics of Gd_2O_3 Gate Dielectric on Sulfided GaAs Substrate

研 究 生：曾 治 國　　Student：Chih-Kuo Tseng

指導教授：簡 昭 欣 博士　　Advisor：Dr. Chao-Hsin Chien

國 立 交 通 大 學

電子工程學系　電子研究所碩士班

碩 士 論 文

A Thesis

Submitted to Department of Electronics Engineering & Institute of Electronics

College of Electrical Engineering and Computer Science

National Chiao Tung University

in partial Fulfillment of the Requirements

for the Degree of

Master

in

Electronics Engineering

June 2007

Hsinchu, Taiwan, Republic of China

中華民國九十六年六月

閘極介電層氧化釓於硫鈍化後
砷化鎵基板之電物性研究

研 究 生：曾 治 國　　　指 導 教 授：簡 昭 欣 博士

國立交通大學

電子工程學系　　　電子研究所碩士班

摘　要

本論文中， 將選擇跟砷化鎵基板有較穩定特性的稀土族元素釓之氧化物作為閘極介電材料，接著我們利用表面預備製以及後熱退火來探討氧化釓與其砷化鎵之介面的電物性研究。

首先，對於砷化鎵基板的濕式化學清潔，發現鹽酸溶液對於表面會呈現砷化物居多的情形，接著做氨水蝕刻溶液去除多餘的砷化物。當清潔步驟完成時，接著馬上進行硫鈍化砷化鎵表面的工作。在介電質沉積之前，硫鈍化的目的可以降低時表面產生的大量介面缺陷氧化層，缺陷氧化層就會使得往後的電物性結果受到極大的影響。我們發現硫化物同時和砷或鎵形成反應，而硫化鎵鍵結比硫化砷鍵結更容易隨著硫化處理的溫度增加而讓鍵結穩定，那是因為堅強的鍵結情形，這樣的話就能降低氧化釓與其砷化鎵電容結構的表面自然氧化層以及介面捕捉狀態密度。

我們也發現硫化銨與水溶液或醇類溶液結合可以有效解決金屬與砷化鎵的費米能階釘札情形。混合的硫化銨和丁醇(butanol)是最有效率可以降低蕭基特能位障的溶液，這是因為硫鈍化可以去除大量的介面氧化層。

另外，後退火幫助氧化釓與砷化鎵接面的品質得到改善；改變不同退火環境可以得到在電容-電壓以及電流-電壓不同的特性。在500-600度的含氧氣體下呈現較少色散的電容-電壓曲線和低的漏電流程度，反之惰性的氬氣或氮氣含量氣體則得到相反結果。另一方面，吸水造成的衰退情形對我們已沉積的高介電質氧化釓並沒有太大明顯，透過韋伯(Weibull)分佈研究下，氧化釓在砷化鎵上的電容即使一個月時間依然可以得到相同的電特性。因此，我們推斷高穩定的氧化釓與其砷化鎵介面可以整合硫鈍化預先處理和介電質退火過程去實現金屬-氧化物-半導體結構的高速元件應用。

The Electrical and Material Characteristics of Gd_2O_3 Gate Dielectric on Sulfidized GaAs Substrate

Student: Chih-Kuo Tseng   Advisor: Dr. Chao-Hsin Chien

Department of Electronics Engineering and Institute of Electronics

National Chiao Tung University, Hsunchu, Taiwan

ABSTRACT

In this thesis, the rare-earth oxide of Gd_2O_3 was used as high-*k* gate dielectric material, which is highly stabilized with GaAs, and we studied the material and electrical properties of the Gd_2O_3/GaAs structures through surface preparation procedures and post thermal annealing, respectively.

At first, for the wet chemical cleaning, it was found that the GaAs surface preferred to form arsenic chemical species after etching in HCl solution, and subsequent NH_4OH solution assisted to remove these excess arsenic-related defects. After that, we performed various kinds of the sulfur-based pretreatment to passivate the cleaned GaAs substrate. The purpose of formed sulfur–terminated GaAs surface is to restrain the growth of defective oxide layers prior to and during the dielectric deposition; since they indeed cause the degradation of the following electrical characteristics. We found that sulfur atoms can react with both arsenic and gallium elements; an increase in sulfidized temperature intends to form the Ga-S rather than As-S chemical bonding

because of the stronger bonding strength, which in turn facilitating to decrease surface native oxides and interface trap density in Gd_2O_3/GaAs capacitors.

We also observed that $(NH_4)_2S$ aqua or combining with alcohol-based solution can alleviate the well-known Fermi level pinning on metal/GaAs interface. The mixed solution of the $(NH_4)_2S$ and the butanol was found to be effectively decrease the Schottky barrier height due to the removal of substantial interfacial oxides as well as the definite sulfide passivation.

In addition, the post-deposition annealing further boosted the quality of Gd_2O_3 thin film with improved Gd_2O_3/GaAs interface; moreover, changing the annealing atmosphere showed several characteristic differences in *C*-*V* and *I*-*V* curves. The O_2-contained gas at 500-600 ^{o}C revealed the smaller *C*-*V* frequency dispersion and lower leakage current level, whereas the inert Ar or N_2-contained gas revealed the opposed results. On the other hand, the humidity induced degradation is not obvious for deposited Gd_2O_3 high-*k* dielectric that the identical electrical properties can be preserved in Gd_2O_3/GaAs capacitors up to one month through investigation of the Weibull distribution. Therefore, we conclude that the highly stable Gd_2O_3/GaAs interface can be achieved integrating the sulfide pretreatment and dielectric annealing processes, which can be considered as the potential structure for metal-oxide-semiconductor device application.

致　謝

在短短兩年的碩士班研究生涯，首先感謝指導教授　簡昭欣 博士給予實驗室學生豐富專業知識的指導，以及老師為人處事更是我們應當學習的目標，另外老師對學生的用心及精神更是讓大家感動不已。其次感謝國家奈米實驗室裡的楊明瑞學長，不管在實驗或討論問題上提供了相當大的幫忙，才得以完成學生的碩士論文。

特別感謝鄭兆欽學長，給予我們極大的鼓勵和幫忙，從學長的做實驗細心態度下學習很多做事情的精神和經驗，相信可以對自己以後有幫助，也祝他在未來人生能一切順利平安。另外，包括楊紹明學長、陳世璋學長以及沈志彥學長，感謝他們不僅解答實驗上的疑問，在日常生活中亦不斷地鼓勵我上進。也謝謝實驗室的其他同學:家豪、熊哥、石頭、小劉、阿壘、阿心和學弟們:弘森、欣哲、Rain、宣凱、敬倫、宇彥、猛飛，陪我一同走過兩年的碩士生活，以及陪我在籃球場上奔跑的日子，謝謝實驗室的大家給我留下許多快樂的回憶。

最後，我要由衷感激親愛的父母，感謝您們辛苦的栽培及默默付出，用心奉獻整個家庭，使得孩子們得以全心投入學業；謝謝優秀的兩位哥哥和老弟的加油與打氣，也因為你們讓爸媽得以減輕辛勞；感謝可愛的女友雅蓮，給了我全力的支持與鼓勵。

Contents

Abstract (Chinese) -- Ⅰ

Abstract (English) -- Ⅲ

Acknowledgement -- Ⅴ

Contents -- Ⅵ

Figure Captions -- Ⅸ

Chapter 1 Introduction

1-1 General Background -- 1

1-2 Motivation -- 3

1-3 Organization -- 4

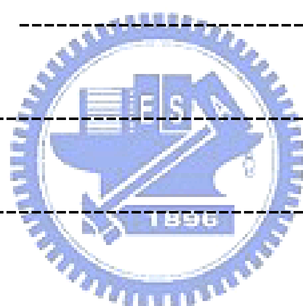

Chapter 2 The Cleaning Process of Gallium Arsenide Substrate

2-1 Introduction -- 7

2-2 Experimental Procedure -- 10

2-3 Results and Discussion -- 11

2-3-1 XPS of cleaning GaAs substrate -- 11

2-3-2 Surface morphology of cleaning GaAs substrate ---------------- 14

2-4 Summary -- 15

Chapter 3 The Sulfur Passivation on Gallium Arsenide Substrate

3-1 Introduction -- 27

3-2 Experimental Procedure -- 29

3-3 Results and Discussion -- 31

3-3-1 *XPS and PL of the sulfided GaAs substrate* ---------------------- 31

3-3-2 *surface roughness of the sulfided GaAs* -------------------------- 35

3-3-3 *electrical characterization of the sulfided GaAs* ---------------- 36

3-4 Summary -- 37

Chapter 4 Electron-beam evaporated Gd_2O_3 Gate Dielectric On GaAs Substrate

4-1 Introduction -- 55

4-2 Experimental Procedure -- 56

4-3 Electrical and Material Characteristics ---------------------------------- 57

4-3-1 *C-V and I-V characteristics of* Pt/ Gd_2O_3/ GaAs structure ------- 57

4-3-2 *xps characteristic of Gd_2O_3 film on GaAs substrate* -------------- 63

4-3-3 *surface morphology of Gd_2O_3 film on GaAs substrate* ---------- 65

4-4 Summary -- 65

Chapter 5 Conclusions and Suggestions for Future Work

5-1 Conclusions --- 93

5-2 Future Work -- 94

References --96

Vita --- 100

Figure Captions

Chapter 1 Introduction

Fig.1-2 Advantage of GaAs substrate compared to general Si material.

Fig.1-2 Predicted band offsets on GaAs with different high-k materials.

Chapter 2 The Cleaning Process of Gallium Arsenide Substrate

Fig. 2-1(a) As 2p and (b) As 3d core-level spectra with different diluted HCl concentration.

Fig. 2-2(a) Ga 2p and (b) Ga 3d core-level spectra after different diluted HCl concentration.

Fig. 2-3(a) As 2p and (b) Ga 2p core-level spectra after different diluted HCl concentration and cleaned cycles.

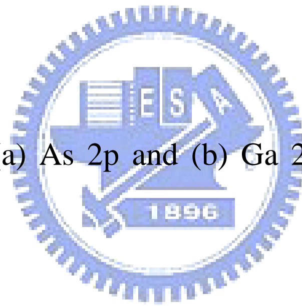

Fig. 2-4 The fitting result of (a) As 2p and (b) Ga 2p core-level spectra after diluted HCl concentration.

Fig. 2-5 The fitting results of As 2p core-level spectra with diluted HCl solution following by different NH_4OH solutions.

Fig. 2-6 The arsenic compound ratio with diluted HCl solution following by different NH_4OH solutions.

Fig. 2-7 AFM image of cleaned GaAs substrate with different clean methods: (a) HCl (b) HCl+NH_4OH (c) NH_4OH.

Fig. 2-8 Surface roughness of cleaned GaAs substrate with different clean methods: (a) HCl (b) HCl+NH_4OH (c) NH_4OH.

Table 2-1 The fitting results of the GaAs component from photoelectron spectra

Table 2-2 The fitting results of the GaAs component from photoelectron As 2p spectum.

Table 2-3 The fitting results of the GaAs component from photoelectron Ga 2p spectum

Table 2-4 The ratio of GaAs component with diluted HCl solution following by different NH_4OH solutions.

Chapter 3 The Sulfur Passivation on Gallium Arsenide Substrate

Fig. 3-1 (a) As 2p and (b) Ga 2p core-level spectra after different sulfide methods.

Fig. 3-2 (a) S 2p spectra by three sulfur passivation before subtraction and (b) after subtraction Ga 2s peak from S 2p peak.

Fig. 3-3 (a) As 2p and (b) Ga 2p core-level spectra of the sulfided samples against moisture with spectra after 1week .

Fig. 3-4 Photoluminance of Gd_2O_3/ GaAs sulfided by $(NH_4)_2S$ solution with different (a) temperature and (b) concentration.

Fig. 3-5 Photoluminance of Gd_2O_3/ GaAs sulfided by Na_2S solution with different (a) temperature and (b) concentration.

Fig. 3-6 (a) As 2p (b) Ga 2p core-level spectra of sulfided GaAs at various treatment temperature: (i) without sulfide (ii) sulfide at room temperature (iii) sulfide at 50°C (iv) sulfide at 80°C.

Fig. 3-7 GaAs component ratio of the HCl cleaned with two sulfide temperature.

Fig. 3-8 (a) As 2p and (b) As 3d spectra of GaAs after two sulfur concentration: (i) cleaned (ii) sulfide at 0.5% concentration (iii) sulfide at 2% concentration.

Fig. 3-9 (a) Ga 2p and (b) Ga 3d spectra of GaAs after two sulfur concentration: (i) cleaned (ii) sulfide at 0.5% concentration (iii) sulfide at 2% concentration.

Fig.3-10 (a) As 2p and (b) Ga 2p core level spectra after HCl+NH_4OH solution with two sulfided temperature.

Fig. 3-11 GaAs component ratio of the HCl、NH_4OH solutions cleaned with two sulfide temperature.

Fig. 3-12 Surface morphology of HCl cleaned GaAs substrate after different sulfide condition: (a) without sulfidation (b) 1%, RT (c) 1%, 80^oC.

Fig. 3-13 Surface morphology of HCl +NH_4OH cleaned GaAs substrate after different sulfide condition: (a) without sulfidation (b) 1%, 80^oC.

Fig. 3-14 Surface morphology of NH_4OH cleaned GaAs substrate after different sulfide condition: (a) without sulfidation (b) 1%, 80^oC.

Fig. 3-15 Surface roughness of cleaned GaAs with different sulfidation

Fig. 3-16 I-V curves of Al metal contact to n-GaAs substrate with different surface treatment.

Fig. 3-17 Extraction of Schottky barrier height(SBH) with Al metal on n-type GaAs

Fig. 3-18 Schottky diode parameters with $(NH_4)_2S$ solution after (i) no-anneal (ii) 400^oC N_2 anneal (iii) 500^oC N_2 anneal.

Fig. 3-19 Schottky diode parameters with sulfur solution and different solvents: (i) H_2O (ii)

C_3H_7OH (iii) C_4H_9OH.

Fig. 3-20 Schottky barrier height(SBH) with sulfur solution and different solvents: (i) H_2O (ii) C_3H_7OH (iii) C_4H_9OH.

Fig. 3-21 I-V curves of Schottky diode (a) with and (b) without sulfide.

Chapter 4 Electron-beam evaporated Gd_2O_3 Gate Dielectric On GaAs Substrate

Fig. 4-1 (a)-(d) Multi-frequency *C-V* characteristics of Pt/Gd_2O_3/GaAs MOS capacitor with different surface treatment.

Fig. 4-2 (a)-(d) The hysteresis of 10kHz frequency of Pt/Gd_2O_3/GaAs MOS capacitor with different surface treatment.

Fig. 4-3 (a) Multi-frequency *C-V* curve with HCl+NH_4OH +Sulfide treatment (b) The C-V dispersion with different surface treatments for Pt/Gd_2O_3/GaAs MOS capacitors.

Fig. 4-4 (a) The 10kHz frequency *C-V* and (b)hysteresis characteristics of Pt/Gd_2O_3/GaAs MOS capacitor with different clean and sulfide method.

Fig. 4-5 (a) The *I-V* curve characteristics and (b) Jg(@V=+1v) of Pt/Gd_2O_3/GaAs MOS capacitor with different clean and sulfide method.

Fig. 4-6 Density of state on Gd_2O_3/GaAs interface with different clean and sulfide method.

Fig. 4-7 (a)-(d) Multi-frequency *C-V* and hysteresis using 10k Hz frequency characteristics of Pt/Gd_2O_3/GaAs MOS capacitor with two cleaning method: (i) HCl+NH_4OH (ii)

NH_4OH

Fig. 4-8 (a) Multi-frequency *C-V* (b) the hysteresis using 10k Hz frequency and (c) density of state characteristics of Pt/Gd_2O_3/GaAs MOS capacitor with two cleaning method: (i) HCl+NH_4OH (ii) NH_4OH

Fig. 4-9 (a) The *I-V* curve characteristics and (b) Jg(@V=+1v) of Pt/Gd_2O_3/GaAs MOS capacitor with different clean methods and sulfide methods.

Fig. 4-10 (a)-(c) Multi-frequency *C-V* frequency characteristics of Pt/Gd_2O_3/GaAs MOS capacitor with three cleaning methods: (i) HCl (ii) HCl+NH_4OH (iii) NH_4OH

Fig. 4-11 (a)-(c) The C-V characteristics and D_{it} of Pt/Gd_2O_3/GaAs MOS capacitor with three cleaning methods: (i) HCl (ii) HCl+NH_4OH (iii) NH_4OH under optimum sulfidation.

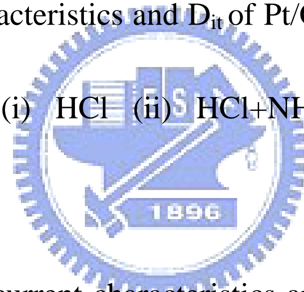

Fig. 4-12 (a)-(b) The leakage current characteristics and J_g v.s CET of Pt/Gd_2O_3/GaAs MOS capacitor with three cleaning methods: (i) HCl (ii) HCl+NH_4OH (iii) NH_4OH under optimum sulfidation.

Fig. 4-13 The Weibull distribution of Pt/Gd_2O_3/GaAs MOS capacitor with three cleaning methods: (i) HCl (ii) HCl+NH_4OH (iii) NH_4OH after 1 week.

Fig. 4-14 The TEM picture of Pt/Gd_2O_3/GaAs MOS capacitor with NH_4OH under optimum sulfidation.

Fig. 4-15 The EDS distribution signal of Pt/Gd_2O_3/GaAs MOS capacitor with NH_4OH under optimum sulfidation.

Fig. 4-16 (a)-(e) Multi-frequency *C-V* frequency characteristics of Pt/Gd_2O_3/GaAs MOS capacitor with different gas ambient : (i) O_2 500°C (ii) Ar 500°C (iii) $N_2$500°C (iv) Ar / O_2 500°C (v) Ar / O_2 600°C

Fig. 4-17 (a)-(e) The hysteresis width of Pt/Gd_2O_3/GaAs MOS capacitor with different gas ambient : (i) O_2 500°C (ii) Ar 500°C (iii) $N_2$500°C (iv) Ar / O_2 500°C (v) Ar / O_2 600°C

Fig. 4-18 (a) The 10k Hz frequency and (b) hysteresis trend of Pt/Gd_2O_3/GaAs MOS capacitor with different gas ambient : (i) O_2 500°C (ii) Ar 500°C (iii) N_2 500°C (iv) Ar / O_2 500°C (v) Ar / O_2 600°C

Fig. 4-19 (a) The dispersion and (b) leakage distribution characteristics of Pt/Gd_2O_3/GaAs MOS capacitor with different gas ambient : (i) O_2 500°C (ii) Ar 500°C (iii) $N_2$500°C (iv) Ar / O_2 500°C (v) Ar / O_2 600°C

Fig. 4-20 XPS spectra of the annealed Gd_2O_3 film at 500°C for 10 s. (a) the As 3d core level; (b) the Ga 3d core level.

Fig. 4-21 XPS spectra of the annealed Gd_2O_3 film at 500°C for 10 s. (a) the Gd 3d core level; (b) the Gd 4d core level.

Fig. 4-22 XPS spectra of the annealed Gd_2O_3 film at 500°C for 10 s. (a) the As 3d and Ga 3d core level; (b) the O 1*s* core level.

Fig. 4-23 The ratio of GaAs in the annealed Gd_2O_3 film at 500°C for 10 s with surface

treatment.

Fig. 4-24 XRD spectra of (i) n-GaAs(100) and (ii) 500°C annealed Gd_2O_3/ n-GaAs(100)

Fig. 4-25 Surface roughness of Gd_2O_3 on GaAs substrate after Ar/O_2 (500°C 10s) anneal with different surface treatments.

Fig. 4-26 Surface roughness of Gd_2O_3 on GaAs substrate after Ar/O_2 (500°C 10s) anneal with different clean methods.

Chapter 1
Introduction

1-1 General Background

Advancements in the performance of CMOS devices employing silicon substrates have been consistently achieved by shrinking critical MOSFET dimensions. Whiles critical dimensions keep decreasing to meet the demand for smaller and faster chips, the associated challenges will become increasingly difficult to address. As theoretical limits are reduced in the silicon CMOS world, referenced to MOSFETs based on compound semiconductor substrates have appeared in the International Technology Roadmap for Semiconductor [2] .Nanoscale device technology is driving intense study of thin dielectric layers on semiconductors. The aggressive scaling of Si CMOS technology calls for identifying high k dielectrics to replace SiO_2 and oxynitride in gate related applications [3]. About the substrate, Si and GaAs will be compared in the Fig. 1-1. The fundamental material requirements for the alternative gate dielectric are very challenging in order to achieve performance comparable to SiO_2. These requirements include dielectric constant, band gap, conduction band offset, high recrystallization temperature (for amorphous dielectrics only), low oxygen

diffusivity, The rare earth dielectric oxides have a high conduction band offset over 1 eV and show good thermodynamic stability in contact with GaAs, hence are considered as a very attractive candidate among several binary metal oxides currently in contention[4] .The GaAs metal-oxide-semiconductor field-effect transistor (MOSFET) in the driven by their applications in the high-speed circuit, which a low-leakage current ,and high-electrical strength[5]. Fig. 1-2 illustrate the energy band offset about GaAs substrate [6], and the difference of conduction band between GaAs and Gd_2O_3 is 1.8e V, which can reduce the thermal leakage current.

1-2 Motivation-Development of Gate Dielectric of GaAs Substrate.

Over the last few decades, there has been a dramatic increase in the number of publications on gate oxide with GaAs. For instance, in 1963 Revesz first appear that who use “anodic oxide” method to growth oxide, but the film morphology was too coarse [7]. In 1965, Becke, Hall and White used hot oxidation to growth SiO2 as gate oxide [8]. Hasegawa *et al*. have introduced the SiO2 or Si3N4 ultrathin film as an interfacial control layer between a GaAs and a gate dielectric [9].Wada have proposed an atomic layer passivation method using atomically thin compound layer [10]. Of the proposed alternative gate dielectrics for the GaAs, an epitaxially grown Gd_2O_3 film stands out as a stable insulating layer for the MOSFETs due to a lowest interface-state density below 10^{10} cm^{-2} eV^{-1} for both the inversion channel and the depletion-mode GaAs MOSFETs[11]、[12]. Therefore, the Gd_2O_3 on GaAs is the better surface passivation required for the efficient protection of GaAs from the air exposure and the deposition-induced degradation.

1-3 Organization of the Thesis

In Chapter 2, we developed the cleaning process of GaAs substrate. Different diluted etching solutions were treated for GaAs wafer cleaning. Various material analysis techniques, such as Atomic Force Microscopy (AFM) and X-ray Photoelectron Spectroscopy (XPS) were performed to observe the surface morphology and surface binding behavior of GaAs substrate after the cleaning procedure.

In Chapter 3, with the optimized cleaning procedure of GaAs wafer, the surface passivation was needed. The chemical wet solution was prepared to treat the GaAs surface in order to reduce the growth of native AsO_x and GaO_x oxide when exposed to air ambient. Various material analysis techniques, such as Atomic Force Microscopy (AFM), X-ray Photoelectron Spectroscopy (XPS) and Photoluminescence (PL), were performed to observe the surface morphology, surface binding behavior of GaAs substrate and surface trap after the cleaning and passivation procedure. Electrical analysis was discussed with Schottky barrier height reduction according to aluminum contact with n-type GaAs.

In Chapter 4, the thesis research focus on this chapter, the metal-insulator-semiconductor structure was fabricated, the optimized surface

treatment, post deposition anneal and e-beam evaporated Gd_2O_3 high-k films were included. Various material analysis techniques, such as Atomic Force Microscopy (AFM), X-ray Photoelectron Spectroscopy (XPS) were performed to observe the films morphology and surface binding behavior of GaAs substrate after the film deposition procedure and metal-insulator-semiconductor structure cross section behavior. Electrical analysis such as C-V and I-V characteristics were used to discuss the capacitor properties.

Finally, in Chapter 5 gave the conclusion and suggestions of this thesis for the future work.

Properties@300K	Si	GaAs
Mobility ($cm^2/V \cdot s$)		
electrons	1450	8000
holes	500	400
Energy gap (eV)	1.12	1.43
Intrinsic resistivity (Ω-cm)	$3.3x10^5$	$2.9x10^8$

Fig.1-1 Advantage of GaAs substrate compared to general Si material.

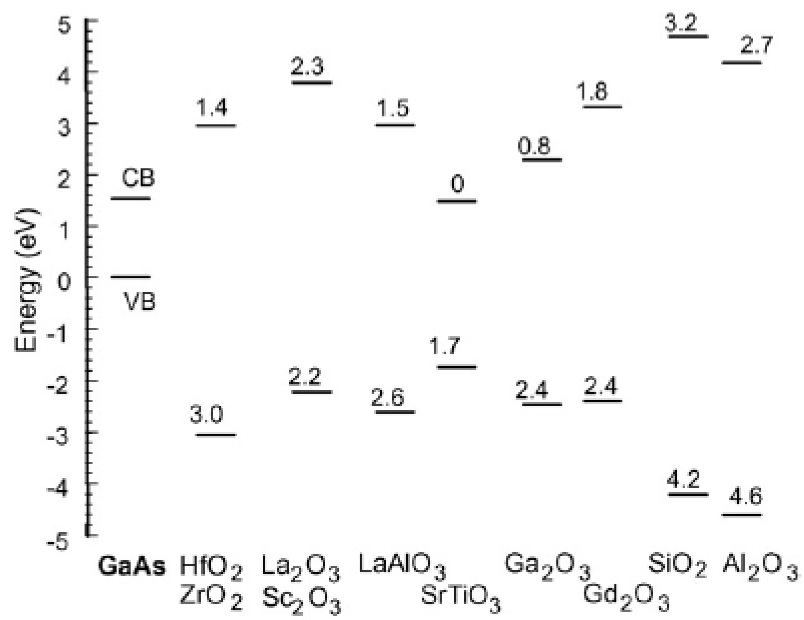

Fig.1-2 Predicted band offsets on GaAs with different high-k materials.

Chapter 2

The Cleaning Process of Gallium Arsenide Substrate

2-1 Introduction

The last two decades have seen growing importance places on research in Gallium Arsenide surface clean. Surface clean is the most important process in order to improve the device performance. Gallium Arsenide is easy to oxidize during the short time, and the native oxides description change with the acid or alkaline solution. In order to achieve the high-quality surface properties, the following conditions are: (1) metal and particle-free surface (2) the thin surface native oxide (3) flat surface morphology. For example of the mainstream silicon devices, surface terminated by silicon hydride are gaining popularity for the growth of gate oxide, which is used in the fabrication of deep submicron ultra-large integrated circuits. Accordingly, several different methods for GaAs surface cleaning have been reported. In the earlier stage, heating cleaning at high temperature can desorption the surface oxide [13]-[18], when the temperature is

above 200°C will is mainly gallium oxide whereas it is an arsenic-rich mixture of As and Ga oxides after the standard procedure [13]. The desorption temperature: (1) AsO_x: around 200 ^{o}C; (2) As element: around 350 ^{o}C; (3) GaO_x: around 500 ^{o}C [14]. Since volatile or unstable oxides are removed during the temperature ramp, it is only a Ga_2O_3-like oxide that remains on the surface above 500 ^{o}C. Menda et al provide an excellent review of the method and findings issues related to wet cleaning use [15]. In the thermal treatments at temperature higher than 570 ^{o}C, thermal facets are introduced on GaAs surface. It reported that the native oxide on the GaAs surface dipped in a HF solution can be removed in vacuum at 490 ^{o}C and this is arsenic-rich from their analysis. Alternative method of reduction of the density of protrusions on a cleaned GaAs surface by arsenic-free high-temperature surface cleaning was found decrease the temperature ramp-up rate of the thermal cleaning. Two-step-heating sequence in arsenic-free high-temperature surface method for two-dimensional electron gas transistor has increased about 50% electron mobility compared to

one-step heating [16]. The following is an instance of ion-cleaning, an undoped substrate after conventional thermal cleaning under an As_4 flux is smoother than that of a Si-doped substrate. The surface roughness of Si-doped was greatly improved by cleaning using hydrogen radicals(H・) at temperature of about 400 ^{o}C, the results indicate that the (H・) treatment of non-smooth substrate is useful for obtaining smooth and clean surface[17]-[18]. However, the above-mentioned cleanings were thermal heating method. The wet chemical cleaning results of this study could have considerable impact on passivation of surface behavior. The effective wet chemical cleaning process used NH_4OH mixture to remove particles and metals as a first step of wet-chemical cleaning and acidic peroxide mixture to remove residual metallic contaminants and control the components of oxide layer as a second step of wet-chemical cleaning [20]. Surface modification of GaAs during argon ionic cleaning and nitridation has reported [21]. During argon ionic bombardment, the values of FWHM of Ga3d peak and energy gap will vary, and nitridation process at substrate temperature equal to 500 ^{o}C: N_2

gas can due to a new contribution of Ga-N bonds in the XPS spectra. After cleaning with HCl or H_3PO_4, elemental As remained on GaAs surface , but elemental As is easily remove by NH_4OH cleaning [22].Unlike the silicon substrate was only one elemental in comparison to the binary of GaAs substrate. The study searched some wet chemical treatments, which were tested in our fabrication process, and sought for the optimized cleaning procedure for GaAs substrate.

2-2 Experimental Procedure

The experimental wafers were the n-type (Si doped) 2-inch GaAs(100), and the doped concentration is about 10^{18} cm^{-3}. Wet-cleaning method was the feasible cleaning method for the experiments. The samples were washed with deionized water (D.I.W) for 3min to remove the larger particles. In this work, we propose the following two procedure cleaning method. First, the HCl acid solution was capable stripper the native oxide and other contamination. After the

solution remove the native oxide, these wafers were washed with deionized water (D.I.W) for 3min to bear the residual oxide and Ca-Cl bond. And the NH_4OH alkali solution was used as cleaning and broad-spectrum way. After the solution, wafers were washed with deionized water (D.I.W) for 3min to remove cation. Eventually, all samples were dry with N_2 blowing, and the surface morphology was characterized immediately by atomic force Microscopy(AFM); surface chemistry was measure by X-ray Photoelectron spectroscopy (XPS).

2-3 Results and Discussion

2-3-1 XPS of cleaning GaAs substrate

In this study, by the use of X-ray photoelectron spectroscopy, the GaAs surface oxides accurately measure the binding energies associated with the 2p and 3d in the X-ray photoemission spectra. The X-ray photoelectron experiment was performed at the National Device Laboratory (NDL) in Hsinchu, Taiwan. The excitation was accomplished using a monochromatic Al Kα ration source(hν=1486.6eV). Fig. 2-1 shows the As 2p peak and As 3d peak spectra with different HCl solution [22]. In Fig.2-1(a) spectra, the substrate peak As(GaAs)

binding energy is assigned as 1322.7 ± 0.05eV; As-As metal peak signal is assigned as 1323.7 ± 0.05eV, which is spacing to As(GaAs) signal with 1eV and results from following equation:

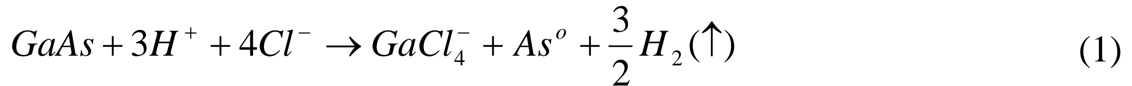

$$GaAs + 3H^+ + 4Cl^- \rightarrow GaCl_4^- + As^o + \frac{3}{2}H_2(\uparrow) \quad (1)$$

And then, 1325.7 ± 0.05eV for As_2O_3; 1326.5 ± 0.05eV for As_2O_5 [23]-[28], and the clean method of HCl/D.I.W.(10%) can reduce the arsenic oxide of GaAs compared to the method of HCl/D.I.W.(10%) or added H_2O_2 solution to diluted HCl solution. In Fig.2-1(b) spectra, the As 3d spectra also can see the oxide signal at high binding energies, the substrate peak As(GaAs) binding energy is assigned as 41.1 ± 0.05eV; As-As metal peak signal is assigned as 41.7 ± 0.05eV which spacing is similar to As 2p with 1eV; 44.5 ± 0.05eV for As_2O_3; 45 ± 0.05eV for As_2O_5. Two orbit spectra both can see the cleaning surface chemistry after HCl solution. Fig.2-2 is the Ga orbit spectra, and in Fig. 2-2(a) the GaAs substrate of Ga 3d spectra is assigned at Ga(GaAs):1117 ± 0.05eV;As opposed to arsenic metal, gallium metal was not easily to form; 1118 ± 0.05 for Ga_2O; 1119 ± 0.05eV for Ga_2O_3.The method of HCl/D.I.W.(1%) received the broader peak width compared to other method. In the Fig. 2-2(b), the Ga 3d also

indicate the same message, the gallium oxide peak is less than the method of HCl/D.I.W.(10%) solution. And the assigned peaks are described as follows: 19.2 ± 0.05eV for Ga(GaAs); 19.9 ± 0.05eV for Ga_2O ;21.05 ± 0.05eV for Ga_2O_3.To go a step further, finding the optimum concentration and cleaning cycle are described as follows. Fig. 2-3 shows the As 2p peak and Ga2p peak spectra with different HCl solution cycles. The concentration of 10% (HCl/D.I.W.) and 1% both had advantage of different orbit spectra. In the Fig.2-3(a) is the As 2p peak spectra, the concentration of 10% has resulted in As_2O_3 (~1326eV) component slightly less than another. On the contract, the concentration of 1% has caused Ga-O less than 10% solution shown in Fig.2-3(b). The fitting results of photoelectron spectra are shown in Fig. 2-4, and Table 2-1 is the ratio of component. Because of sensitivity (photo-ionization cross sections) to different elements, the ratio of arsenic to gallium is needed divide by 1.27(As2p3=27.2 / Ga2p3=21.4). After HCl solution with concentration of 10%, the GaAs surface is arsenic oxide-rich and the ratio percentage is 165%. It also remains As elemental, the percentage of As element over total arsenic signal was 14%. The As element easily reacted with oxygen compared to Ga elemental, and the arsenic oxides were unstable during thermal process [29]. Table 2-2 and Table 2-3 are the fitting results of the GaAs

component from photoelectron As 2p and Ga 2p spectra. The Equation (2) is the arsenic oxides reaction equilibrium equation. The arsenic oxide desorbs at around 200°C, and the other for As element at around 350 °C. On the contrast, Ga oxide (Ga_2O) starts to desorb at around 500 °C, and the volatile Ga_2O is result from Eq.(3). The Ga_2O_3 remains on the surface above 500 °C, and it has advantage of thermal stability [14].

$$As_2O_3 + 2GaAs \rightarrow Ga_2O_3 + 2As_2 (or As_4 \uparrow) \quad (2)$$

$$Ga_2O_3 + 4GaAs \rightarrow 3Ga_2O \uparrow + 2As_2 (or As_4 \uparrow) \quad (3)$$

Fig. 2-5 and Table 2-4 illustrate improvement experiments, by adding NH_4OH solution after HCl solution cleaning [22]、[30]. Three ammonia conditions were NH_4OH/D.I.W.(1%,RT) 、 NH_4OH/D.I.W.(10%,RT) and NH_4OH/D.I.W. (10%,80°C), respectively. The As element over total arsenic signal ratio really is reduced because of As elemental is dissolved in NH_4OH solution, and arsenic oxide over gallium oxide ratio also had decreased. The better conditions of ammonia solution are 1% and 10% at room temperature. Fig. 2-6 shows the arsenic compound ratio with different NH_4OH method, and the fewer As element and arsenic oxide are in the 1% & 10% NH_4OH etching solution,

respectively.

2-3-2 Surface morphology of cleaning GaAs substrate

Fig. 2-7(a) shows the surface of n-type GaAs substrate after cleaning of diluted HCl / D.I.W. etching solution with concentration of 10%. After HCl solution cleaning, the wafer was washed by D.I.W. for three minutes because the Ga-Cl bond is highly soluble in the water [22].The As element appearance had discuss in chapter 1. Fig. 2-7 (b) shows the surface roughness of n-type GaAs substrate after cleaning of diluted HCl/D.I.W.(10%) and NH_4OH/D.I.W.(1%) , and D.I.W. was used after each step cleaning. It is known that the NH_4OH cleaning leads to the obvious decrease of As elemental component, and the surface roughness of NH_4OH-cleaned GaAs was flatter. The surface roughness also slightly results from As element. In the Fig. 2-7(c), only one etching solution of NH_4OH/ D.I.W.(1%) was used in the n-type GaAs substrate. The surface roughness is the same as two-step clean method. As shown in the Fig. 2-8, the GaAs surface roughness cleaned by different methods are between 0.354nm to.266 nm.

2-4 Summary

In this chapter, the suitable HCl and NH_4OH solution both effectively clean GaAs substrate. These physical properties can be of enormous value to GaAs device. Finally, the optimum condition for HCl/D.I.W. solution is 10% at room temperature, effectively remove surface native oxide; the solution of NH_4OH/D.I.W.is 1% at room temperature, which remove As elemental and arsenic oxide/gallium oxide ratio equal to one. If next chapter 3, we can use the cleaning method to develop surface treatment by sulfur solution, and the sulfur passivation can improve the interface density (D_{it}) of high-k film on GaAs substrate. The improved interface density can solve the Fermi level pinning, and the unpinned metal-oxide-semiconductor will come true.

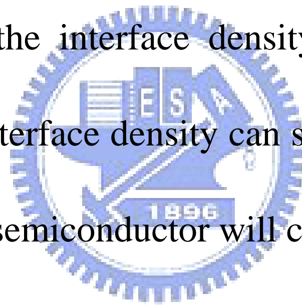

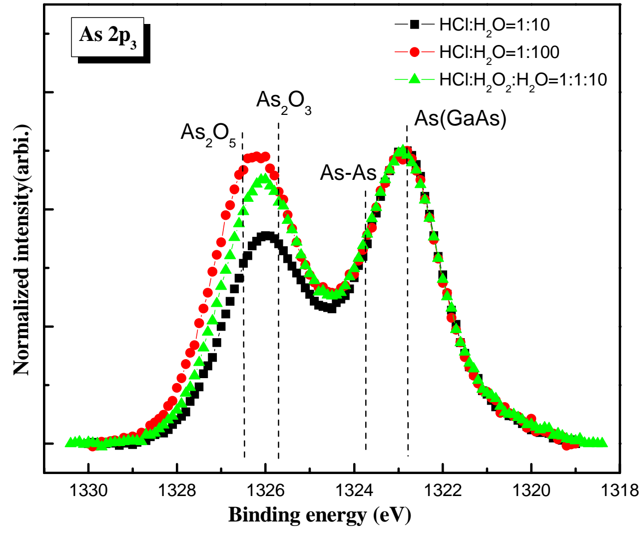

(a)

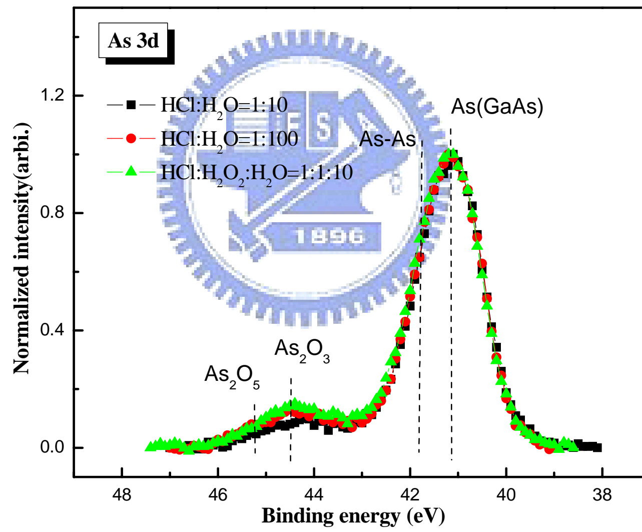

(b)

Fig. 2-1 (a) As 2p and (b) As 3d core-level spectra with different diluted HCl concentration.

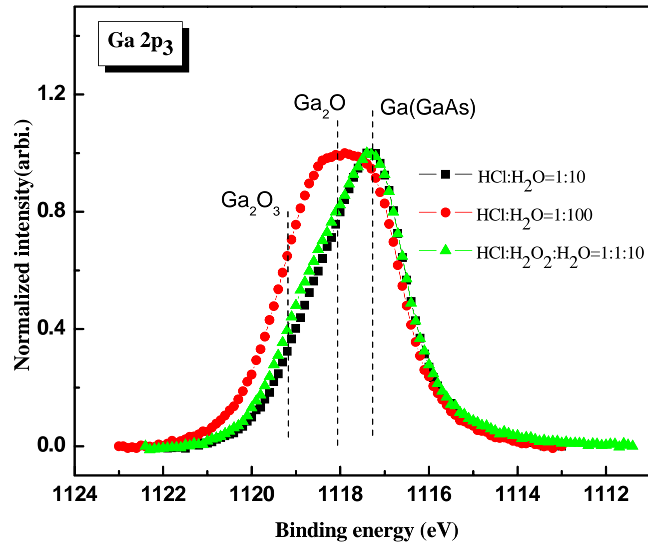

(a)

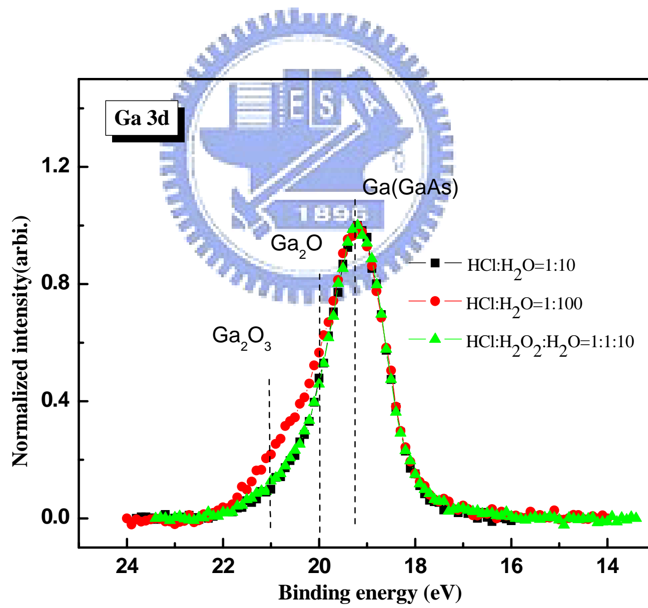

(b)

Fig. 2-2 (a) Ga 2p and (b) Ga 3d core-level spectra after different diluted HCl concentration.

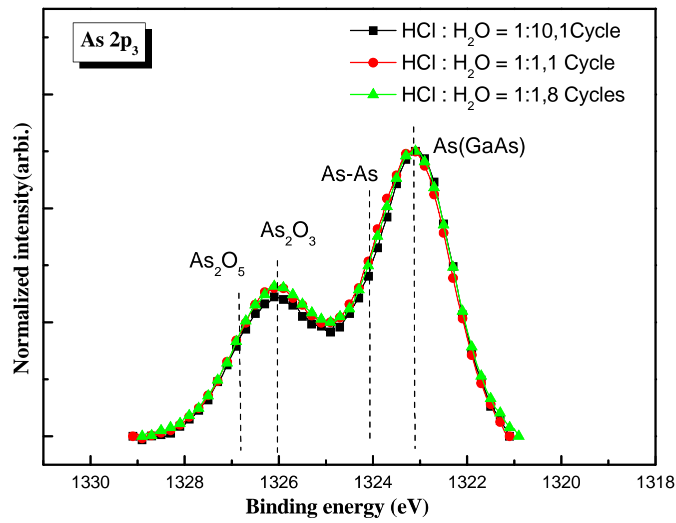

(a)

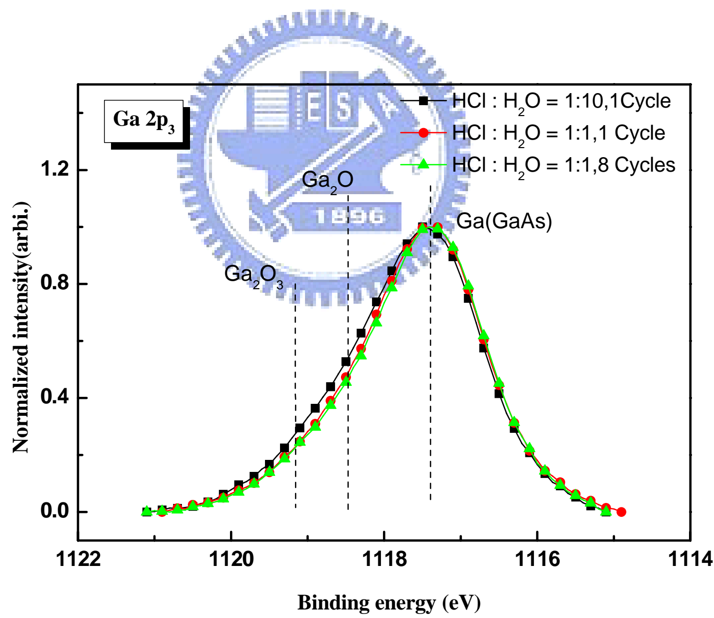

(b)

Fig. 2-3 (a) As 2p and (b) Ga 2p core-level spectra after different diluted HCl concentration and cleaned cycles.

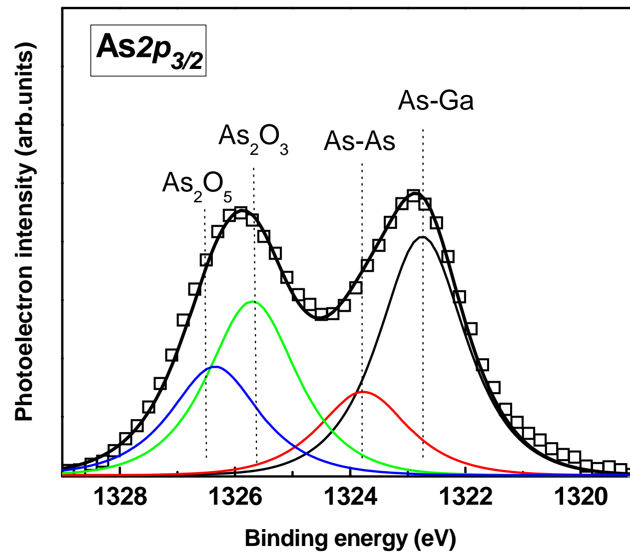

(a)

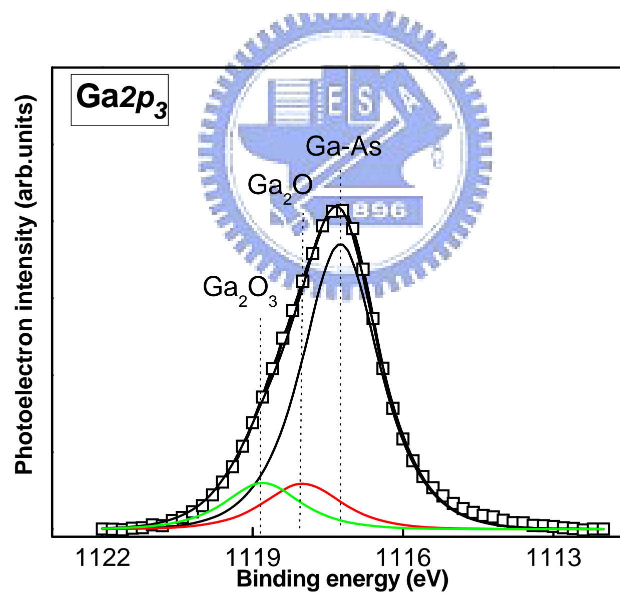

(b)

Fig. 2-4 The fitting result of (a) As 2p and (b) Ga 2p core-level spectra after diluted HCl concentration.

Clean process	As_{oxide} / Ga_{oxide}	$As_{substrate}$ / $Ga_{substrate}$	As_{total} / Ga_{total}	As^{O} / As_{total}
$HCl:H_2O$=1:10	165%	37%	84%	14%

Table 2-1 The fitting results of the GaAs component from photoelectron spectra.

	Position (eV)	FWHM (eV)	Area	%Lorentzian - Gaussian(0:G,100:L)
As (GaAs)	1322.75	1.75	419939.8	75
As-As	1323.77	1.8	150880.7	75
As_2O_3	1325.7	1.8	314532.4	70
AS_2O_5	1326.35	1.8	199913.2	80

Table 2-2 The fitting results of the GaAs component from photoelectron As 2p spectum .

	Position (eV)	FWHM (eV)	Area	%Lorentzian-Gaussian(0:G,100:L)
Ga (GaAs)	1117.25	1.8	780783.4	74
Ga_2O	1118	1.8	122867.4	70
Ga_2O_3	1118.5	1.75	123057.4	75

Table 2-3 The fitting results of the GaAs component from photoelectron Ga 2p spectum .

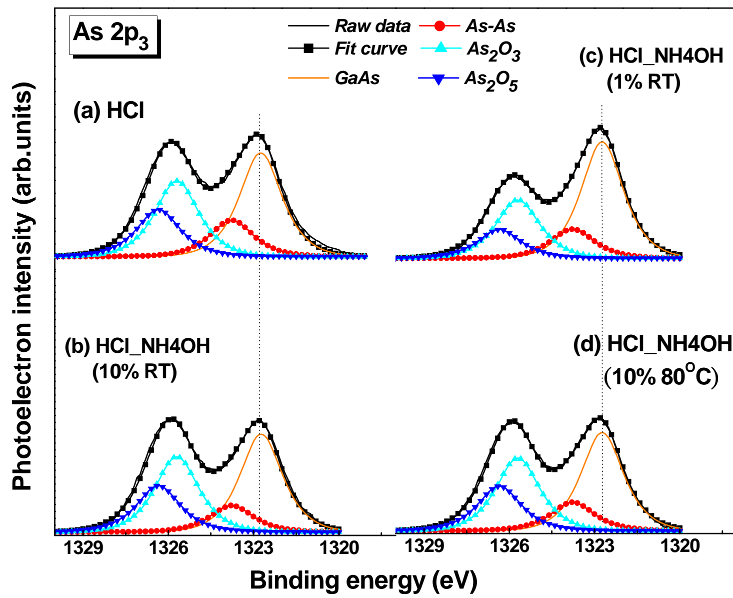

Fig. 2-5 The fitting results of As 2p core-level spectra with diluted HCl solution following by different NH_4OH solutions.

Clean process	As_{oxide}/ Ga_{oxide}	$As_{substrate}$/ $Ga_{substrate}$	As^{O} / As_{total}	As_{total}/ Ga_{total}
HCl Clean	165%	37%	14%	84%
HCl+NH4OH(10%,RT)	102.3%	36.6%	10.8%	64.2%
HCl+NH4OH(1%,RT)	94%	38.6%	12.7%	59.4%
HCl+NH4OH(10%,80oC)	124.1%	33.1%	12%	63.3%

Table 2-4 The ratio of GaAs component with diluted HCl solution following by different NH_4OH solutions.

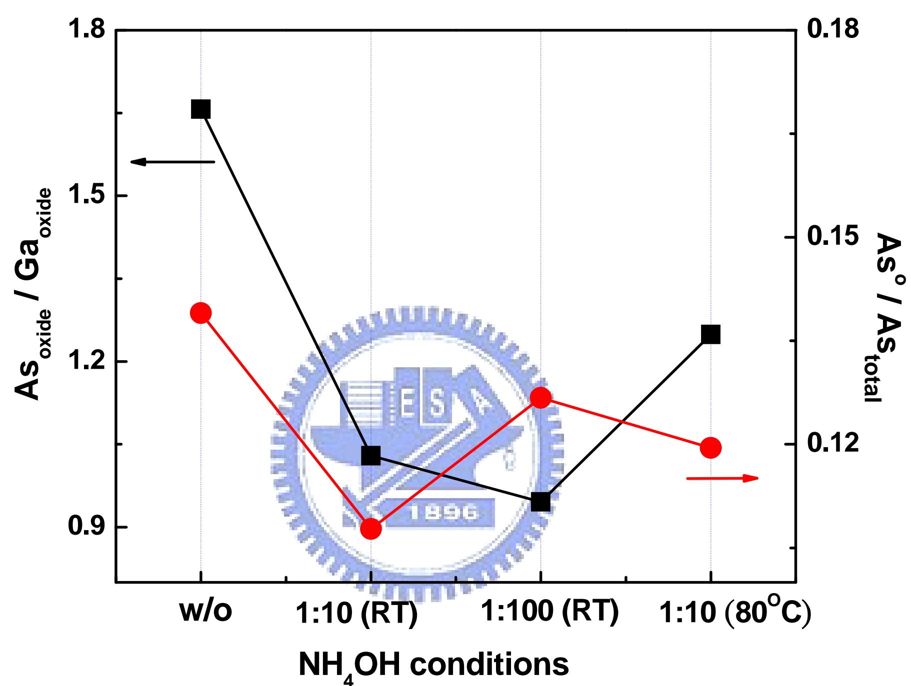

Fig. 2-6 The arsenic compound ratio with diluted HCl solution following by different NH_4OH solutions.

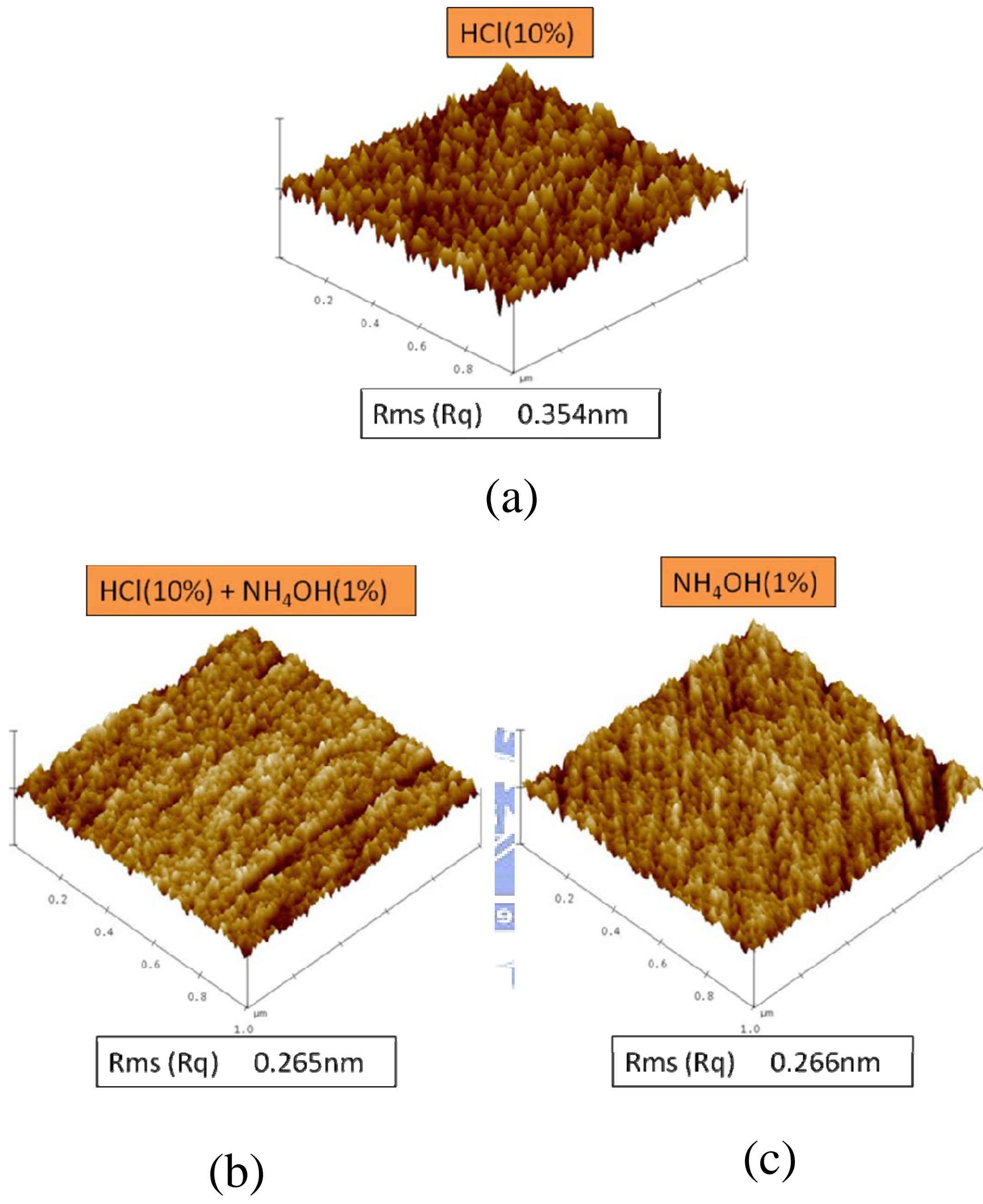

Fig. 2-7 AFM image of cleaned GaAs substrate with different clean methods: (a) HCl (b) HCl+NH_4OH (c) NH_4OH.

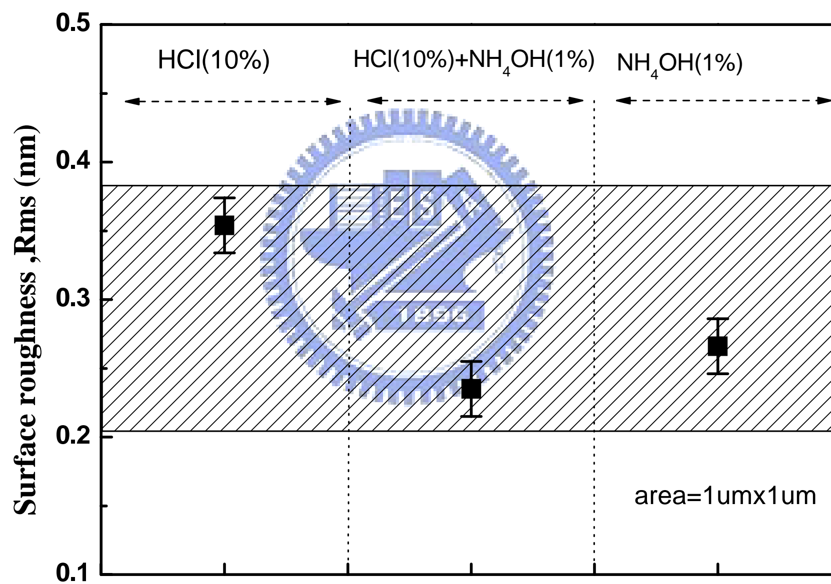

Fig. 2-8 Surface roughness of cleaned GaAs substrate with different clean methods: (a) HCl (b) HCl+NH_4OH (c) NH_4OH.

Chapter 3

The Sulfur Passivation on Gallium Arsenide Substrate

3-1 Introduction

It is well known that the high density of surface states and difficult task of passivating them have been responsible for the slow development of GaAs MIS technology and other small geometry devices such as GaAs MESFETs, HBTs and HEMTs. Therefore, extensive effort has been expended over the past two decade to passivate the GaAs surface to realize GaAs MIS capacitors and MISFETs [31]-[45]. Among them, the sulfur chemical treatment of GaAs surface has received considerable attention because of its simplicity and suitability for commercial exploitation. Thus, even though a number of sulfur compounds such as $Na_2S \cdot 9H_2O$ [31]- [36] and $(NH_4)_2S$ [34]-[45]. In 1987, Sandroff was the first man to passivating the GaAs by sulfur using room-temperature Photoluminescence(PL) and low-temperature PL spectroscopy [31]. This can be attributed to the formation of native oxide on GaAs surface. It has been found that with the decrease in the solvent dielectric constant , in such solution the surface sulfur coverage increases , the thickness of the native oxide layer decreases, and the efficiency of band-edge

photoluminescence will increases [36]-[38]. The thermal stability of Ga-S bond is better than As-S bond. Annealing experimental show that As-S chemical bonds were broken at a relatively low temperature, approximately 200°C-300°C, whereas desorption of sulfur from the surface, through breaking of Ga-S bonds, occurs above 500 ^{o}C. At 500 ^{o}C-600 ^{o}C, only Ga-S remained stable, and the increasing density of sulfur from As to Ga atoms[39]-[44].Compared to the conventional basic $(NH_4)_2S$ solution treatment, a thick Ga sulfur layer and Ga-S bond were formed on the GaAs surface after dipping GaAs in the neutralized $(NH_4)_2S$ solution [45].

3-2 Experimental Procedure

The cleaning GaAs samples resulted from HCl and NH_4OH-based solution were immersed in sulfur solution for 1minute. Before immersing in sulfur solution, we dry the samples with N_2 gas blowing to remove the excess surface moisture. This blowing can assure fewer effects during interface reaction between sulfur and semiconductor. We treat the cleaned samples with alcohol and deionized water-based sulfur-solvent solution, and adjust the sulfur concentration and temperature ramped from RT to 80°C by hot-plate machine to obtain the higher passivation efficiency. After sulfur passivation, we washed deionized water for 3minute to remove away the excess sulfur bond. Finally, dry the samples with N_2 gas to blow excess moisture. The sulfided samples immediately were measured by X-ray Photoelectron Spectroscopy(XPS) and atomic force Microscopy(AFM) to get the surface chemistry and morphology .The electrical properties of sulfided samples were fabricated as metal-semiconductor device to calculate the Schottky barrier height, and we discuss passivation effect on barrier height. The gate electrode was 500nm Al deposited through a shadow mask to form a top electrode on the topside. The backside was 30nm indium(In) layer for ohmic contact and follow by 20nm platinum(Pt) layer for fast electric conductivity and protection. After backside

contact deposition, hot-plate with 90 ^{o}C and 10min was used to repair metal quality. A precision impedance meter of HP4284 was used for *C*-*V* measurement, and a semiconductor parameter analyzer of Keithley 4200 was used for *I*-*V* measurement.

3-3 Results and Discussion

3-3-1 XPS and PL of the sulfided GaAs substrate

The surface treatment of GaAs in sulfur solution results in a dramatic decrease surface state density in the middle of the band gap. Reduction of surface recombination velocity enables an improvement in the performance and reliability of many devices. For the beginning, three sulfur passivation methods were used to increase the efficiency on HCl-cleaned GaAs substrate, which was shown in the Figure 3-1.

First, Sodium sulfide is the salt of a strong base and a week acid, after its dissolution in D.I.W.:

$$Na_2S + H_2O \rightleftharpoons 2Na^+ + HS^- + OH^- \quad (1)$$

Second, Ammonium sulfide is the salt of a week base and a weak acid. In the D.I.W. reaction occurs:

$$2NH_4^+ + S^{2-} \rightleftharpoons NH_3 + NH_4^+ + HS^- \rightleftharpoons 2NH_3 + H_2S \quad (2)$$

Both above sulfur coat formation can occur either by reaction (3) [37].

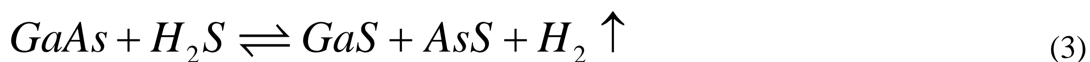

$$GaAs + H_2S \rightleftharpoons GaS + AsS + H_2 \uparrow \quad (3)$$

Finally, the organic twelve-carbon thiol with long-chain molecule type was used. The molecule was sulfur-terminated molecule which can be bonded with gallium or arsenic element of substrate. Fig. 3-1 shows the set of (a) As 2p and (b) Ga 2p core-level spectra after three sulfide treatment. The substrate peaks were normalized to the same height and substrate signals shifted to the same binding energy which was As(GaAs):1323 $\pm$ 0.5eV; Ga(GaAs):1117.5 $\pm$ 0.5eV. This study has taken a step in the direction of defining the relationship between sulfur and GaAs surface passivation in order to suppress the oxides. The sulfur signal also can be seen from the S 2p orbit spectra, as shown in the Fig. 3-2, and Fig. 3-2(a) points out the sulfur peak, which is overlap with Ga 3s peak, and the spacing about 1.1eV. Fig.3-2 (b) is the subtraction of S 2p and Ga 3s orbit, and we can subtract Ga 2s peak of no-sulfided sample from S 2p peak of sulfided one. The S 2p orbit can see the sulfur peak signal, but we don't like to use this indirect way. The suppression of sulfided samples after 1week compared to no-sulfided one is shown in Fig. 3-3. Clearly, the sulfided sample can decrease the growth rate compared to no-sulfided one. Hence, the sulfur passivation for GaAs substrate is useful and further research is required. There are two sulfur methods with PL analysis as shown in Fig. 3-4 and Fig. 3-5. The Fig. 3-4(a) is the Photoluminescence(PL) intensity treated by $(NH_4)_2S$/D.I.W.

liquid. It shows that sulfided temperature increasing the PL intensity before 400 ^{o}C, and it decreases at 500 ^{o}C. This is because arsenic bonds fully broke before 400 ^{o}C, and Ga compound bonds began to desorb. Then, the solvent effect was replaced with C_3H_7OH solution, whose results were shown in Fig.3-4(b). When anneal at 400°C and highest concentration with 10% will obtain the highest PL intensity. The highest PL intensity cause may be the more sulfur bond coverage. The Fig. 3-5 is the Photoluminescence(PL) intensity treated by Na_2S/D.I.W. liquid . Fig. 3-5(a) shows that sulfided temperature increasing the PL intensity at 400°C, and it decrease at 500 ^{o}C. Then, the solvent was chosen with C_3H_7OH solution, whose results were shown in Fig.3-5(b). When the PDA anneal at 400 ^{o}C, highest concentration with 2.5% will increase PL intensity.

Fig. 3-6(a) and (b) illustrate XPS spectra of the sulfide temperature effect. When the temperature is increasing, the Ga-S bonds will increase and As-S bonds decrease. This is because that thermal stability of Ga-S bonds is better than As-S bonds. Fig.3-7 shows different ratio of GaAs surface signal, and we divide into five parts: (i) As element (ii) As-S (iii) Ga-S (iv) As-O (v) Ga-O. After sulfidation, the As element decrease from 13.9% to 3.5%, and oxides decrease one half at least. About sulfur composition, the high sulfided temperature causes the Ga-S bonds increasing compared to As-S bonds

decreasing. Fig.3-8 (a) and (b) are spectra of GaAs with two sulfur concentration, we believe that sulfur really suppresses the GaAs oxide under $80^{o}C$ passivation solution. Fig. 3-9 (a) and (b) are sulfur concentration at Ga orbit spectra. They also show the same behavior compared to Fig. 3-8. In the Fig. 3-10(a) and (b), we discuss the alkaline NH_4OH solution effect combining with sulfur passivation on the GaAs surface. From the Fig. 3-10 (a), we find the As element peak magnitude of (i) and (ii) are different. With NH_4OH solution cleaned, the As element component will decrease, because of As(OH) bonds can remove easily compared to Ga(OH) bonds. When sulfided temperature increase, the As-O and As element both expressed decreasing behavior. Fig. 3-10 (b) is the Ga 2p spectrum, we find that the Ga-S peak increase with $80^{o}C$ sulfur temperature compared to RT treatment. The Ga element likes to react with sulfur solution at high temperature. Simply stated, the NH_4OH solution etching can reduce As compound bonds and get a Ga-termined surface .Fig. 3-11 shows different ratio of GaAs surface signal, and we divide into five parts: (i) As element (ii) As-S (iii) Ga-S (iv) As-O (v) Ga-O. After NH_4OH and sulfur solution, the As element decrease from 9.6% to 4.7%, and oxides also decrease. About sulfur composition, the high sulfide temperature cause the Ga-S bonds increase .On the other hand, As-S bonds decrease with high sulfided

temperature.

3-3-2 surface roughness of the sulfided GaAs

Fig. 3-12 shows the variation of surface roughness of GaAs after the cleaning of diluted HCl/D.I.W. (10%) etching solution with three sulfide conditions of (a) without (b) 1%, RT (c) 1%, 80°C.The surface roughness decrease as sulfide temperature increase from 0.354nm to 0.237nm. Fig. 3-13 shows the variation of surface roughness of GaAs after the cleaning of diluted HCl/D.I.W.(10%) and NH_4OH/D.I.W.(1%) etching solution with two sulfide conditions of (a) without (b) 1%, 80°C. The surface roughness ranges from 0.265nm to 0.235nm. Fig. 3-14 shows the variation of surface roughness of GaAs after the cleaning of diluted NH_4OH/D.I.W.(1%) etching solution with two sulfide conditions of (a) without (b) 1%, 80°C. The surface roughness ranges from 0.266nm to 0.245nm. All the variation of surface roughness after different treatment is summarized in Fig.3-15, and the GaAs surface roughness is smooth with different surface treatment.

3-3-2 electrical characterization of the sulfided GaAs

In Fig. 3-16, we treatment the HCl cleaned GaAs substrate with two sulfur solutions combined with three solvents. The curves were measured at room temperature, and we find that the I-V curves depend on surface treatment. As displayed in Fig. 3-17 was the extraction of Schottky barrier height(SBH) by following equation:

$$J=J_s(1-e^{-qV/nkT}) \quad (1)$$

Where $J_s = A^*T^2 e^{-q\Phi_B/kT}$, A^* is the Richardson constant; n is the ideal factor; Φ_B is the barrier height. Fig. 3-18 and 3-19 show the variation of barrier height with different sulfide treatment. Because that the ideal barrier height difference of Al metal contact to n-GaAs substrate is about 0.4 eV, and the barrier height of sulfided GaAs is smaller than no-sulfidation one. From the Fig. 3-19, the barrier height decreased with decreasing dielectric constant of solvent solution. This is because that efficiency for different solvents solution. Fig. 3-20 shows I-V curves difference before and after sulfidation, and we find that original Schottky-like diode curve has change to ohmic-like curve.

3-4 Summary

After sulfur passivation, the GaAs surface elements bond with sulfur element. The formation of As-S or Ga-S bond depends on clean method and sulfided temperature. The HCl etching solution remains the As-terminated surface, but NH_4OH remains the Ga-terminated surface. We can use the sulfided temperature to mathch with GaAs surface element. Because of thermal stability for As-S bonds are worse better than Ga-S bonds. We need to increase the sulfided temperature up to 80^oC, and Ga-S bonds remain stable. The Schottky barrier height (SBH) can be changed to ideal-like value by sulfidation, especially in solvent solution.

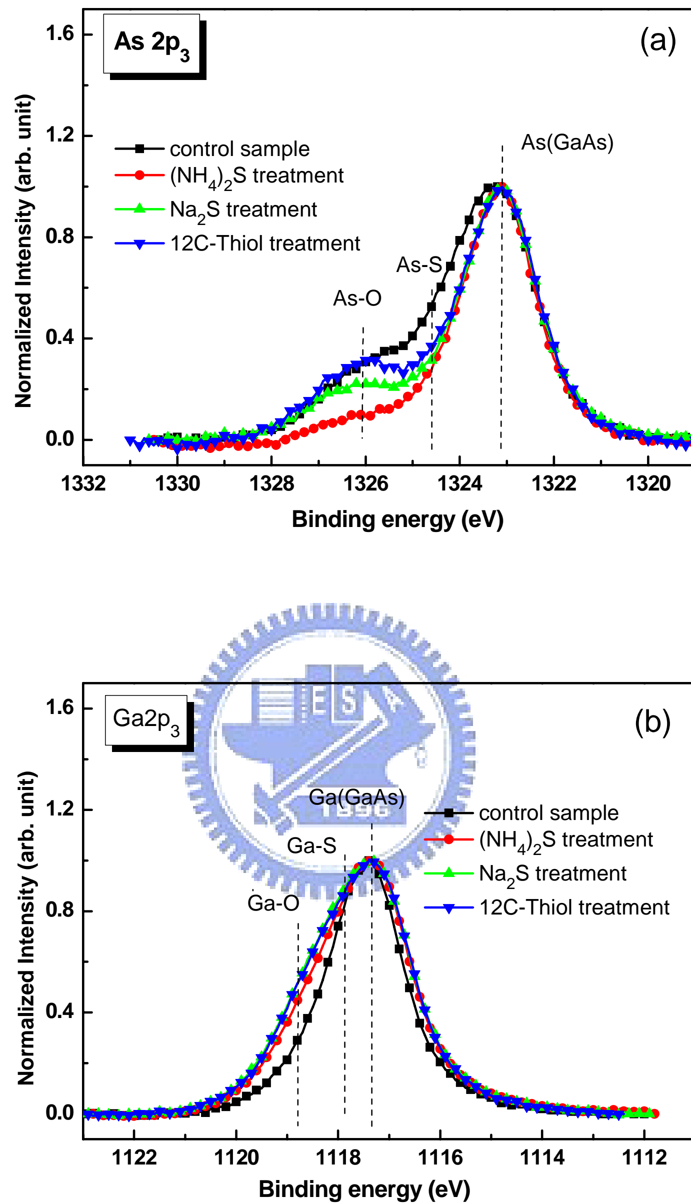

Fig. 3-1 (a) As 2p and (b) Ga 2p core-level spectra after different sulfide methods.

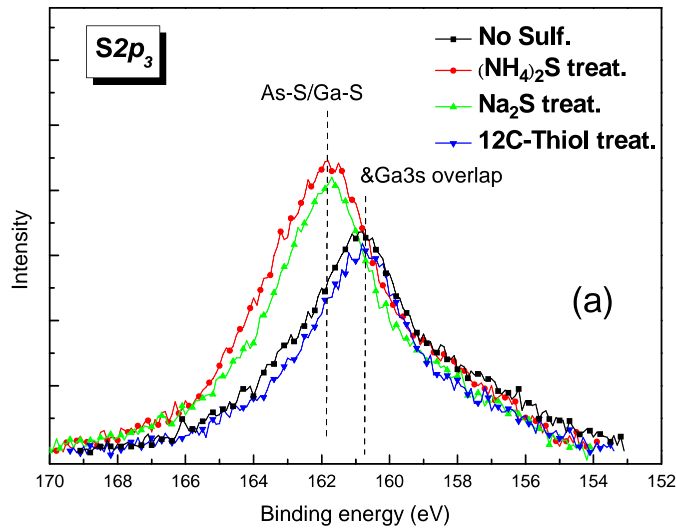

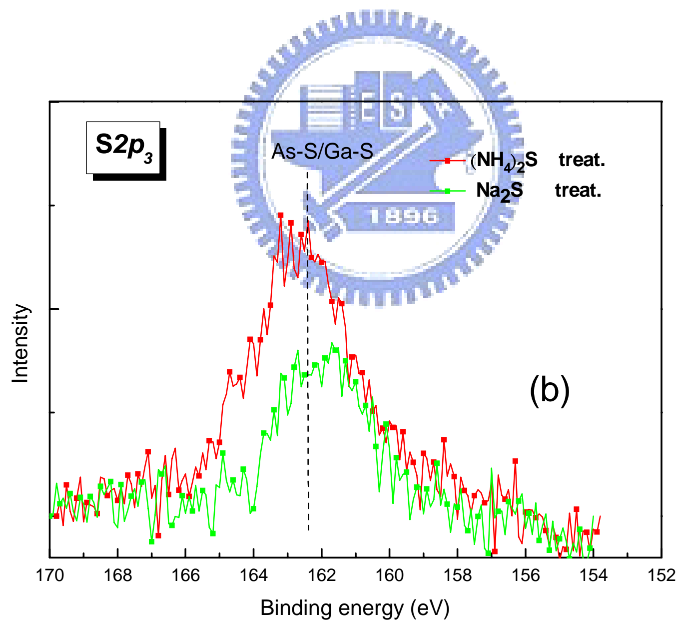

Fig. 3-2 (a) S 2p spectra by three sulfur passivation before subtraction and (b) after subtraction Ga 2s peak from S 2p peak.

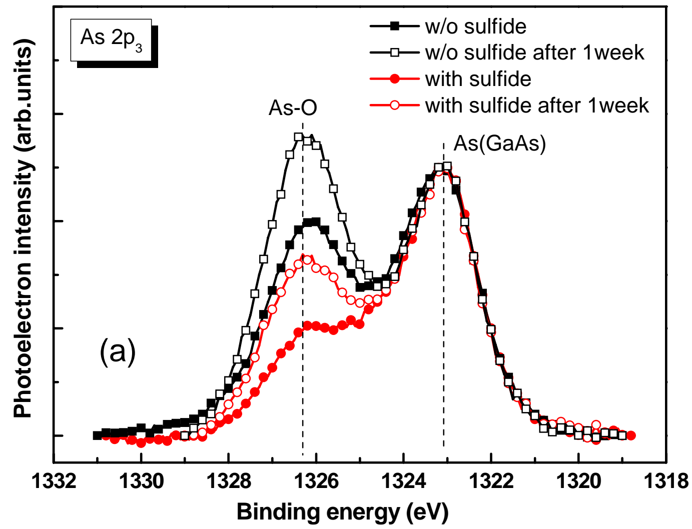

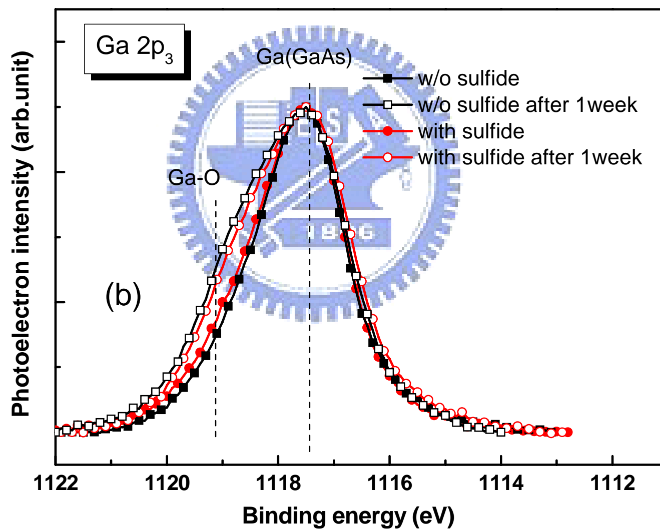

Fig. 3-3 (a) As 2p and (b) Ga 2p core-level spectra of the sulfided samples against moisture with spectra after 1week .

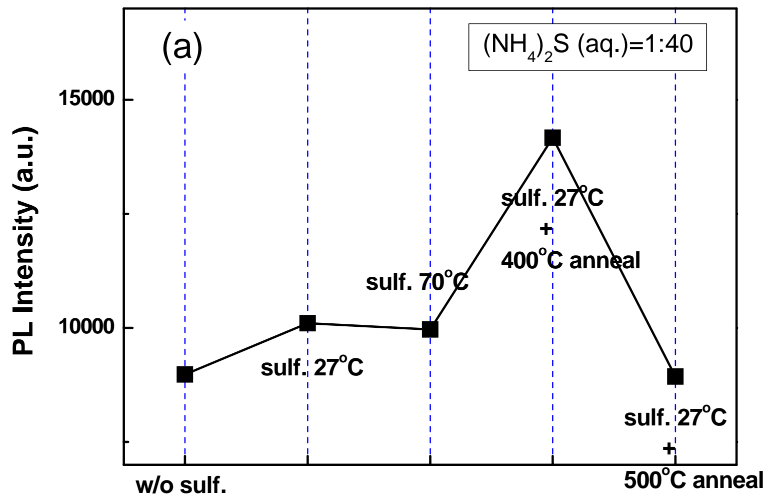

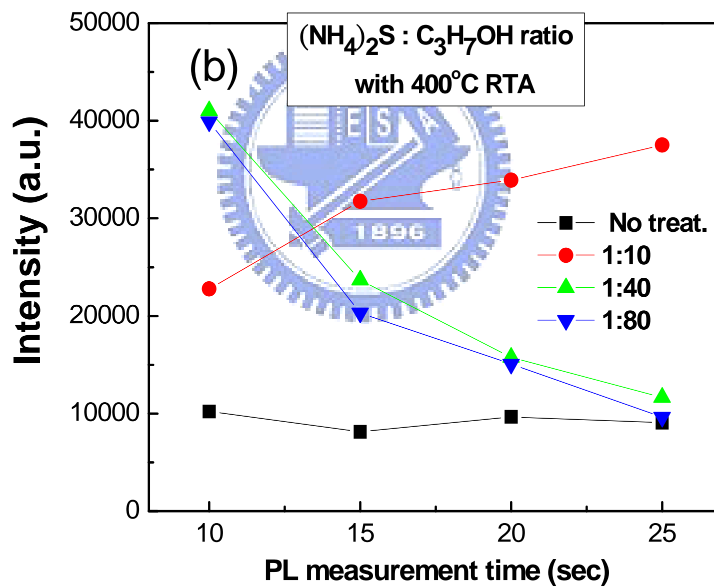

Fig. 3-4 Photoluminance of Gd_2O_3/ GaAs sulfided by $(NH_4)_2S$ solution with different (a) temperature and (b) concentration.

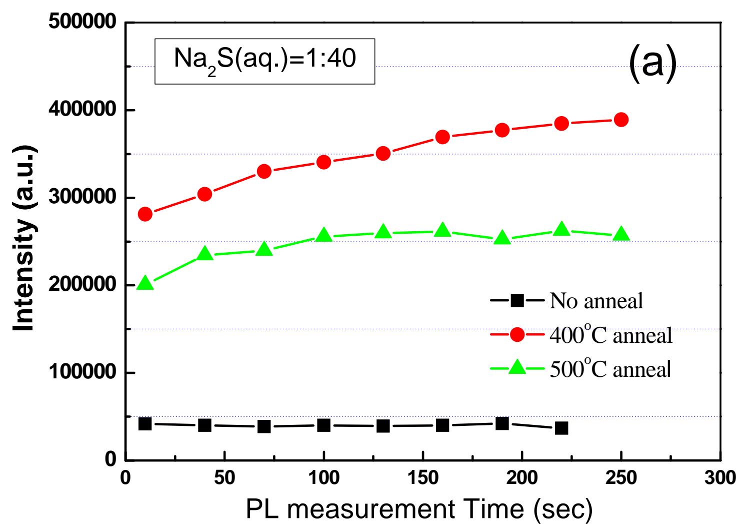

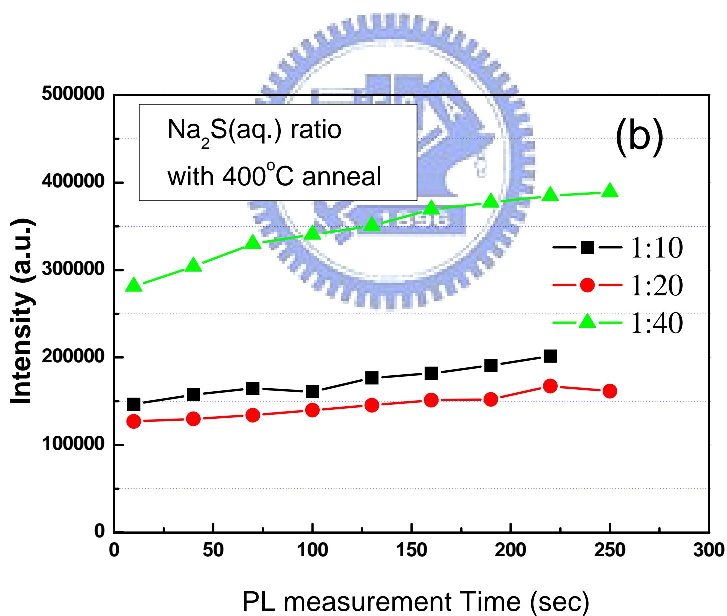

Fig. 3-5 Photoluminance of Gd_2O_3/ GaAs sulfided by Na_2S solution with different (a) temperature and (b) concentration.

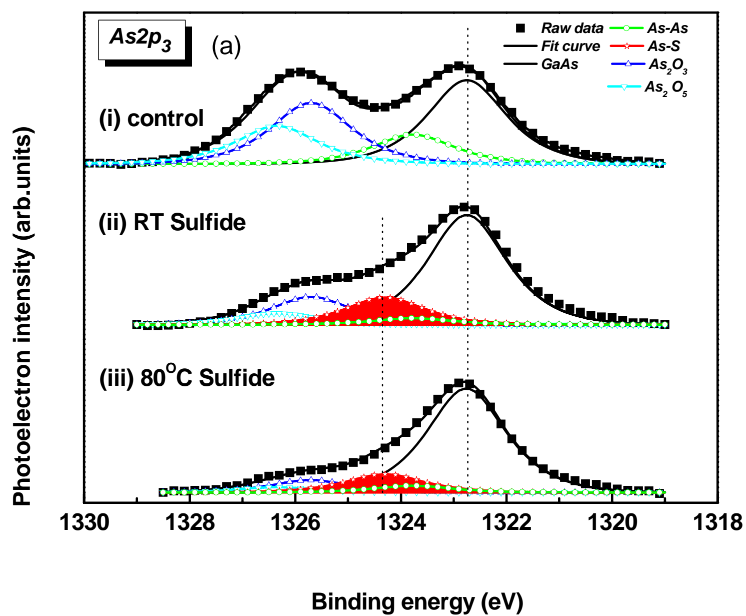

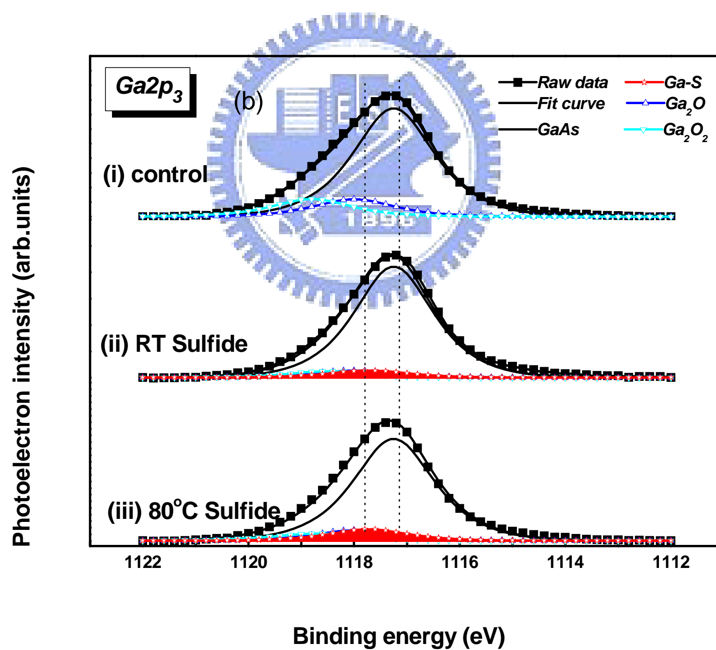

Fig. 3-6 (a) As 2p (b) Ga 2p core-level spectra of sulfided GaAs at various treatment temperature: (i) without sulfide (ii) sulfide at room temperature (iii) sulfide at 50°C (iv) sulfide at 80°C.

Wet Clean	As-As As_{Total}	As-S As_{Total} Ga-S Ga_{Total}	As_2O_x/As_{Total} Ga_2O_x Ga_{Total}
HCl	13.9%	-- --	47.4% 24%
HCl+Sulf.(RT)	3.5%	14.9% 5.5%	21.4% 13%
HCl+Sulf.(80°C)	4.6%	12.4% 8.4%	12.1% 14.1%

Fig. 3-7 GaAs component ratio of the HCl cleaned with two sulfide temperature.

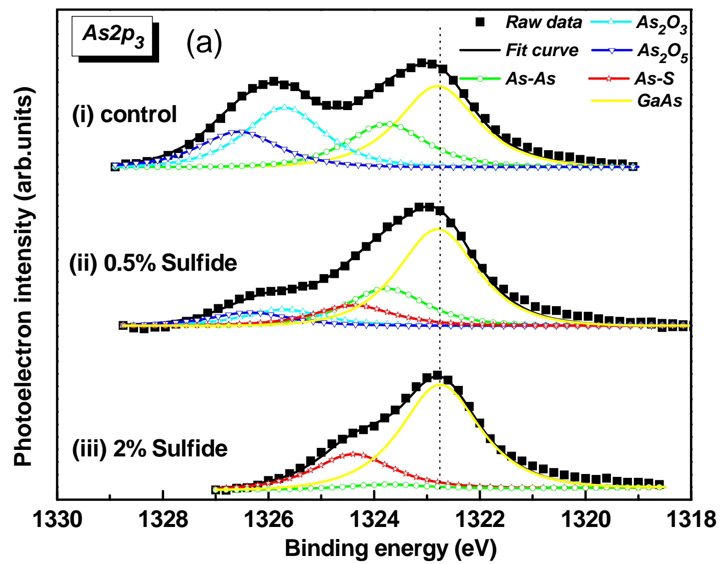

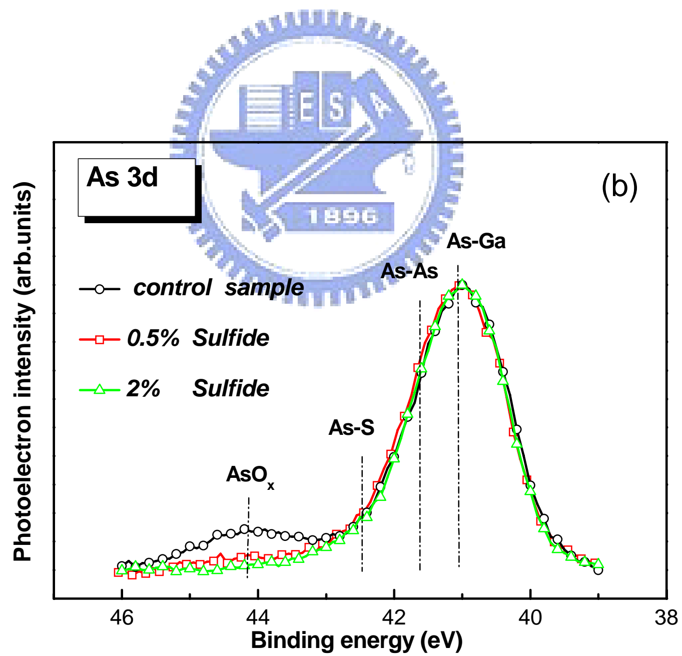

Fig. 3-8 (a) As 2p and (b) As 3d spectra of GaAs after two sulfur concentration: (i) cleaned (ii) sulfide at 0.5% concentration (iii) sulfide at 2% concentration.

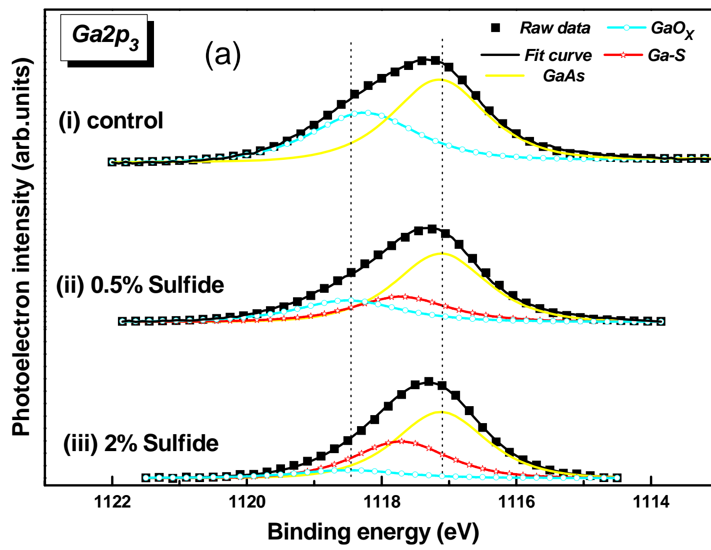

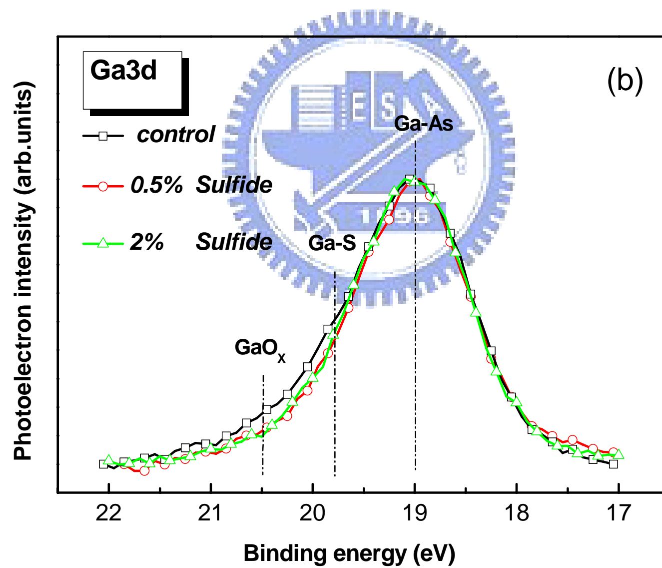

Fig. 3-9 (a) Ga 2p and (b) Ga 3d spectra of GaAs after two sulfur concentration: (i) cleaned (ii) sulfide at 0.5% concentration (iii) sulfide at 2% concentration.

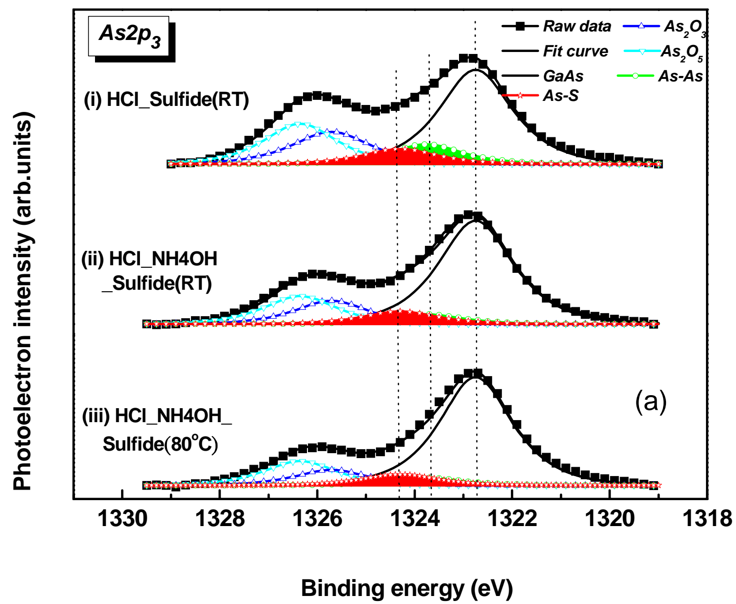

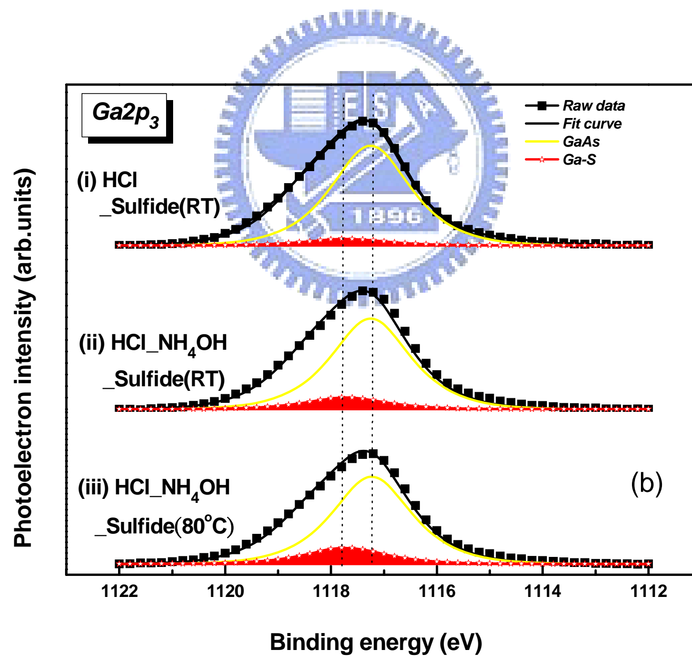

Fig.3-10 (a) As 2p and (b) Ga 2p core level spectra after HCl+NH_4OH solution with two sulfided temperature.

Wet Clean	As-As/As_{Total}	As-S/As_{Total}	Ga-S/Ga_{Total}	As_2O_x/As_{Total}	Ga_2O_x/Ga_{Total}
HCl+Sulf.(RT)	9.6%	7.3%	4.3%	36.4%	30.1%
HCl+NH_4OH+Sulf.(RT)	5.5%	7.1%	8.3%	28.1%	28%
HCl+NH_4OH+Sulf.(80°C)	4.7%	6.4%	11.9%	23.6%	23.8%

Fig. 3-11 GaAs component ratio of the HCl、NH_4OH solutions cleaned with two sulfide temperature.

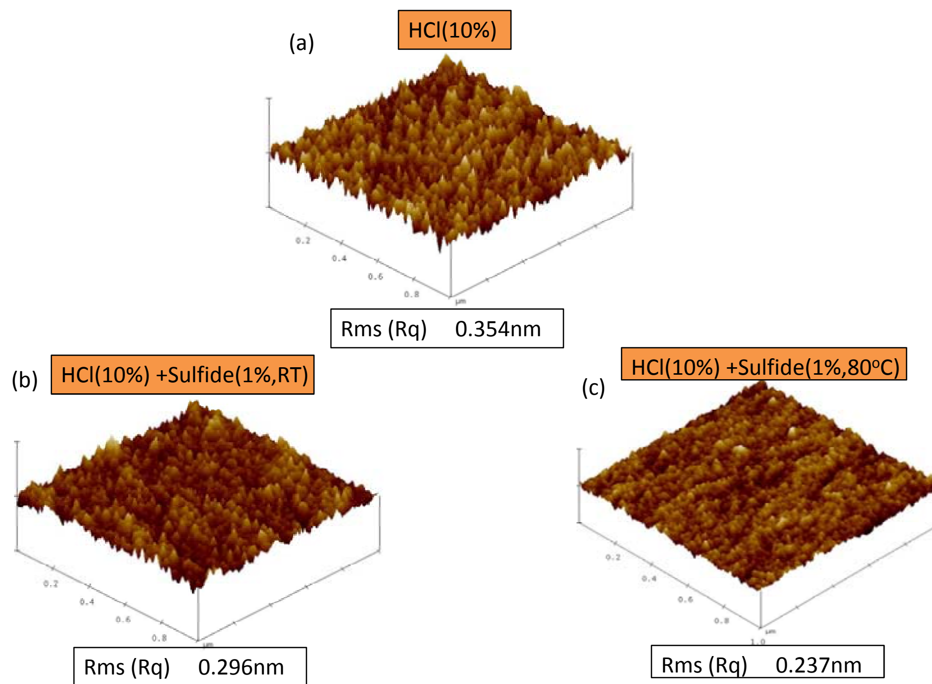

Fig. 3-12 Surface morphology of HCl cleaned GaAs substrate after different sulfide condition: (a) without sulfidation (b) 1%, RT (c) 1%, 80°C.

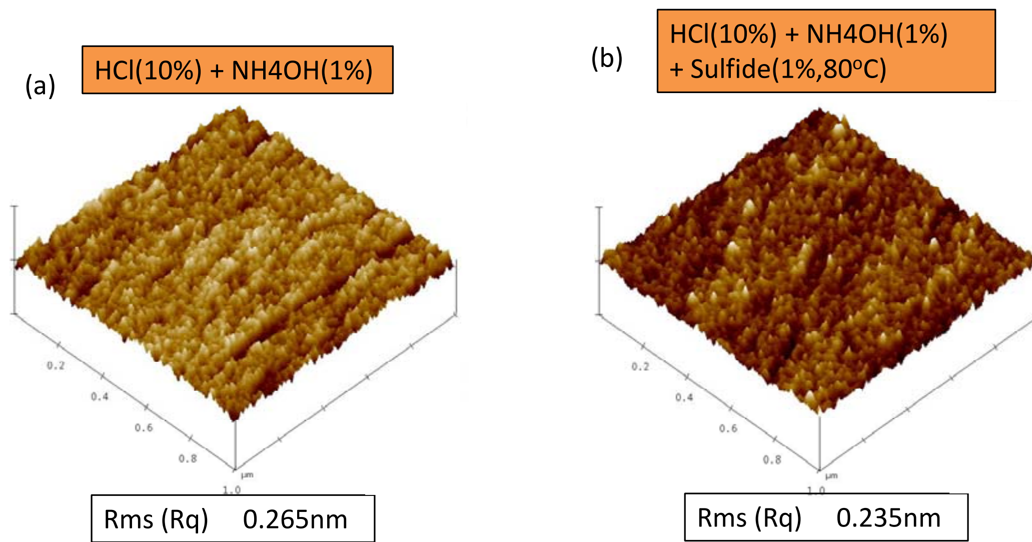

Fig. 3-13 Surface morphology of HCl +NH_4OH cleaned GaAs substrate after different sulfide condition: (a) without sulfidation (b) 1%, 80^oC.

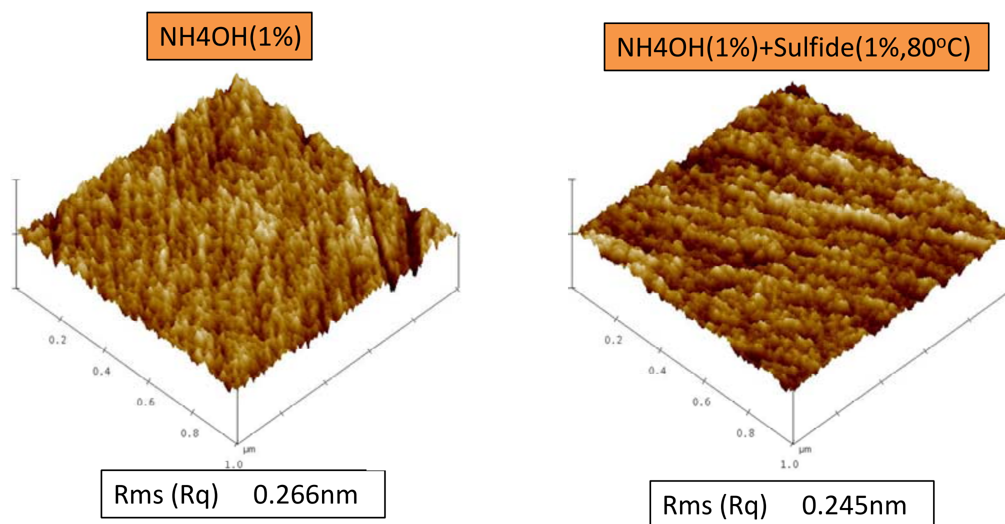

Fig. 3-14 Surface morphology of NH_4OH cleaned GaAs substrate after different sulfide condition: (a) without sulfidation (b) 1%, 80°C.

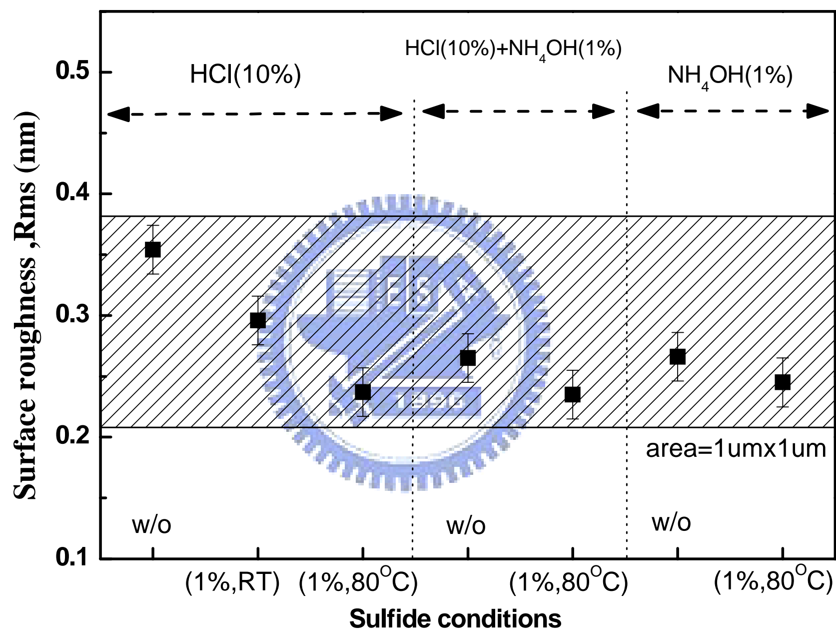

Fig. 3-15 Surface roughness of cleaned GaAs with different sulfidation

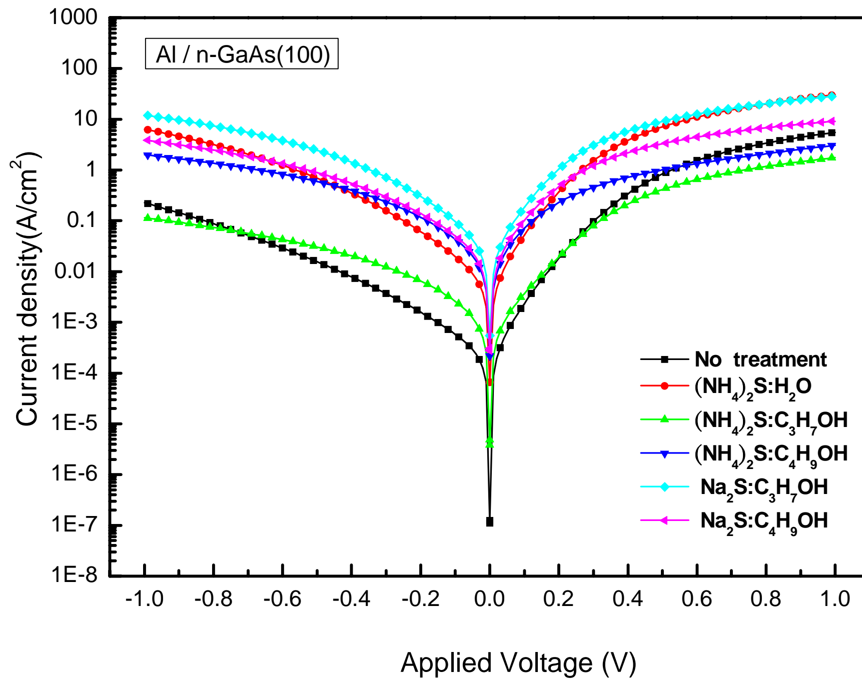

Fig. 3-16 I-V curves of Al metal contact to n-GaAs substrate with different surface treatment.

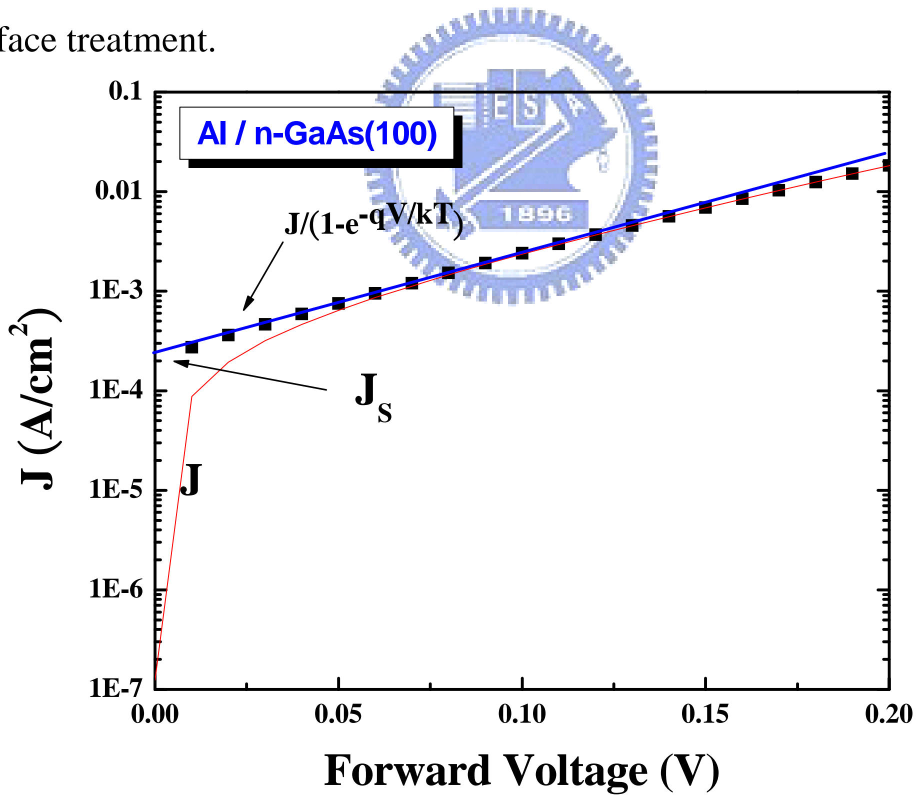

Fig. 3-17 Extraction of Schottky barrier height(SBH) with Al metal on n-type GaAs

Method	n (ideal factor)	Is (A)	Φ_B (eV)
M1(No treat.)	1.97	5.73E-6	0.774
M3(H_2O, No anneal)	1.86	1.72E-6	0.686
M5(H_2O, 400°C anneal)	1.98	9.98E-6	0.640
M7(H_2O, 500°C anneal)	1.83	1.73E-5	0.626
M4(C_3H-OH, No anneal)	1.88	4.26E-6	0.662
M6(C_3H-OH, 400°C anneal)	2.12	2.25E-6	0.679
M8(C_3H-OH, 500°C anneal)	2.07	2.17E-5	0.620

* error of Φ_B is about ±0.01eV

Fig. 3-18 Schottky diode parameters with $(NH_4)_2S$ solution after (i) no-anneal (ii) 400°C N_2 anneal (iii) 500°C N_2 anneal.

Method	n (ideal factor)	Is (A)	Φ_B (eV)
No sulfur treatment	1.97	5.73E-6	0.774
$(NH_4)_2S+H_2O$	1.86	1.72E-6	0.686
$(NH_4)_2S+C_3H$-OH	1.88	4.26E-6	0.662
$(NH_4)_2S+C_4H_9OH$	2.74	3.24E-4	0.550
Na_2S+C_3H-OH	2.12	6.34E-6	0.652
$Na_2S+C_4H_9OH$	2.01	1.00E-5	0.640

* error of Φ_B is about ±0.01eV

Fig. 3-19 Schottky diode parameters with sulfur solution and different solvents: (i) H_2O (ii) C_3H_7OH (iii) C_4H_9OH.

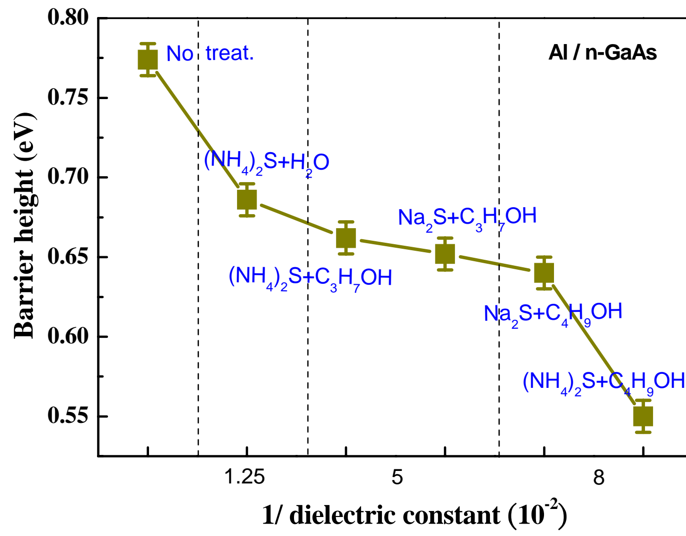

Fig. 3-20 Schottky barrier height(SBH) with sulfur solution and different solvents : (i) H_2O (ii) C_3H_7OH (iii) C_4H_9OH.

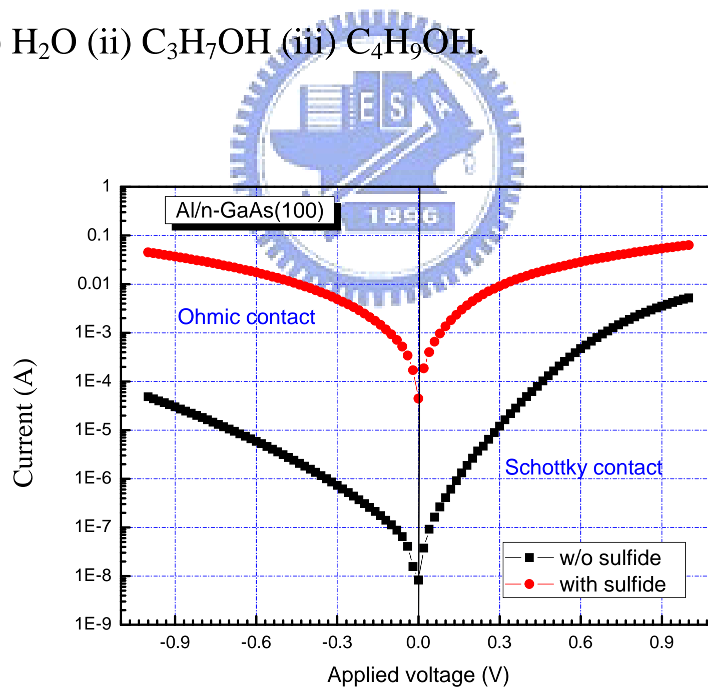

Fig. 3-21 I-V curves of Schottky diode (a) with and (b) without sulfide.

Chapter 4

Electron-beam evaporated Gd_2O_3 Gate Dielectric On GaAs Substrate

4-1 Introduction

In recent years, high-*k* gate dielectrics on Si substrate have been proved being able to significantly reduce the leakage currents as compared to the traditional SiO_2/Si system, while still maintain excellent reliability and high-level of transistor performance. In order to further enhance device driving capability, GaAs is a great potential semiconductor material due to its higher electron mobility for carrier transport. Interestingly, the lack of sufficiently stable native GaAs oxide makes the integration of high-*k* gate dielectric on top of GaAs substrate receive more and more attentions. Up to now, several metal oxides, e.g., Al_2O_3 [46], Ga_2O_3 [47] showed high breakdown field and sharp interface in atomic scale with low interface state density with n-GaAs substrate. Epitaxial growth of single-crystal gadolinium oxide dielectric thin films om GaAs is reported [48]. Ultrathin Gd metal was evaporated on GaAs surface covered with native oxides, and the oxides could be reduced during the deposition of Gd metal [49]-[50].By directly evaporated Gd_2O_3 oxide on GaAs

substrate to keep a stable interface [51]-[54]. In our work, we systematically investigated the impact of surface treatment on the electrical and material properties of Gd_2O_3 dielectric on the GaAs substrates.

4-2 Experimental Procedure

The real time cleaning GaAs samples result from HCl and NH_4OH-based were immersed in sulfur solution, before immersing in sulfide solution, we dry the samples with N_2 blowing to remove the excess surface moisture. This blowing can assure the less causes during interface reaction between sulfur and semiconductor. We treat the immediate samples with $(NH_4)_2S$ liquid solution, we also adjust the sulfur concentration and temperature to obtain the higher efficiency. After sulfur passivation, we washed deionized water for 3min to wash away the excess sulfur bond. Finally, dry the samples with N_2 blowing. The Gd_2O_3 film was deposited on the GaAs substrate by e-beam evaporation from a source under 4×10^{-6} torr at room temperature. The deposition rate of 0.05nm /s was calibrated using a quartz-crystal. The post-dielectric anneal (PDA) with O_2/Ar mixed gas and 25 torr vacuum ambient was performed to improve the Gd_2O_3 film quality and electrical characteristics. The accomplished Gd_2O_3 film samples were measured chemical composition detected by X-ray

Photoelectron Spectroscopy(XPS), surface morphology was characterized immediately by atomic force microscopy(AFM). Then, the gate electrode was 70nm Pt metal deposited through a shadow mask to form a top electrode on the topside, and the backside was 30nm indium (In) layer for ohmic contact and follow by 20nm platinum (Pt) layer for fast electric conductivity and protection. After the backside contact deposition, hot-plate with 90 ^{o}C and 10min was used to repair metal quality. The electrical properties of sulfided samples were fabricated as metal-insulator-semiconductor (MIS) device to calculate the electrical properties. A precision impedance meter of HP4284 was used for *C-V* measurement, and a semiconductor parameter analyzer of Keithley 4200 was used for *I-V* measurement.

4-3 Electrical and Material Characteristics

4-3-1 C-V and I-V characteristics of Pt/ Gd_2O_3/ GaAs structure

Fig.4-1(a)-(d) shows multi-frequency *C-V* characteristics of Pt/ Gd_2O_3/ GaAs MOS capacitor with different surface treatment. If the sulfur temperature increases to 80°C, the high frequency C-V curve will raise at accumulation region. It shows that high sulfur temperature can reduce interface state in electrical characteristics. Plotted in Fig. 4-2 is the hysteresis as functions of the

clean method and sulfide temperature at 10k Hz frequency. We find that the sulfide temperature up to 80°C, the hysteresis reduce to about 20-30mv at capacitance of flat band. We believe that As-S bonds are unstable compared to Ga-S bonds, and As-S bonds broke by post dielectric anneal (PDA) about 200-300°C. And the broken As-S bonds capture carrier easily during the Gd_2O_3/ GaAs interface. Their corresponding frequency dispersion as shown in Fig. 4-3(a) is estimated by the equations below:

$$\Delta C(@\,C_{acc.}) \triangleq \frac{(1KHz - 1MHz)}{1KHz} \tag{4.1}$$

$$\Delta V(@\,C_{fb}) \triangleq 1KHz - 100KHz \tag{4.2}$$

Fig. 4-3 displays the definition of dispersion and dispersion trend of Pt/Gd_2O_3/GaAs MOS capacitor with sulfided conditions. It is observed that NH_4OH and sulfidation(80°C) can reduce frequency dispersion. Plotted in Fig. 4-4(a) is the 10k Hz frequency curve with different treatment, and the accumulation capacitance increases with NH_4OH etching solution because of Ga-terminated surface remain stable after post dielectric anneal (PDA).On the other hand, sulfide concentration increase 10% will decrease accumulation capacitance because of residual sulfur element on the Gd_2O_3/ GaAs interface.

Fig.4-4(b) shows the C-V curve hysteresis which place value on sulfided temperature. The resultant difference in hysteresis value was evaluated at C_{fb} , and 80°C condition resulted in less hysteresis below to 50mV. In Fig. 4-5(a), we study the leakage distribution with different treatment, and the condition: HCl+NH_4OH+Sulside (1%, 80°C) can obtain the lowest leakage current. In contrast, higher sulfide concentration (10%) and low temperature (RT) led to the larger leakage current for the Pt/Gd_2O_3/GaAs MOS capacitor. Fig. 4-5(b) is leakage current trend at V_g =+1V result from Fig. 4-5 (a).These differences will be discussed in depth later in combination with the material analysis. In Fig. 4-6, we studied the variation of density of state (D_{it}) using single-frequency method [55], and equation is shown below.

$$D_{it} = \frac{(2/qA)(G_{\max}/\omega)}{[(G_{\max}/\omega C_{ox})^2 + (1 - C_m/C_{ox})^2]} \qquad (4.3)$$

Where G_{max} is the maximum conductance in the G-V plot with its corresponding capacitance (Cm). The D_{it} shows the decreasing trend with sulfided temperature and the input of NH_4OH solution.

Fig. 4-7 (a)-(d) show multi-frequency *C-V* and hysteresis width

characteristics of Pt/Gd_2O_3/GaAs MOS capacitor with two best clean methods and the NH_4OH concentration was chosen as 10% because of less As element compared to 1% NH_4OH/D.I.W.. Their corresponding frequency dispersion is estimated by the equation (4.1) and (4.2), as shown in Fig. 4-8(a).Plotted in Fig. 4-8 (b) is the hysteresis as functions at 10k Hz frequency of the two clean way with the same sulfide condition. The two clean ways mean that they are HCl_NH_4OH and NH_4OH procedure. In Fig. 4-8 (c), we study the variation of density of state (D_{it}). This shows that NH_4OH/D.I.W. (10%) concentration only less As element, but worst electrical characteristics. According to equation below, the As-O will react with GaAs substrate, so we need to think about this important thing.

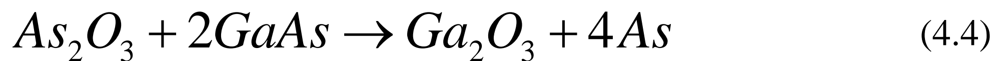

$$As_2O_3 + 2GaAs \rightarrow Ga_2O_3 + 4As \quad (4.4)$$

In Fig. 4-9(a), we study the leakage distribution with different NH_4OH solution and sulfidation. In contrast, higher sulfide concentration (2%) and NH_4OH/H_2O_2/D.I.W. led to larger leakage current, whereas result in the smaller leakage current for Gd_2O_3/GaAs gate stacks, especially for the case of 1% combined with NH_4OH/D.I.W. Fig. 4-9(b) is Weibull current distribution at V_g

=+1V result from Fig. 4-9(a).The slope of fitting line is not sharp, especially in the NH_4OH with Sulfide method. We find that leakage distribution result from non-uniform wet chemical clean and sulfidation.

In previous work, an improved *C-V* curves and *I-V* leakage current are observed with NH_4OH solution. We find that the As element will effect electrical characteristics, and surface oxides also significantly determine properties because of reaction between oxides and GaAs substrate. Following are the electrical properties of Pt/Gd_2O_3/GaAs MOS capacitor with the NH_4OH/D.I.W.(1%) solution, which solution can suppress smaller oxide but a little As element compared to the NH_4OH/D.I.W.(10%) solution.

Three possible clean methods were prepared to explain the observed difference between the Gd_2O_3 /GaAs interface. Fig.4-10 plots multi-frequency *C-V* frequency characteristics of Pt/Gd_2O_3/GaAs MOS capacitor with three cleaning methods: (i) HCl (ii) HCl+NH_4OH (iii) NH_4OH .According to the Chaptr 2 and Chapter 3, the Ga-termined surface can obtain by NH_4OH etching solution, and Ga-termined compound is thermal stable compared to HCl cleaned As-termined one. Fig. 4-11 (a) and (b) show the C-V dispersion and hysteresis of Pt/Gd_2O_3/GaAs MOS capacitor. Clearly, the NH_4OH solution and sulfidation can reduce more dispersion and hysteresis because cleaned Ga-termined surface

likes to react with high temperature sulfur element. The Ga-S bonds can against the 500-600 °C PDA temperature. Next, from the single frequency method, we observe that the density of state on the Gd_2O_3/GaAs MOS capacitor in Fig. 4-11 (c). The lowest density of state by wet chemical and sulfur passivation on GaAs substrate in this work has reduce to $6x10^{12}$ $cm^{-2}e\ V^{-1}$. According to (4-4) and (4-5) equilibrium reaction equation, leakage current result from the metal-like As element.

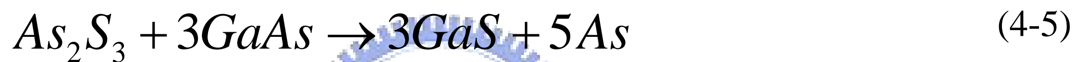

$$As_2S_3 + 3GaAs \rightarrow 3GaS + 5As \qquad (4\text{-}5)$$

Equation (4.5) shows that the more As-O and As-S components increasing, and the right hand of (4.5) equation will produce more As element. In Fig. 4-12(a) is the leakage current with different clean methods. The NH_4OH solution and sulfidation method is the best condition because of less arsenic compound component. Remarkably, the Gd_2O_3/GaAs with surface passivation revealed extremely low J_g range from $1e^{-3}$ to $1e^{-5}$ of magnitude with about CET equal to 2nm shown in Fig. 4-12(b).We find that Gd_2O_3 on Si and GaAs substrate locate on the same distribution line of this figure. Figure 4-13 shows the J_g distribution for annealed Gd_2O_3 film under moisture test. Because that rare-earth oxides will

absorb moisture contamination, and gate dielectric will degrade with time in the electrical characteristic behaviors. According to the leakage current test, in our work, the Gd_2O_3 film also keeps the same leakage current after 1week or 1 month. So we think that the Gd_2O_3 film don't absorb moisture contamination during a short period time. Finally, we show the TEM picture and EDS signal with NH_4OH solution under optimum sulfidation fabricated MOS capacitor which is shown in Fig.4-14 and Fig.4-15. The interfacial layer between Gd_2O_3/GaAs interface is about 0.5nm, and oxide thickness is 0.96nm.

Following is the PDA conditions at different gas ambient. Fig. 4-16 (a)-(e) plot multi-frequency *C-V* frequency characteristics of Pt/Gd_2O_3/GaAs MOS capacitor with different gas ambient: (i) O_2 500^oC (ii) Ar 500^oC (iii) N_2 500^oC (iv) Ar /O_2 500^oC (v) Ar /O_2 600^oC. Clearly, the O_2 gas ambient led to Gd_2O_3/GaAs interface oxidized quickly during 10 second. Fig. 4-17 (a)-(e) show the hysteresis width of Pt/Gd_2O_3/GaAs MOS capacitor. Fig. 4-18 is the 10k Hz frequency C-V curve and hysteresis trend. The 600^oC anneal led to Gd_2O_3 film quality more dense because of higher activation to fill Gd_2O_3 vacancy site. In Fig. 4-19(a) is the C-V dispersion and leakage current with different gas ambient methods.

4-3-2 xps characteristic of Gd_2O_3 film on GaAs substrate

Fig. 4-20 shows As and Ga 3d core level spectra from GaAs substrate with different surface treatment after PDA 10s with Ar/O_2 ambient at 500°C. In the As 3d, three oxides components appeared, one could be identified as As_2O_3, two as As_2O_5, and three as As(Gd-O) form their typical chemical shifts; approximately 2、3.5 and 6 eV, respectively [55]. In the Ga 3d, three oxides components appeared, one could be identified as GA_2O, two as Ga_2O_3, and three as Ga(Gd-O) form their typical chemical shifts. After PDA at 500°C, the interface still contains GaAs oxides and GaAs(GdO)-like compound. When Gd_2O_3 film has deposited on the GaAs substrate with 500°C anneal temperature, we can't exactly describe the magnitude of every component. This is because interface GaAs oxides have desorbed after 500°C anneal, and the Gd_2O_3 film combined with this residual element. From the Fig.4-21(a), the Gd-O oxide in the Gd 3d orbit is assigned in 1188 eV which is one of the spin orbit of Gd 3d, and Auger electron spectra of As LMN is 20 eV distance from Gd 3d orbit. We find that a large number of As-O was found in the spectra regardless of surface treatment. Fig.4-21(b) shows the Gd 4d spectra, the two peaks are known as Gd 4d spin orbit peak [52]. In the Fig. 4-22 spectra, we discuss the NH_4OH solution effect to remove cleaned residual native oxides. We know that the As-O of (ii)

and (iii) methods are less than (i) one after cleaned GaAs wafer. When the film and PDA process has finished, according to equation (4-4), the As-O will be desorbed, and it transfers to Ga-O component and remains As element. In the Fig. 4-22 (b), the O1s spectrum has two peaks, they are deconvoluted into one with a binding energy of around 529.8eV (Gd-O[I]) and 532.5eV(Gd-O[II]). It was reported the Gd-O[II] correspond to both the oxygen contaminants and interfacial GaAs oxides whereas Gd-O[I] correspond to the O-Gd bond in the amorphous Gd_2O_3.Fig. 4-23illustrates the Gd_2O_3 film contaminants, the (ii) and (iii) methods contain less Ga_2O component because of NH_4OH solution.Fig.4-24 is the XRD spectra, which show that no serious crystallization behavior on the Ar/O_2 500°C annealed Gd_2O_3 film on GaAs substrate.

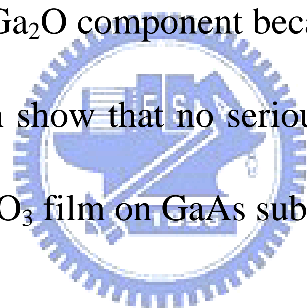

4-3-3 surface morphology of Gd_2O_3 film on GaAs substrate

Fig. 4-25 represents the 1x1 um AFM images of the different surface treatments GaAs substrate surface after the deposition of the Gd_2O_3 films, and images show a relatively smooth surface morphology with a measured Rms roughness ranging from 0.24 to 0.37nm.Because the surface roughness affects the properties of a thin oxide or device, it is desirable to preserve a smooth surface during the process. Fig. 4-26 shows the clean method effect on Gd_2O_3

film under same silfidation, and the Rms roughness ranging from 0.25 to 0.29nm

4-4 Summary

We systematically investigated the surface treatment effect on the electrical and material characteristics of GaAs MOS capacitors with Gd_2O_3 gate dielectric. The higher sulfur temperature and NH_4OH solution was found to obtain the lower EOT of Gd_2O_3/GaAs gate stack, however, with a smaller hysteresis width. A lower EOT of 20Å with a low leakage current of 1×10^{-3} to 1×10^{-5} A/cm^2 @ $V_g = +1$V, which has been achieved after 500°C annealing for 10 seconds. The density of state can reduce to 6×10^{12}cm^{-2}e V^{-1} and lowest leakage current about 1×10^{-5} A/cm^2 @ $V_g = +1$V for the best surface treatment. We believed that the continuous optimization of the interface structure through process modification is expected to further improve the electrical performance of the Gd_2O_3/GaAs gate stack, which thus be considered as a promising gate dielectric of GaAs device.

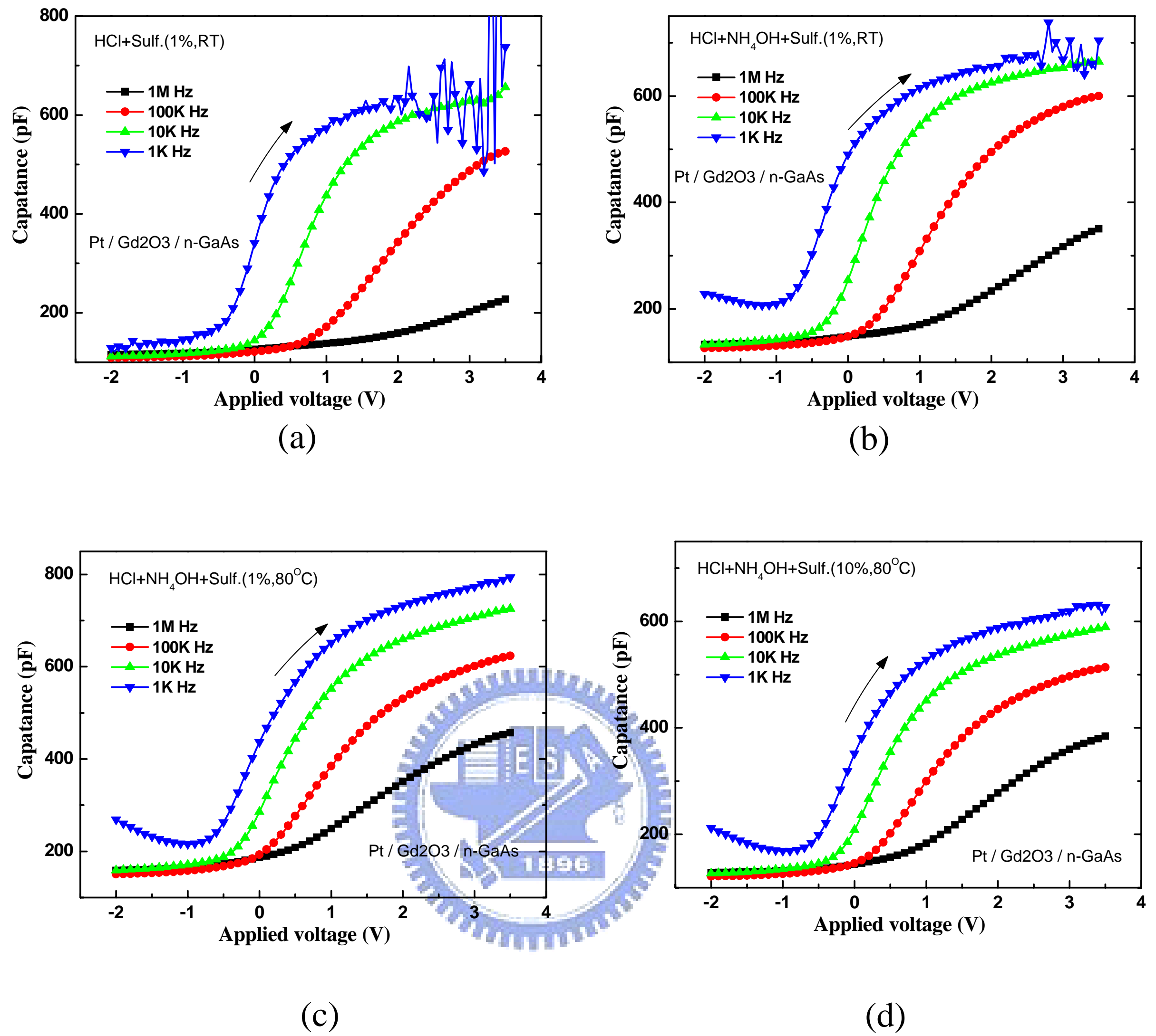

Fig. 4-1 (a)-(d) Multi-frequency *C-V* characteristics of Pt/Gd_2O_3/GaAs MOS capacitor with different surface treatment.

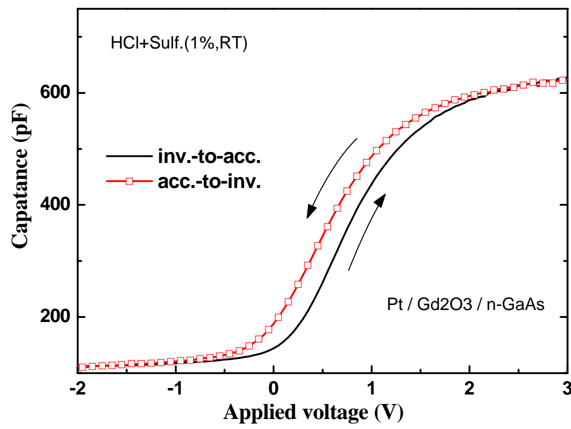

(a)

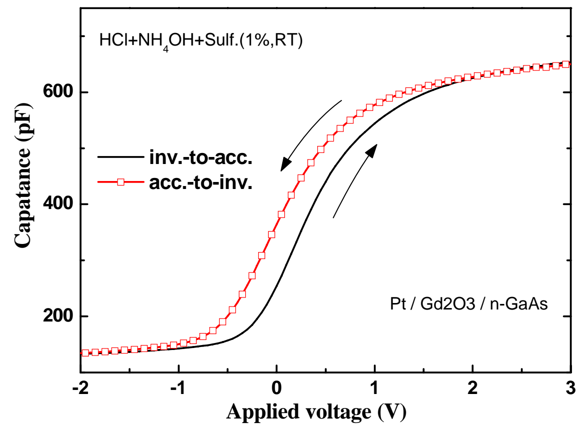

(b)

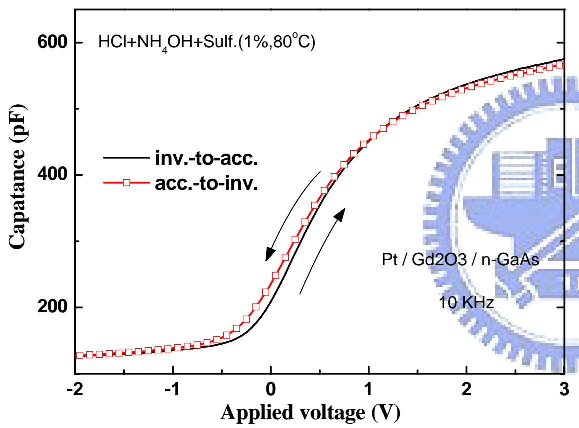

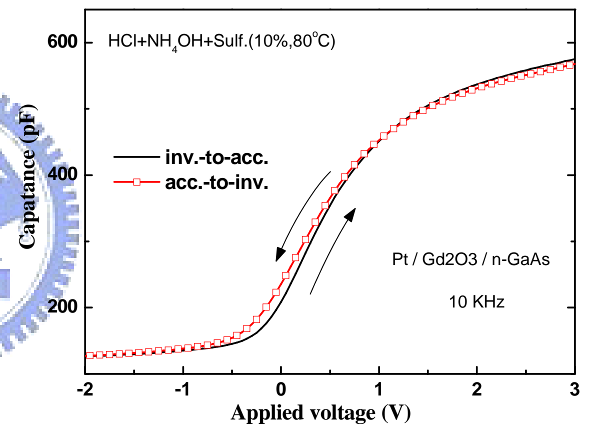

(c)

(d)

Fig. 4-2 (a)-(d) The hysteresis of 10kHz frequency of Pt/Gd_2O_3/GaAs MOS capacitor with different surface treatment.

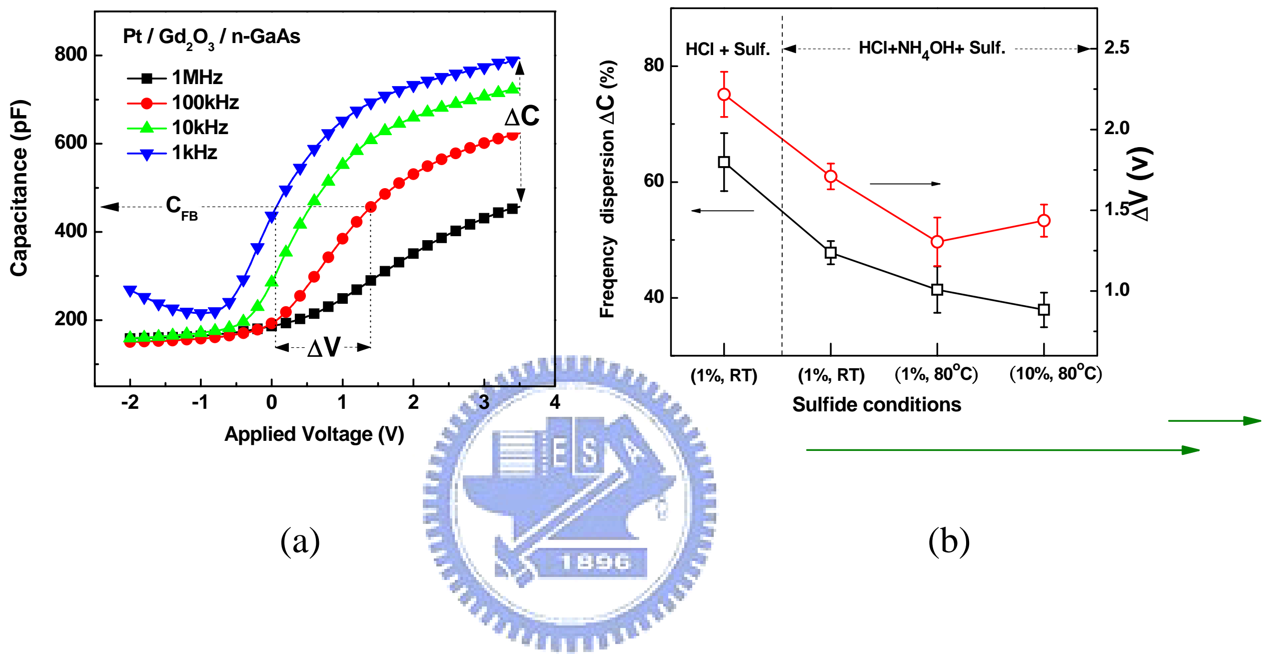

Fig. 4-3 (a) Multi-frequency *C-V* curve with HCl+NH_4OH +Sulfide treatment (b) The C-V dispersion with different surface treatments for Pt/Gd_2O_3/GaAs MOS capacitors.

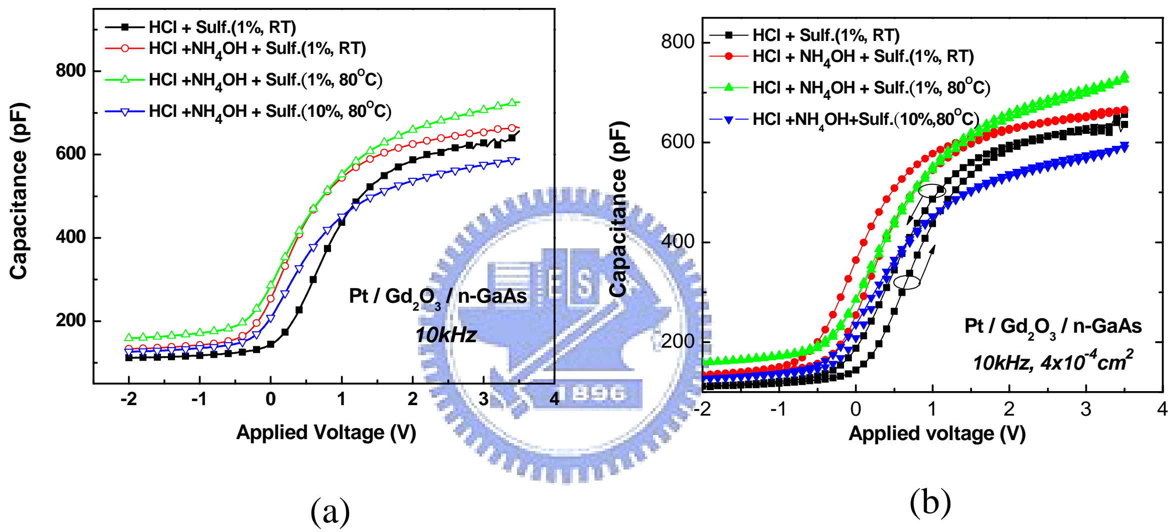

Fig. 4-4 (a) The 10kHz frequency *C*-*V* and (b)hysteresis characteristics of $Pt/Gd_2O_3/GaAs$ MOS capacitor with different clean and sulfide method.

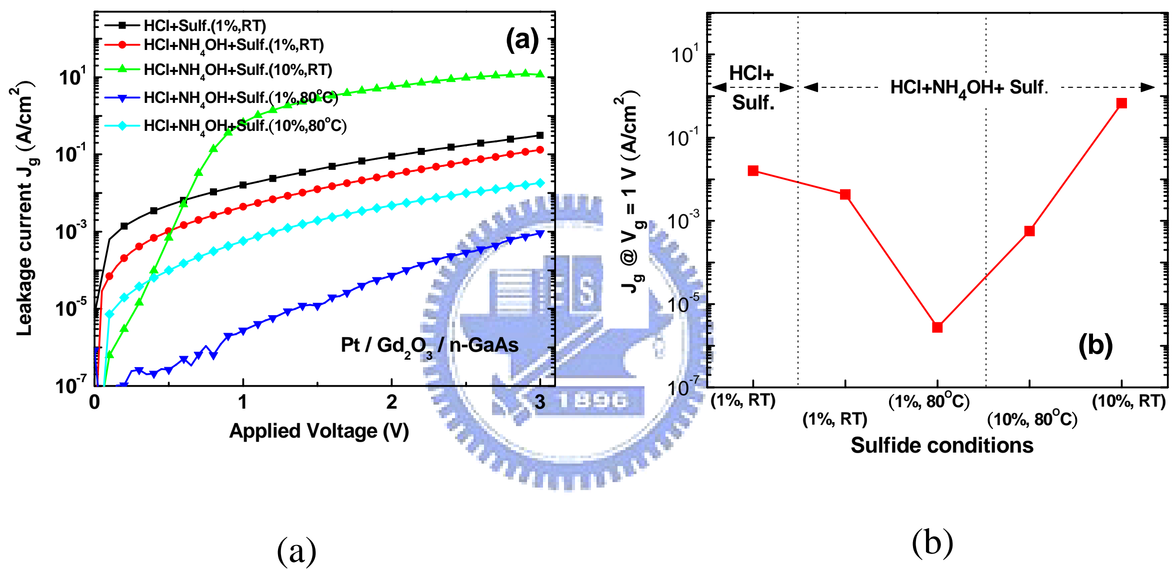

(a) (b)

Fig. 4-5 (a) The *I-V* curve characteristics and (b) Jg(@V=+1v) of Pt/Gd_2O_3/GaAs MOS capacitor with different clean and sulfide method.

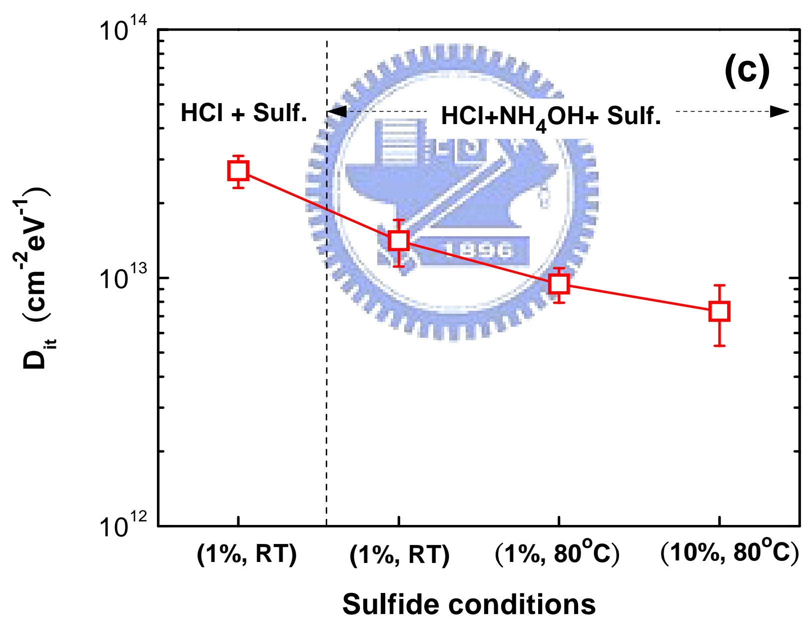

Fig. 4-6 Density of state on Gd_2O_3/GaAs interface with different clean and sulfide method.

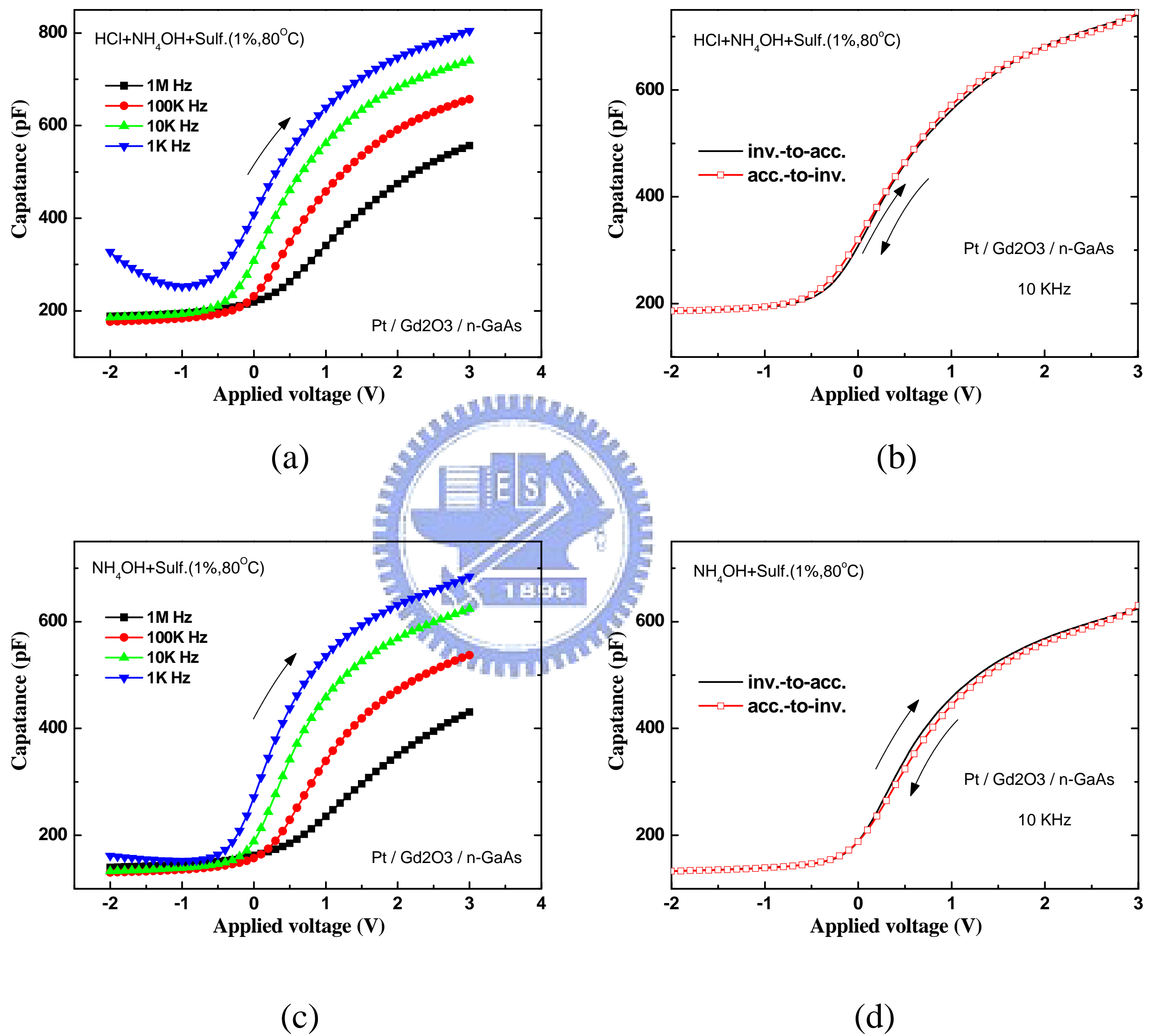

Fig. 4-7 (a)-(d) Multi-frequency *C-V* and hysteresis using 10k Hz frequency characteristics of Pt/Gd_2O_3/GaAs MOS capacitor with two cleaning method: (i) HCl+NH_4OH (ii) NH_4OH

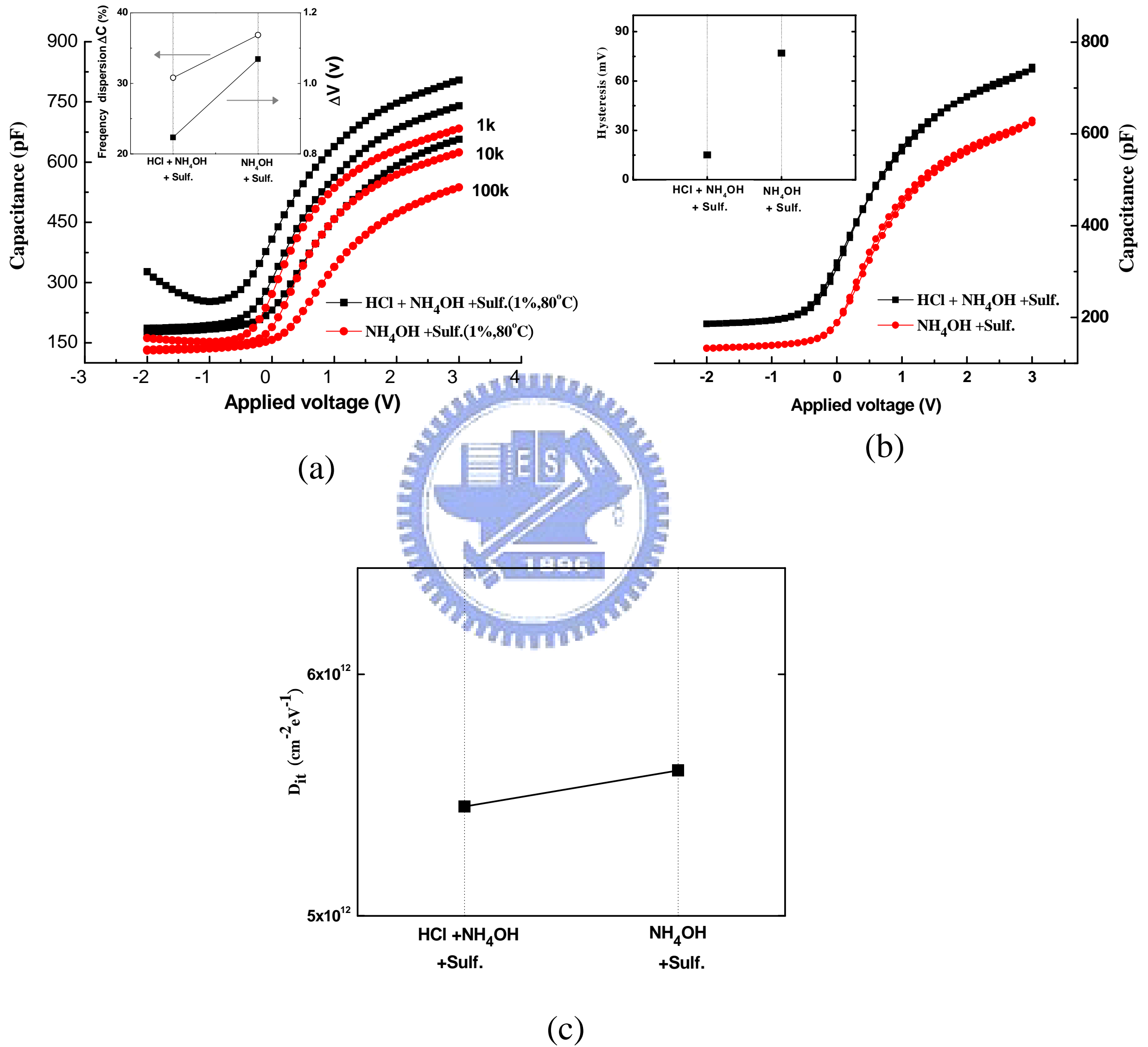

Fig. 4-8 (a) Multi-frequency *C-V* (b) the hysteresis using 10k Hz frequency and (c) density of state characteristics of Pt/Gd_2O_3/GaAs MOS capacitor with two cleaning method: (i) HCl+NH_4OH (ii) NH_4OH

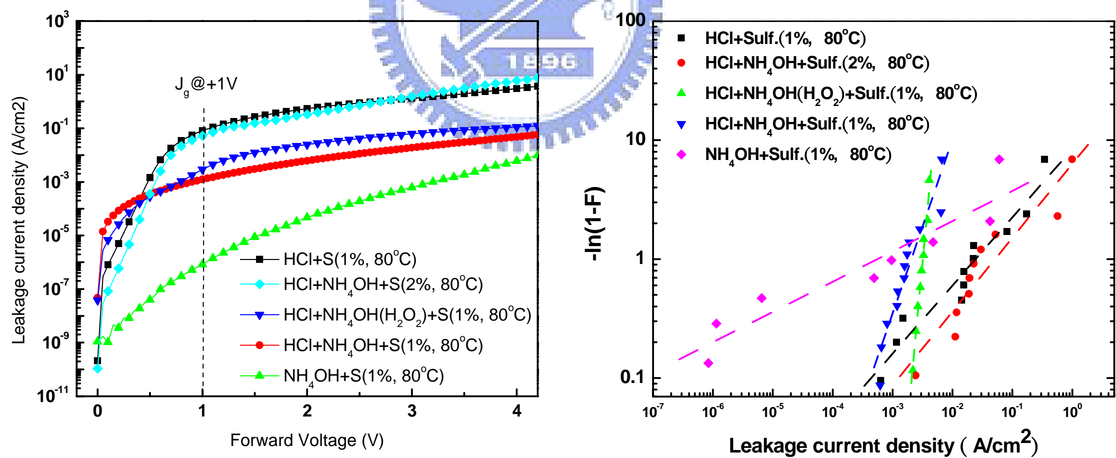

(a) (b)

Fig. 4-9 (a) The *I-V* curve characteristics and (b) Jg(@V=+1v) of Pt/Gd_2O_3/GaAs MOS capacitor with different clean methods and sulfide methods.

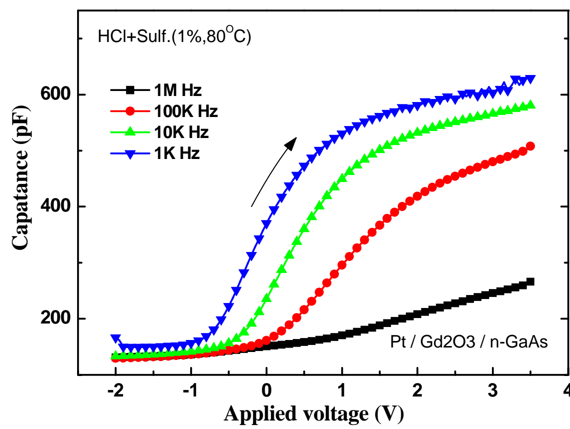

(a)

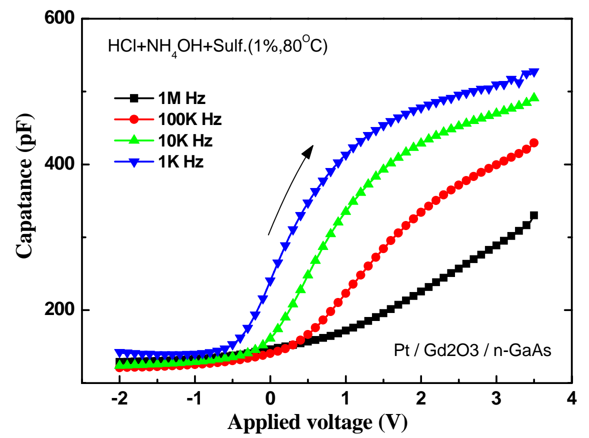

(b)

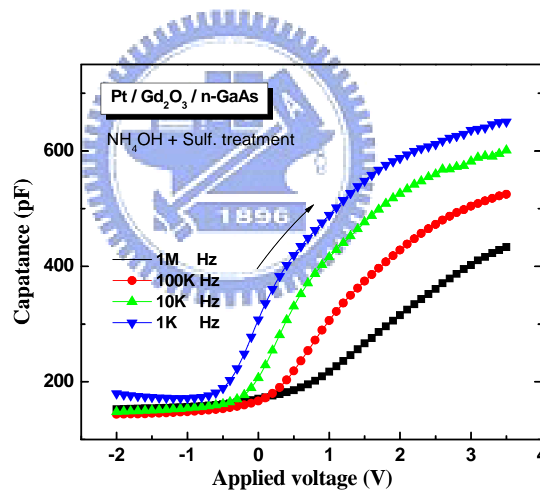

(c)

Fig. 4-10 (a)-(c) Multi-frequency *C-V* frequency characteristics of Pt/Gd_2O_3/GaAs MOS capacitor with three cleaning methods: (i) HCl (ii) HCl+NH_4OH (iii) NH_4OH

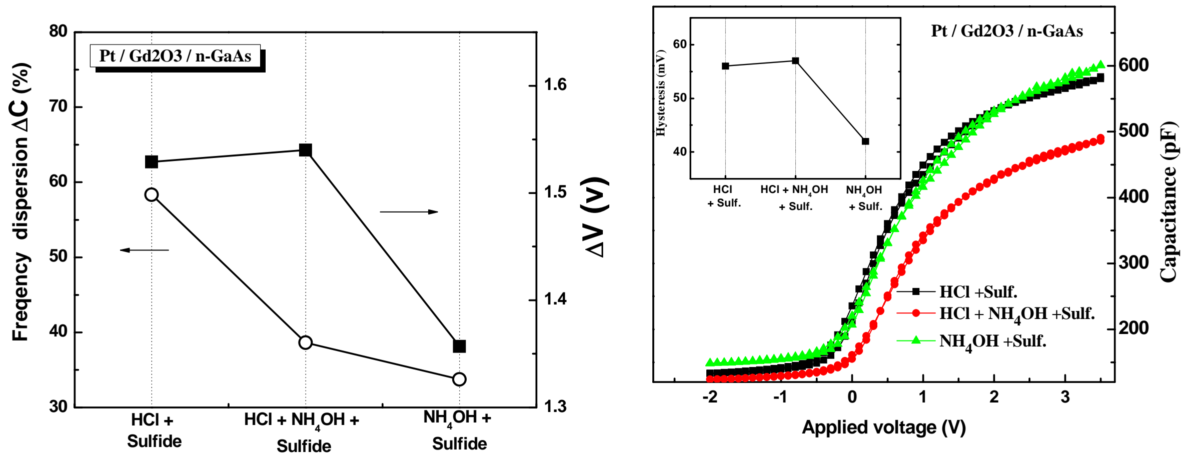

(a) (b)

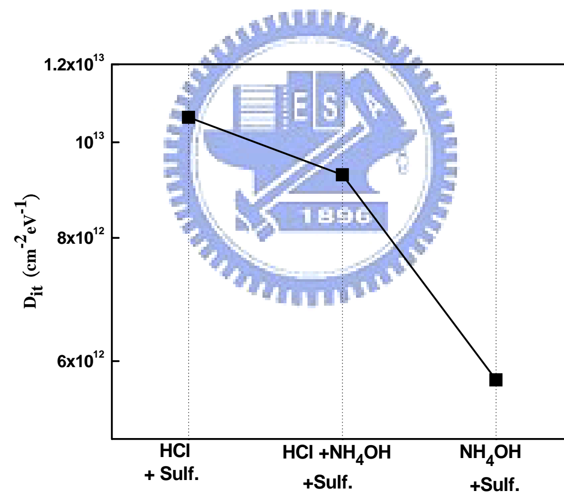

(c)

Fig. 4-11 (a)-(c) The C-V characteristics and D_{it} of Pt/Gd_2O_3/GaAs MOS capacitor with three cleaning methods: (i) HCl (ii) HCl+NH_4OH (iii) NH_4OH under optimum sulfidation.

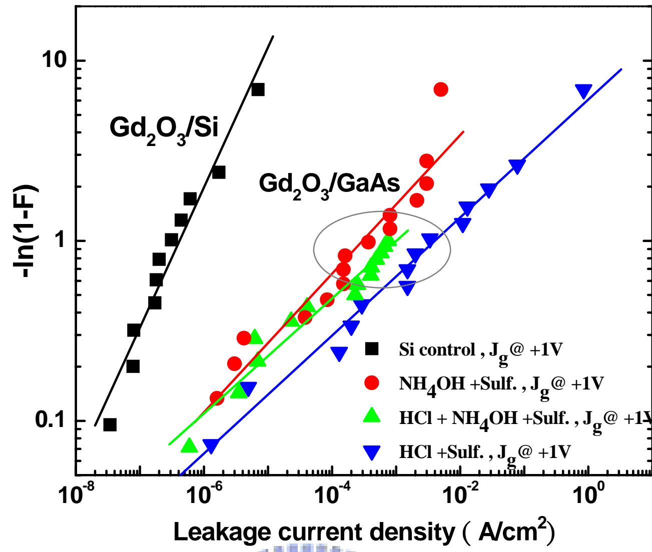

(a)

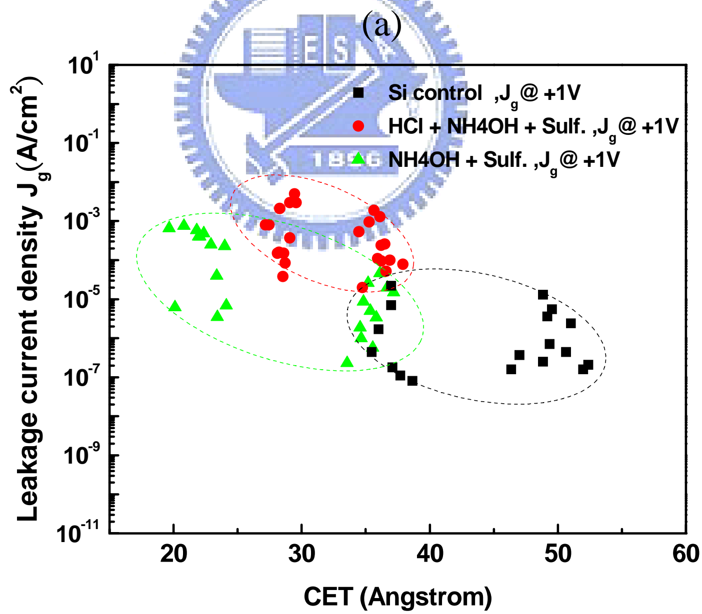

(b)

Fig. 4-12 (a)-(b) The leakage current characteristics and J_g v.s CET of Pt/Gd_2O_3/GaAs MOS capacitor with three cleaning methods: (i) HCl (ii) HCl+NH_4OH (iii) NH_4OH under optimum sulfidation.

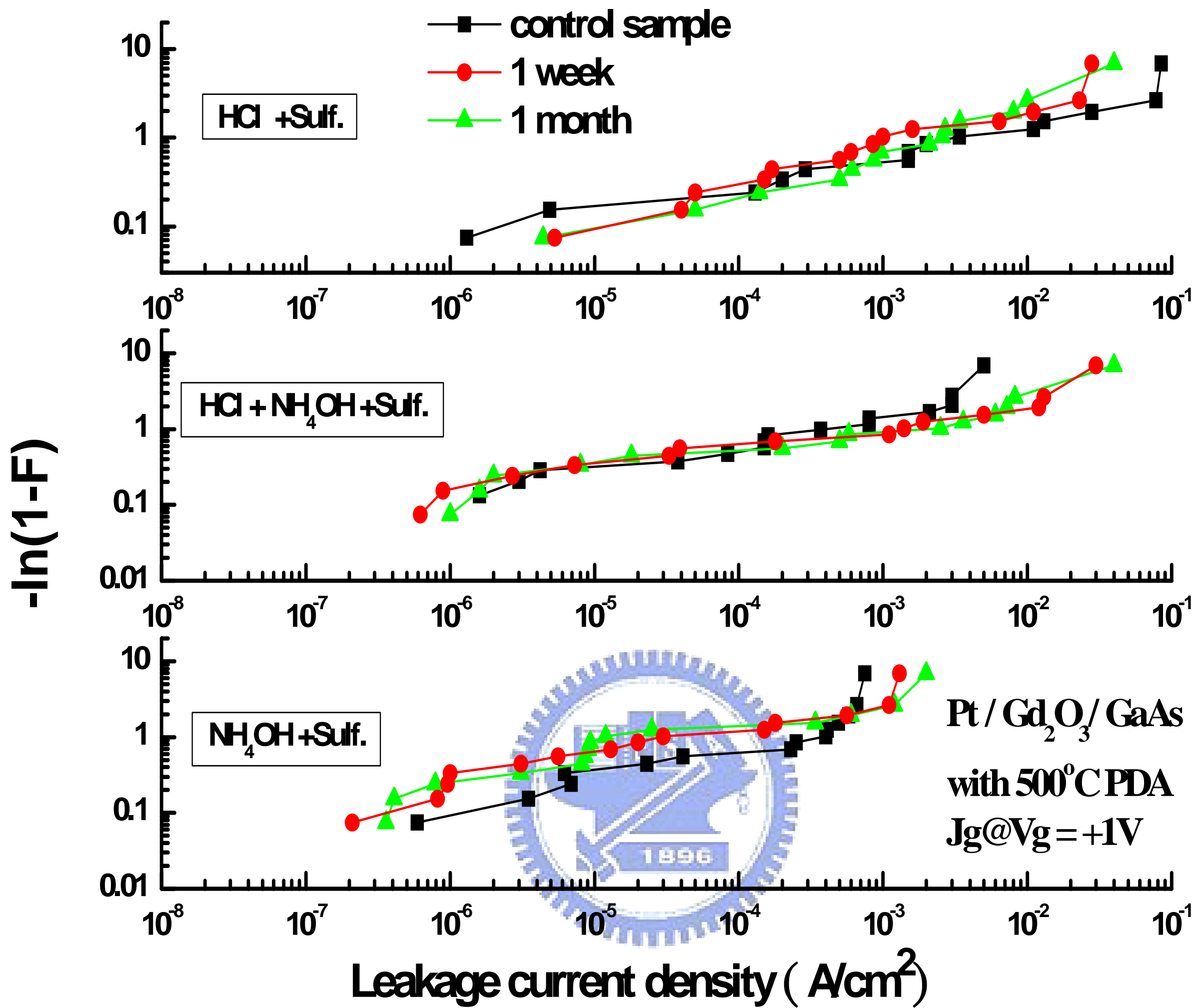

Fig. 4-13 The Weibull distribution of Pt/Gd_2O_3/GaAs MOS capacitor with three cleaning methods: (i) HCl (ii) HCl+NH_4OH (iii) NH_4OH after 1 week/1 month.

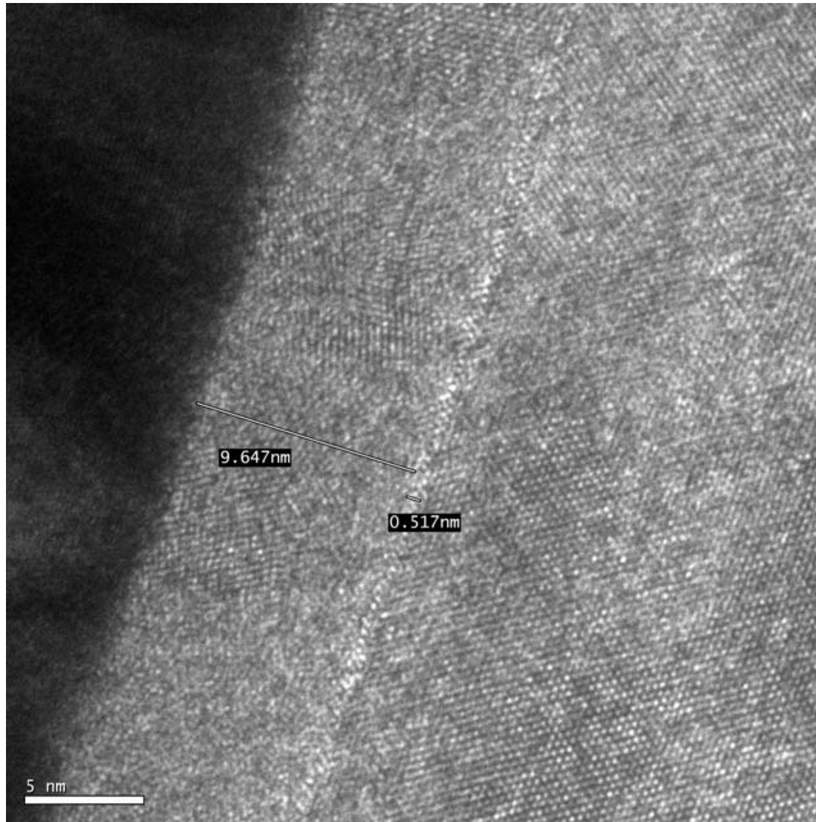

Fig. 4-14 The TEM picture of Pt/Gd_2O_3/GaAs MOS capacitor with NH_4OH under optimum sulfidation.

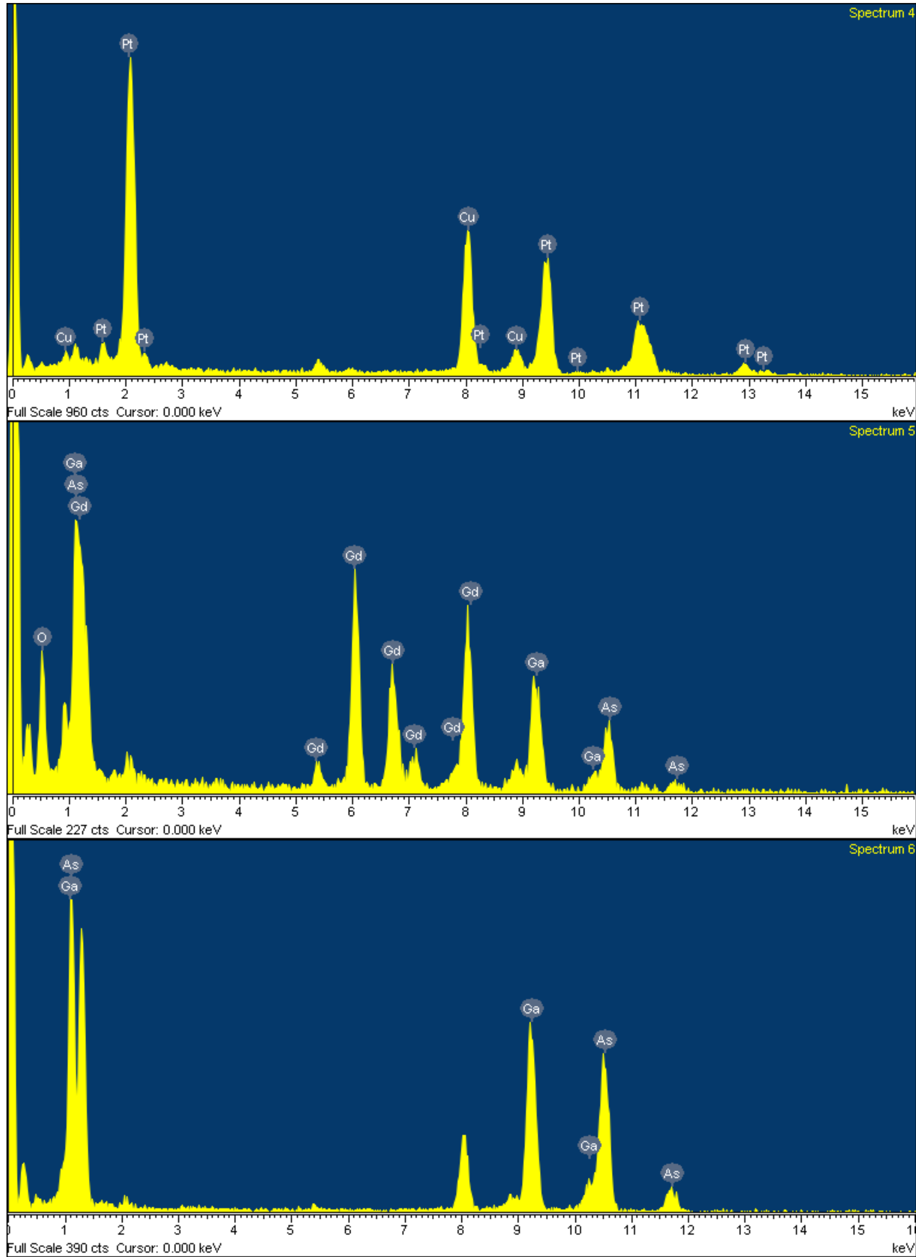

Fig. 4-15 The EDS distribution signal of $Pt/Gd_2O_3/GaAs$ MOS capacitor with NH_4OH under optimum sulfidation.

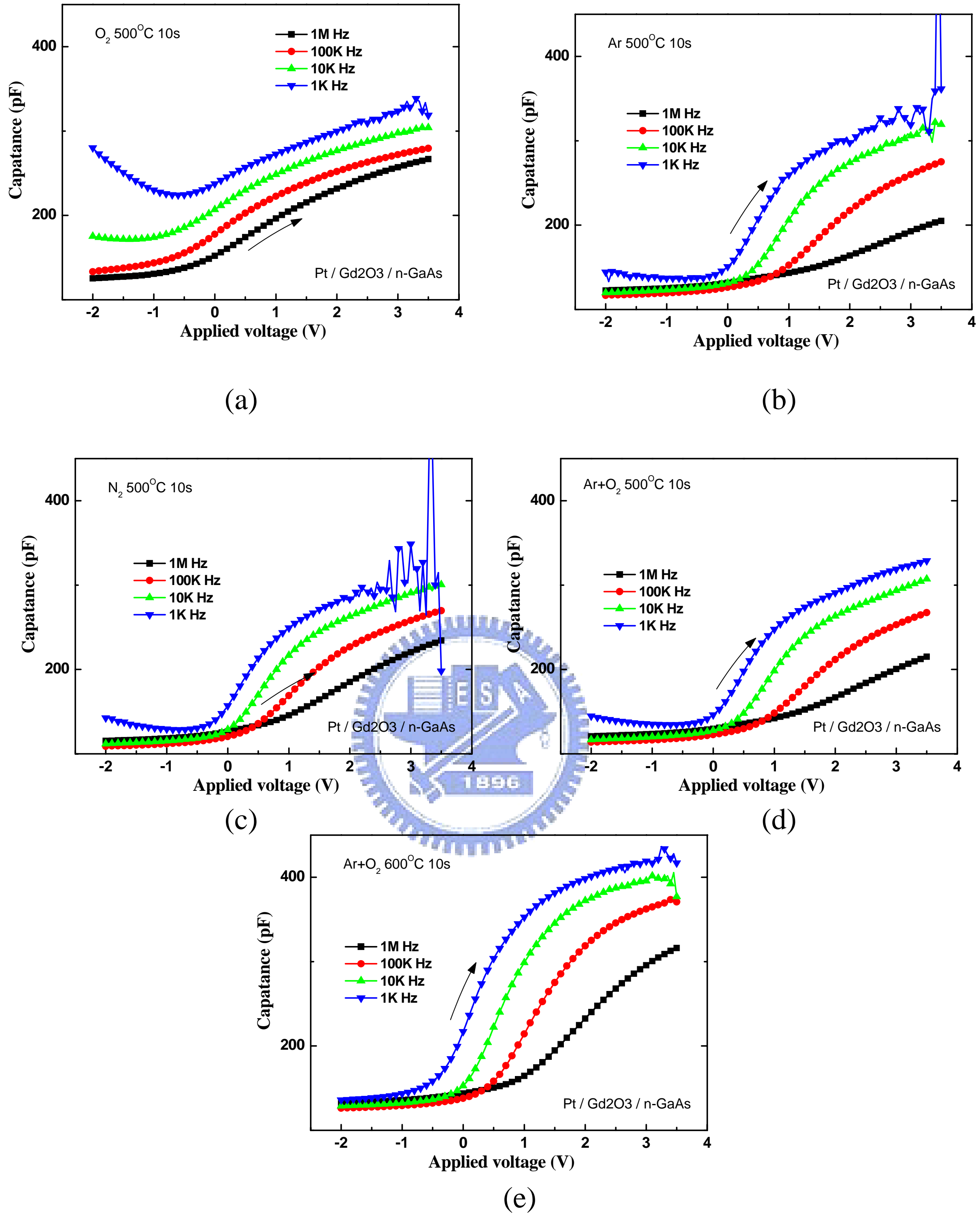

Fig. 4-16 (a)-(e) Multi-frequency *C-V* frequency characteristics of Pt/Gd_2O_3/GaAs MOS capacitor with different gas ambient : (i) O_2 500°C (ii) Ar 500°C (iii) $N_2$500°C (iv) Ar / O_2 500°C (v) Ar / O_2 600°C

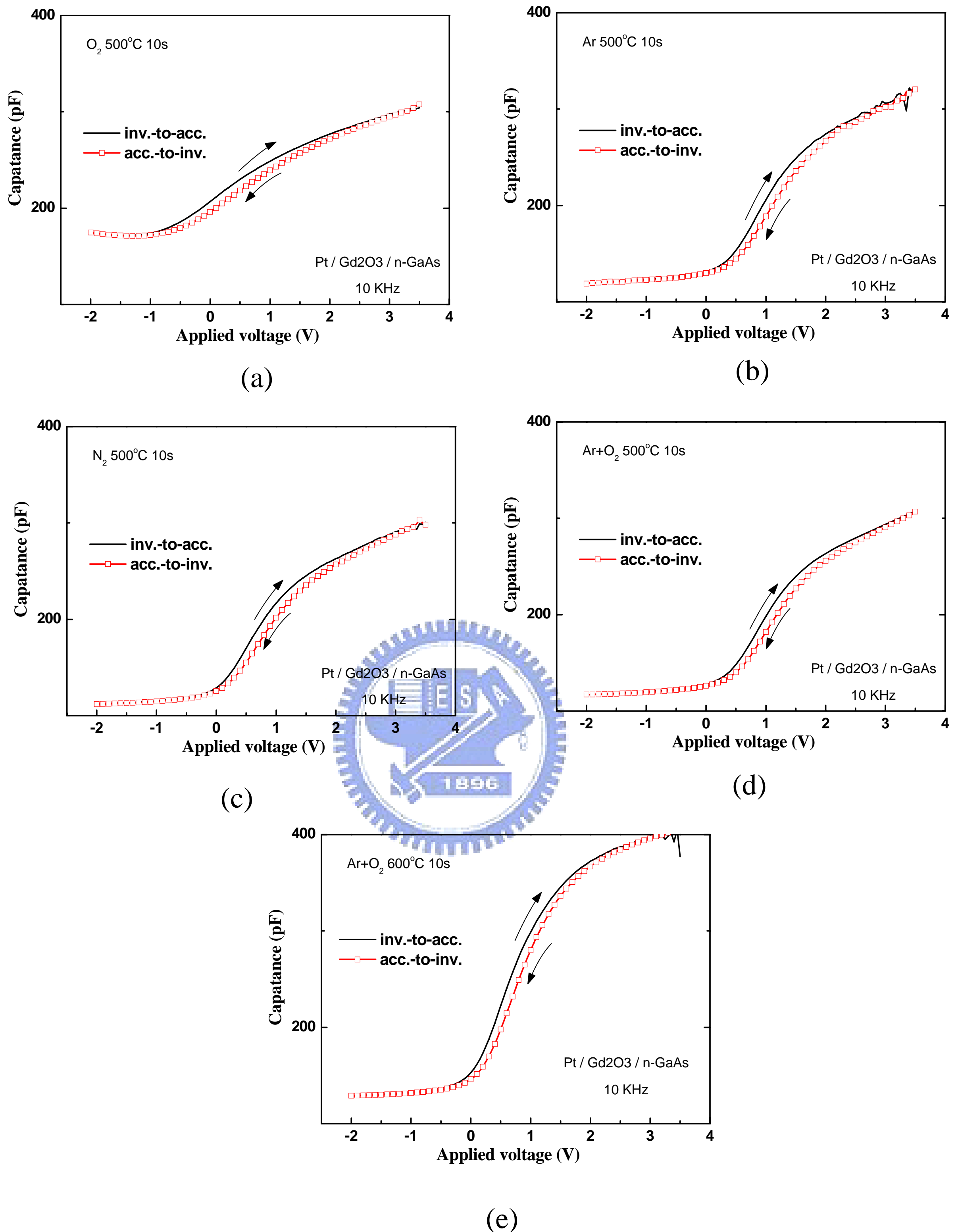

(e)

Fig. 4-17 (a)-(e) The hysteresis width of Pt/Gd_2O_3/GaAs MOS capacitor with different gas ambient : (i) O_2 500°C (ii) Ar 500°C (iii) $N_2$500°C (iv) Ar / O_2 500°C (v) Ar / O_2 600°C

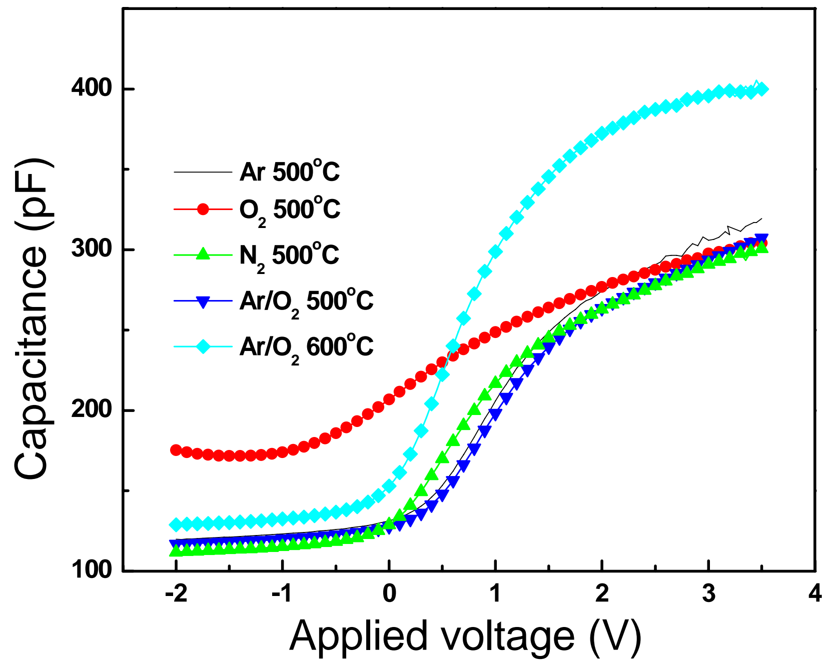

(a)

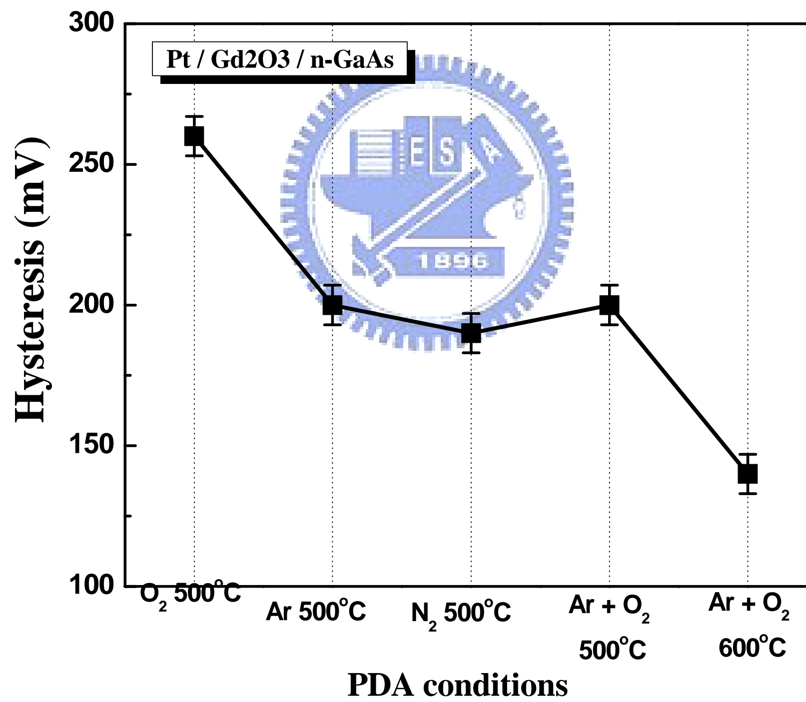

(b)

Fig. 4-18 (a) The 10k Hz frequency and (b) hysteresis trend of Pt/Gd_2O_3/GaAs MOS capacitor with different gas ambient : (i) O_2 500°C (ii) Ar 500°C (iii) N_2 500°C (iv) Ar / O_2 500°C (v) Ar / O_2 600°C

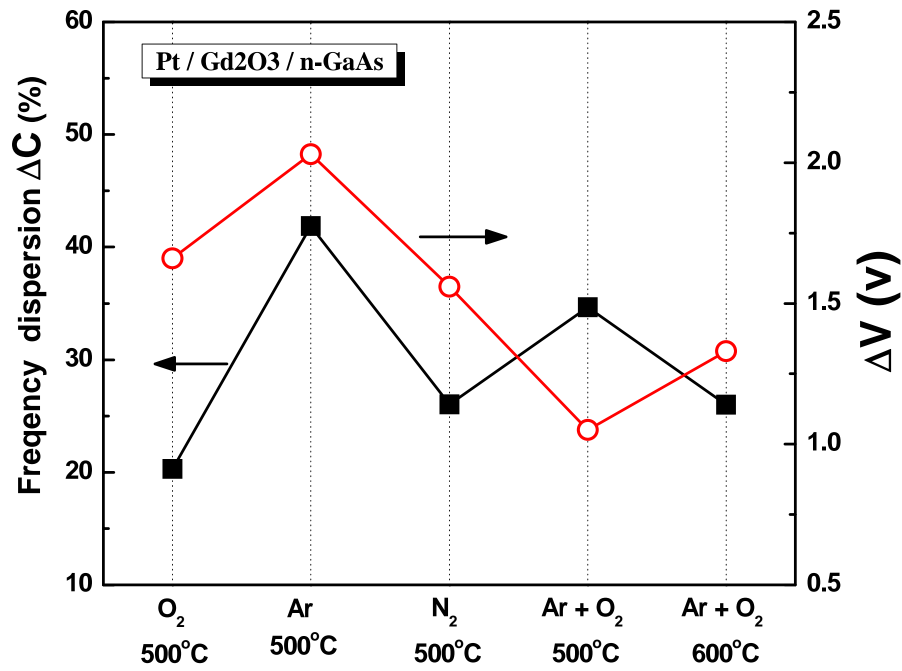

(a)

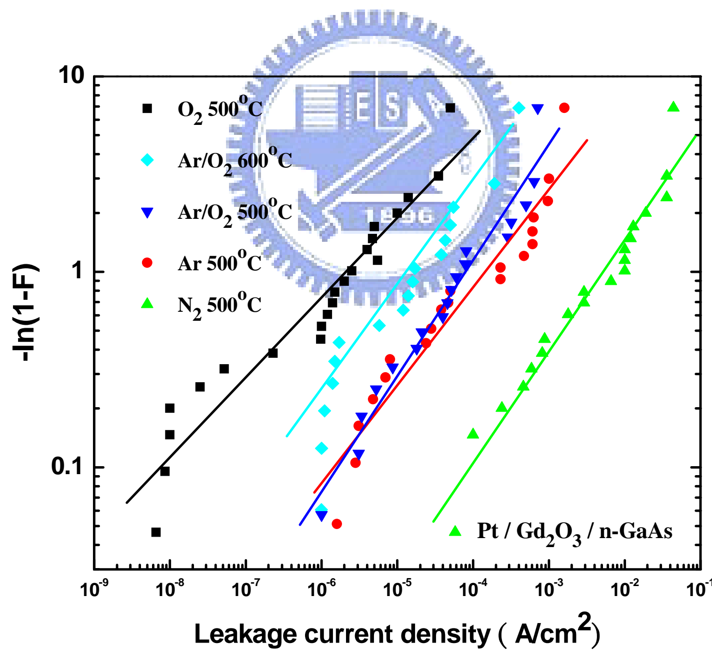

(b)

Fig. 4-19 (a) The dispersion and (b) leakage distribution characteristics of Pt/Gd_2O_3/GaAs MOS capacitor with different gas ambient : (i) O_2 500°C (ii) Ar 500°C (iii) $N_2$500°C (iv) Ar / O_2 500°C (v) Ar / O_2 600°C

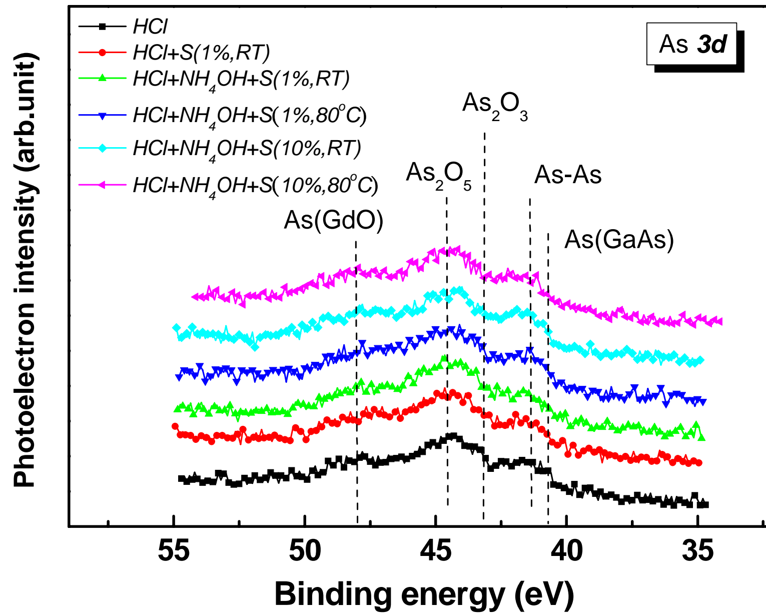

(a)

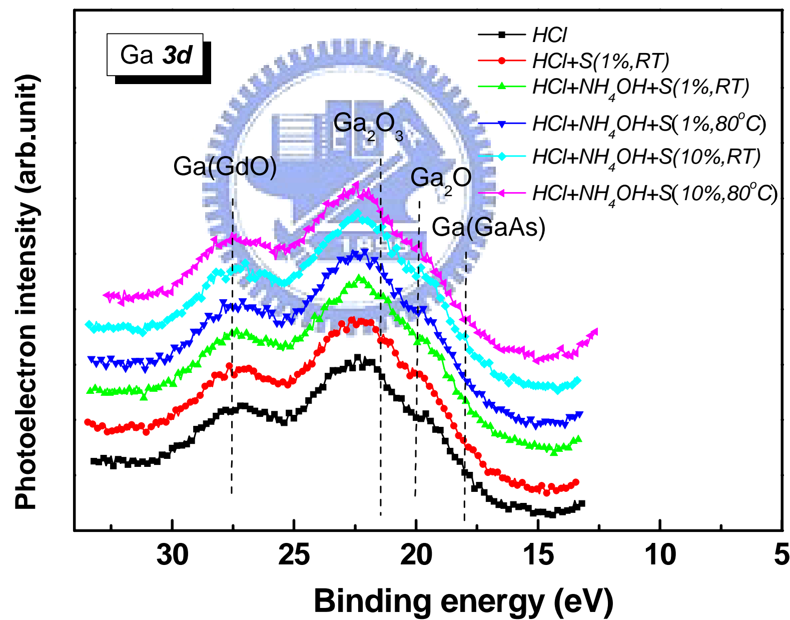

(b)

Fig. 4-20 XPS spectra of the annealed Gd_2O_3 film at 500°C for 10 s. (a) the As 3d core level; (b) the Ga 3d core level.

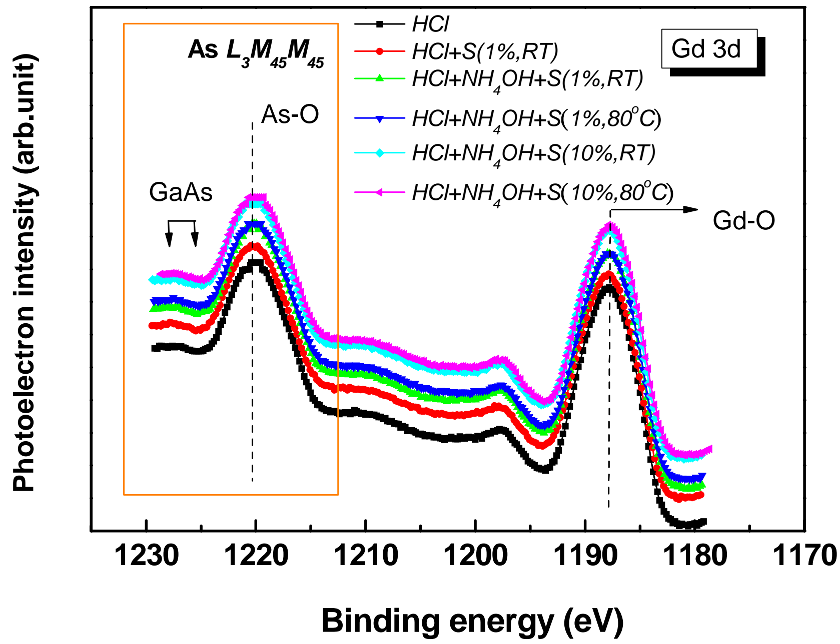

(a)

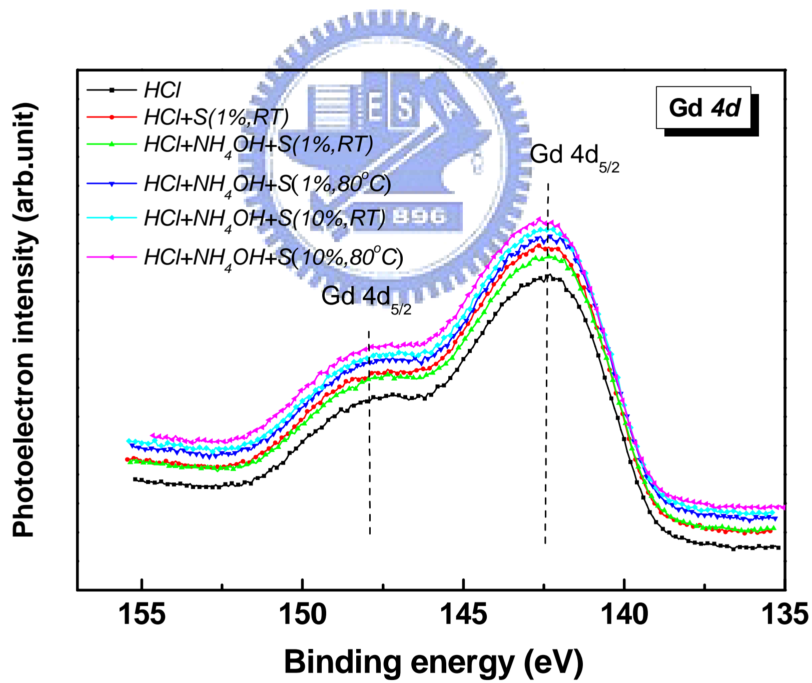

(b)

Fig. 4-21 XPS spectra of the annealed Gd_2O_3 film at 500°C for 10 s. (a) the Gd 3d core level; (b) the Gd 4d core level.

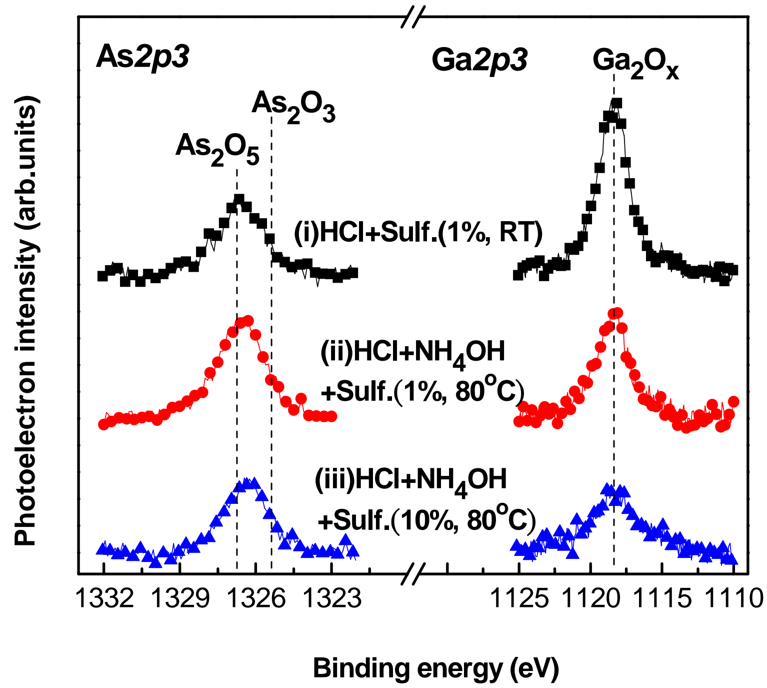

(a)

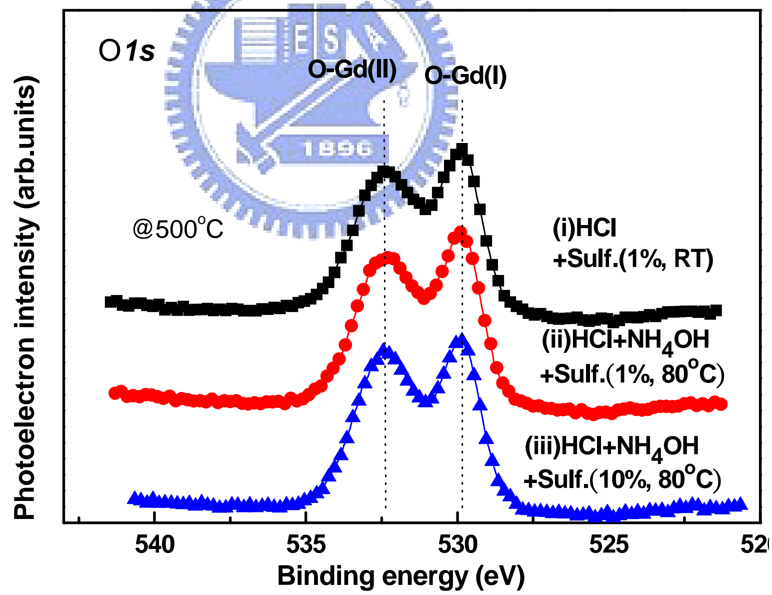

(b)

Fig. 4-22 XPS spectra of the annealed Gd_2O_3 film at 500°C for 10 s. (a) the As 3d and Ga 3d core level; (b) the O 1*s* core level.

GaAsGdO	**Ga**	**As**	**Gd**	**O**
HCl +Sulf.(1%, RT)	**2.51%**	**0.73%**	**28.10%**	**68.63%**
HCl+ NH4OH +Sulf.(1%, 80°C)	**1.27%**	**0.89%**	**27%**	**70.74%**
HCl+NH4OH +Sulf.(10%, 80oC)	**1.01%**	**0.67%**	**27.47%**	**70.76%**

Fig. 4-23 The ratio of GaAs in the annealed Gd_2O_3 film at 500°C for 10 s with surface treatment.

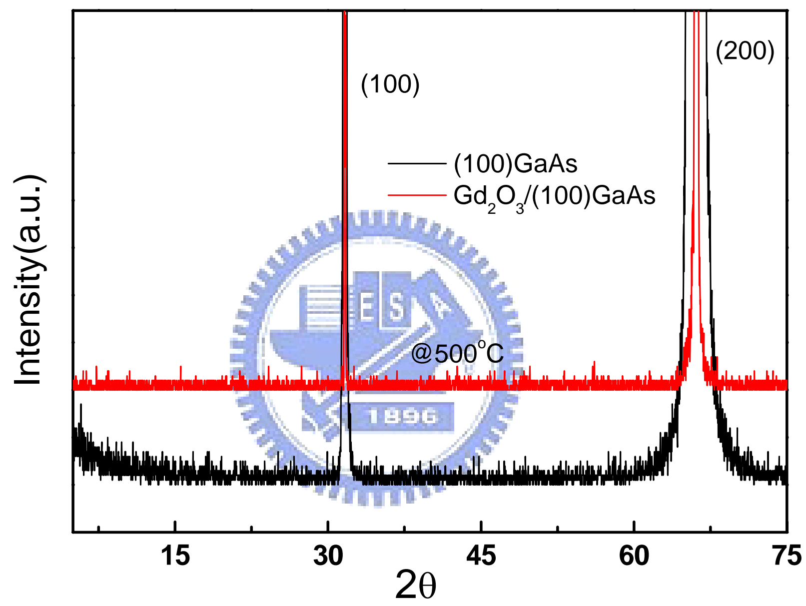

Fig. 4-24 XRD spectra of (i) n-GaAs(100) and (ii) 500°C annealed Gd_2O_3/ n-GaAs(100)

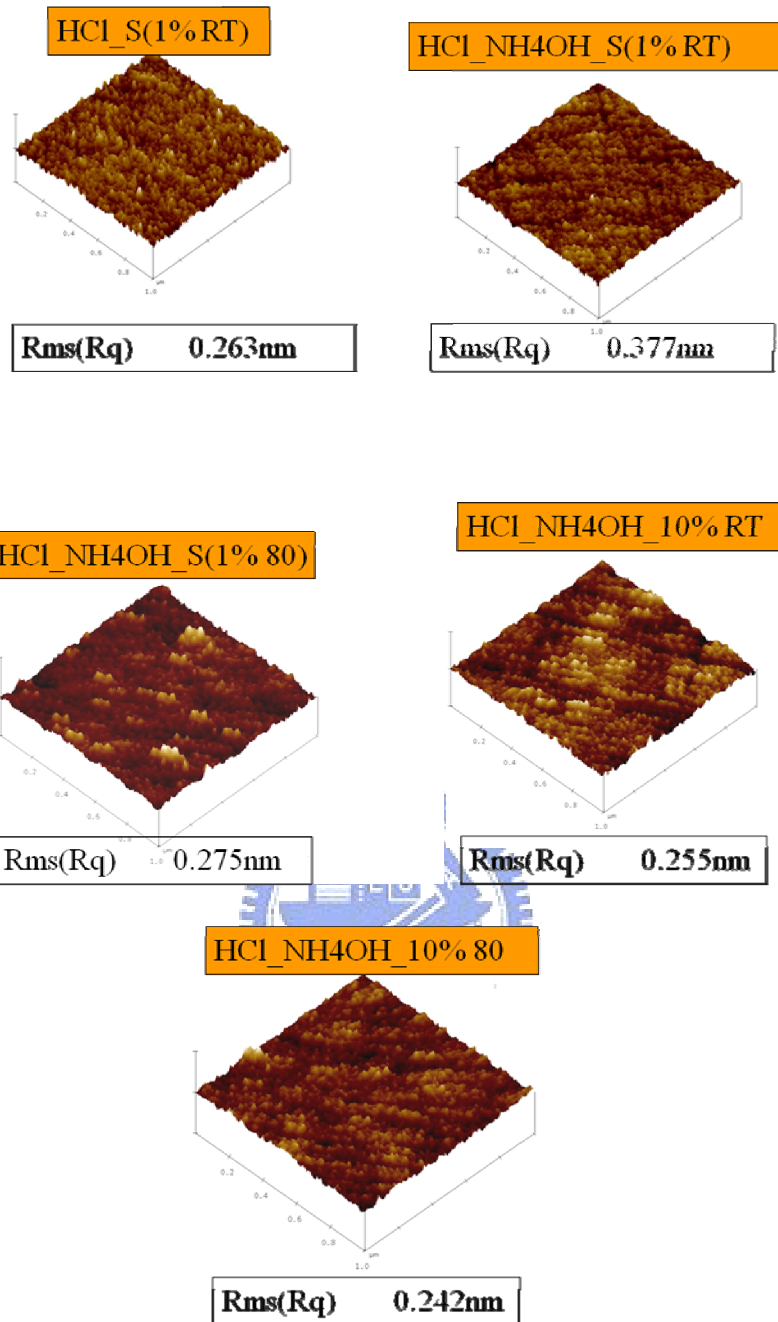

Fig. 4-25 Surface roughness of Gd_2O_3 on GaAs substrate after Ar/O_2 (500°C 10s) anneal with different surface treatments.

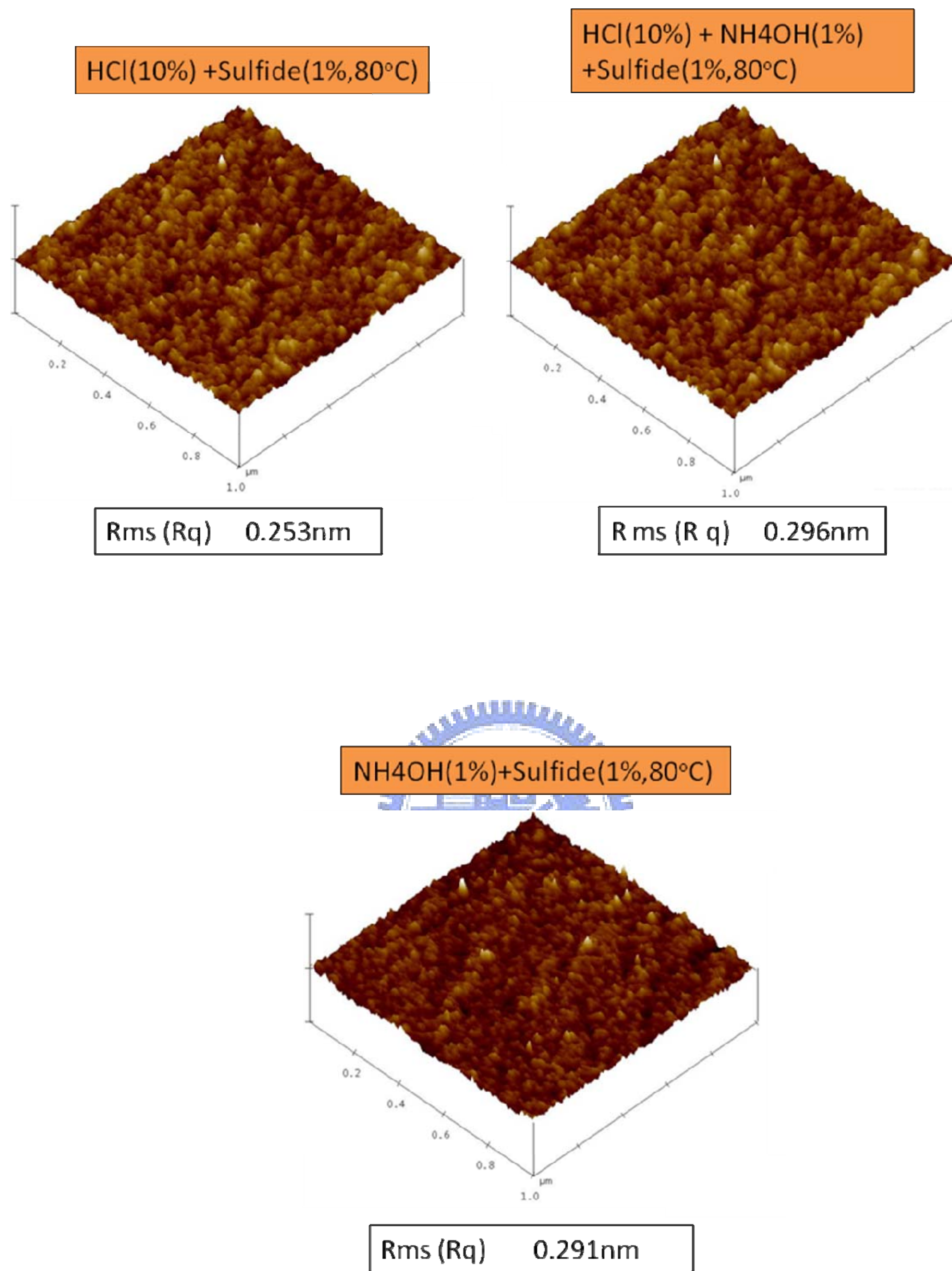

Fig. 4-26 Surface roughness of Gd_2O_3 on GaAs substrate after Ar/O_2 (500°C 10s) anneal with different clean methods.

Chapter 5
Conclusions and Suggestions for Future Work

5-1 Conclusions

Firstly, the flatness of the GaAs surface was needed, but the thermal stable surface is more important. The optimized surface roughness was ~0.266 nm after the NH_4OH/DIW (1%) and DIW solutions. From the XPS examination, it shows that the growth of native oxide on GaAs surface still exists.

Next, surface passivation by sulfur solution is effective wet chemical treatment included material and electrical analysis. The $(NH_4)_2S$ solution with C_4H_9OH solvent can reduce Al/n-GaAs barrier height to 0.55 e V, and it trends to ideal value. This diluted sulfur-solution really suppresses the GaAs oxides, and increases sulfur temperature to bond strongly. The 80°C sulfur solution increases Ga-S bond when NH_4OH cleaned GaAs surface is used.

Subsequently, the electrical and physical properties of e-beam evaporated Gd_2O_3 film deposited on GaAs substrate are studied. For RT-sulfide treatment capacitor, the manifest frequency dispersion with a larger hysteresis is observed in multi-frequency *C-V* characteristics. High-temperature sulfided GaAs substrate results in the improvement of the electrical performances, especially for the *C-V* distortion and gate leakage increment. For NH_4OH clean process, the thermal stability of Ga-termined surface facilitated to obtain passivation result. Through the XPS analysis, the resultant composition of deposited Gd_2O_3

film is found to be (GaAs)GdO mixed oxide. Furthermore, it is found that the surface treatment, e.g., sulfur and NH_4OH pre-treatment, is essential to improve the quality of Gd_2O_3 films on GaAs substrate.

Finally, we believe that the continuous optimization of the surface treatment through process modification is expected to further improve the electrical performance of the Gd_2O_3/GaAs gate stack, which thus be considered as a promising gate dielectric of GaAs device.

5-2 Future Work

For the GaAs cleaning, the absence of the hydrophobic phenomenon gives rise to our attention. Because of such an interest difference between Si and GaAs substrate, how to obtain the suitable cleaning procedures for GaAs wafer and clarify the discrepancy of surface bonding mechanism between these two substrates is an attractive issue.

In the Chapter 3, we have demonstrated that the surface passivation through sulfur is required to improve the GaAs surface, especially the XPS characteristics. On the other hand, the easily oxidized properties of GaAs and the thermal instability of the surface bonds have been noticed in our experiments. Therefore, the attempt of different surface pre-treatments, such as the $(NH_4)_2S$ and Na_2S, in order to change the surface bonding states may be an essential procedure to improve the GaAs surface.

In the Chapter 4, a considerable C-V dispersion observed in e-beam Gd_2O_3 film on GaAs

is the most serious problem, which in turn leads to threshold instability of GaAs device. The PDA resulting in the reliability degradation of dielectric film may be owing to the GaAs incorporation and the formation of As-O and Ga-O bonding, since these events may serve as the trapping states and/or dielectric defects. One solution is the attempt of surface passivation has mentioned above, another is the advanced deposited instrument to growth high quality high-k film. In addition, the Ar/O_2 mixed post deposition annealing of the Gd_2O_3 film is performed. The aims of oxygen incorporation are expected to fill the vacancy inside the gate dielectric and decrease the leakage current. For the material characterization, i.e., XPS, the change of composition bonding and their mechanism for bulk dielectric can be characterized. We suggest that the other high-*k* gate dielectrics with very stable chemical property to GaAs may be good candidates for GaAs device.

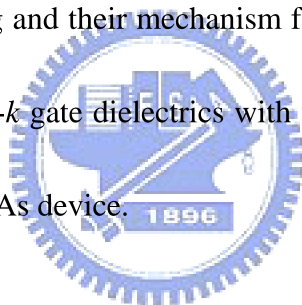

References:

[1] W. Zhu, J.P. Han and T.P. Ma, IEEE Trans. Electron Devices, **51**, 1, (2004)98-105

[2] The International Technology Roadmap for Semiconductors, 2004 Edition.

[3] G.D. Wilk, et al., J. Appl. Phys. **89** (2001) 5243.

[4] K.J. Hubbard, et al., J. Mater. Res,**11** (1996) 2757.

[5]C. W. Wilmsen, *Physics and Chemistry of III–V Compound Semiconductor Interfaces* (Plenum, New York, 1985) p. 165.

[6] J. Robertson , B. Falabretti, "Band offsets of high K gate oxides on high mobility semiconductors" Materials Science and Engineering B 135 (2006) 267–271

[7] M.Hong,"SEMICONDUCTOR-INSULATOR INTERFACES" , p.94

[8] H. Becke, R. Hall, and J. White, Solid-State Electron.,8:812,1965

[9] H. Hasegawa, M. Akazawa, K. Matsuzaki, H. Ishii, and H. Ohno, Jpn. J.Appl. Phys., Part2 **27**, L2265 (1988).

[10] Y. Wada and K. Wada, Appl. Phys. Lett. **63**, 379 (1993).

[11] J. Kwo, D. W. Murphy, M. Hong, R. L. Opila, J. P. Mannaerts, A. M. Sergent, and R. L. Masaitis, Appl. Phys. Lett. **75**, 1116 (2000).

[12] M. Hong, M. Passlack, J. P. Mannaerts, J. Kwo, S. N. G. Chu, N. Moriya,S. Y. Hou, and V. J. Fratello, J. Vac. Sci. Technol. B **14**, 2297 (1996).

[13] J.P.Contour, J.Massies, H.Fronius, and K.Ploog, Jpn.J.Appl.Phys.**27**,2, (1988) L167-L169,

[14] M.Yamada, and Y.Ide, Sur.Sci.**339**(1995)L914-L918.

[15] K.Menda, E.Kanda, and T.Yokoyama, Jpn. J. Appl. Phys. **29,**3,(1990)L391-L393

[16] K.Iizukaa, Y.Sakamakia, T.Suzukia, and H.Okamoto, J. Crystal Growth 227-228(2001) p41-p45

[17] Y.Morishita, Y.Nomura, S.Goto, and M, Yamada, Jpn. J. Appl. Phys. **34**(1995)

pp.L397-L400

[18] S.Goto, M, Yamada, and Y.Nomura, Jpn. J. Appl. Phys. **34**(1995) pp.L1180-L1183

[19] C.C.Surdu-Bob, S.O.Saied, J.L.Sulivan, App.Surf.Sci. **183**(2001)126-136

[20] J.S. Songa, Y.C. Choia, S.H. Seoa, D.C. Ohb, M.W. Chob, T. Yaob, and M.H. Oh, J.Cry. Growth **264** (2004)98-103

[21] L. Bideux a, D. Baca , B. Gruzza , V. Matolin , and C. Robert-Goumet, Surf. Sci. 566-568(2004)1158-1162

[22] M.G.Kang, and H.H.Park, Vac.**67**(2002)91-100

[23] T.V.Buuren, M.K.Weilmeier, I.Athwal, K.M.Colbow, J.A.Mackenzie, and T.Tiedje, Appl.Phys.Lett. **59**,4(1991)464-466

[24] J.P.Contour, J.Massies, and A.Saletes, Jpn. J. Appl. Phys. **24,** 7 (1985) L563-L565.

[25] A.Saletes, J.Masies, and J.P.Contour, **25**, 1 (1986) L48-L51.

[26] D.A.Allwood, R.T.Carline, N.J.Mason, C.Pickering, B.K.Tanner, and P.J.Walker. Thin Solid Films **364**(2000) 33-39.

[27] B.K.Tanner, D.A.Allwood, and N.J.Mason, Material and Science and Engineering B80(2001)99-103.

[28] L.G.Quagliano, App.Sur.Sci.**153**(2000) 240-244

[29] Y.Hiratani, M.Sasaki, S.Yoshida, and M.Yamada, J.Crystal Growth **150**(1995) 404-408.

[30] C.Bryce, and D.Berk,Ind.Eng.Chen.Res.**35** (1996) 4464-4470

[31] B.J.Skromme, C.J.Sandroff, E.Yablonovitch, and T.Gmitter, Appl.Phys. Lett.**51**,24(1987) L2022-L2024.

[32] R.S.Besser, and C.R.Helms, J.Appl.Phys.**65**,11(1989)

[33] V.L.Berkovits, V.N.Bessolov, T.N.Lvova, E.B.Novikov, and V.I.Safarov, R.V.Khasieva, and B.V.A.Tsarenkov, J.Appl.Phys.**70**,7(1991), L3707-L3711.

[34] M.S.Carpenter, M.R.Melloch, and M.S.Lundstrom, App.Phys. Lett.**52**,(25), 20 (1988).

[35] V.N.Bessolov, M.V.Lebedev, A.F.Ivankov, W.Bauhofer, and D.R.T.Zahn, Appl. Sur.Sci.

133(1998)17-22

[36] T.Simonsmeier, A.Ivakov, and W.Bauhofer, J.Appl.Phys.**97**, 084910(2005)

[37] V.N.Bessolov, E.V.Konenkova, and M.V.Lebedev, Material Sci.Eng.B44 (1997) 376-379.

[38] V.N.Bessolov, M.V.Lebedev, N.M.Binh, M.Friedrich, and D.R.T.Zahn, Semicond. Sci.Technol.**13** (1998) 611-614.

[39] S.Shikata, and H.Hayashi, J.Appl.Phys.70(7),(1991)3721-3725.

[40] D.Paget, J.E.Bonnet, V.L.Berkovits, P.Chiaradia, and J.Avila, Phy.Rev.B **53,**8(1996)4604-4614.

[41] S.A.rabasz, E.Bergignat, G.Hollinger, and J.Szuber, Vacuum **80**(2006)888-893.

[42] K.Remashan, and K.N.Bhat, Semicond.Sci.Technol.**17**(2002)243-248.

[43] J.Szuber, E.Bergignat, G.Hollinger, A.Polakowska, and P.Koscielniak, Vacuum **67** (2002) 53-58.

[44] P.Moriarty, and B.Murphy, L.Roberts, A.A.Cafolla, G.Hughess, L.Koenders, and P.Bailey, Phy.Rev.B, vol.**50** (1994) 14237-14245.

[45] Z.L.Yuan, X.M.Ding, H.T.Hu, Z.S.Li, J.S.Yang, X.Y.Miao,X.Y.Chen,X.A.Cao, and X.Y.Hou, Appl.Phys.Lett. **71**(1997) 3081-3083.

[46] P.D.Ye, G.D.Wilk, B.Yang,J.Kwo, S.N.G.Chu, S.Nakahara, H.J.L.Gossmann, J.P.Mannaert, M.Hong, K.K.Ng, J.Bude, Appl.Phys.Lett.**83**(2003) 180.

[47] Z.Yu, C.D.Overgaard, R.Droopad, M.Passlack, J.K.Abrokwah, Appl. Phys. Lett. **82**(2003)2978.

[48] M.Hong, J.Kwo, A.R.Kortan, J.P.Mannaerts,and A.M.Sergent, Science, **283** 19 (1999) 1897-1990.

[49] J.K.Yang, M.G.Kang, and H.H.Park, Thin Solid Films 420-421 (2002)571-574.

[50] J.K.Yang, W.S.Kim, and H.H.Park, Appl.Surf.Sci.**216** (2003) 203-207.

[51] J.K.Yang, M.G.Kang, and H.H.Park, J.Appl.Phys.**96**(2004) 4811-4816.

ES 1896

[52] J.K.Yang, and H.H.Park, Appl.Phys.Lett.**87**, (2005) .

[53] K.H.Kwon, J.K.Yang, H.H.Park, J.Kim, and T.M.Roh, Appl.Surf.Sci.**252** (2006) .7624-7630.

[54] G.K.Dalapati, Y.Tong, W.Y.Loh, H.K.Mun, and B.J.Cho, Appl.Phys.Lett. **90**(2007).

[55] M.G.Kang, and H.H.Park, Thin Solid Films 355-356 (1999)435.

簡　歷

姓 名：曾 治 國

性 別：男

生 日：民 國 72 年 1 月 11 日

籍 貫：台 灣 省 台 中 縣

地 址：台 中 縣 外 埔 鄉 二 崁 路 51 號

學 歷：私 立 逢 甲 大 學　電 機 系

（2001 / 9 ～ 2005 / 6）

國 立 交 通 大 學　電 子 研 究 所 碩 士 班

（2005 / 9 ～ 2007 / 6）

碩 士 論 文 題 目：

閘極介電層氧化釓於硫鈍化後砷化鎵基板之電物性研究

The Electrical and Material Characteristics of Gd_2O_3 Gate Dielectric on Sulfided GaAs Substrate